Physiological and Pharmacological Regulation of the STAT3 Pathway in Cancer

Physiological and Pharmacological Regulation of the STAT3 Pathway in Cancer

A dissertation presented

by

Michael Xiang

to

The Division of Medical Sciences

in partial fulfillment of the requirements

for the degree of

Doctor of Philosophy

in the subject of

Cell Biology

Harvard University

Cambridge, Massachusetts

May 2013

Dissertation Advisor: Professor David A. Frank Michael Xiang

Physiological and Pharmacological Regulation of the STAT3 Pathway in Cancer

Abstract

STAT3 is a critical oncogenic transcription factor, but how it becomes aberrantly activated in cancer is unclear. We have discovered a new pathway whose loss is associated with persistent STAT3 activation in human cancer. We found that the tumor suppressor miR-146b is a direct STAT3 target gene in normal breast epithelial cells. However, STAT regulation of miR-146b is subverted in tumor cells and is suppressed by promoter methylation, which is increased in primary breast cancers. Moreover, we show that miR-146b inhibits NF-κB-dependent IL-6 production, IL-6-dependent STAT3 activation, and IL-6/STAT3-driven functional phenotypes, thereby establishing a negative feedback loop. In addition, miR-146b expression appears to be deregulated in tumors with the highest levels of activated STAT3, and is positively correlated with patient survival. Our results indicate a new mechanism of crosstalk between STAT3 and NF-κB relevant to constitutive STAT3 activation in malignancy and the role of inflammation in oncogenesis.

Despite the importance of STAT3 in cancer, clinically available therapies to inhibit STAT3 are limited. A chemical genomics approach can discover drugs with novel mechanisms of action. In this manner, the FDA-approved drug atovaquone was identified to oppose the gene expression signature of STAT3. At concentrations readily achieved in human plasma, atovaquone inhibits STAT3 phosphorylation, transcriptional activity, and STAT3-dependent

cancer cell viability. Atovaquone is not a kinase inhibitor, but instead downregulates cell-surface gp130 expression, which is required for STAT3 activation in multiple contexts. Additionally, atovaquone activates certain components of the unfolded protein response and inhibits mTOR by inducing REDD1. Importantly, higher atovaquone exposure is associated with improved disease-free survival in patients who underwent hematopoietic stem cell transplant for hematological malignancies. These results establish atovaquone as a novel STAT3 inhibitor with evidence of anti-cancer efficacy in patients.

TABLE OF CONTENTS

CHAPTER 1:

Introduction and Background

Overview of Cancer and STAT Biology

Cancer is a disease built upon a progression of genetic and epigenetic derangements (1) that alter the level or functional activity of specific genes. Such alterations conspire to switch on certain pathways and disable others, bestowing upon cells the features of a transformed phenotype. These properties, shared by all cancers, include inappropriate proliferation and survival, sustained angiogenesis, and invasion and metastatic spread (2). Additionally, cancer cells do not exist in a vacuum: crosstalk with non-malignant stromal cells and signals from the tumor microenvironment play crucial roles in cancer development, growth, and dissemination (3). Thus, based on their specialized abilities and interactions with the host, cancers have become increasingly viewed as heterogeneous, multifunctional, organ-like tissues (2).

Gene expression alterations not only underlie cancer cells' perturbed intracellular circuitry, but also serve to link it to the phenotypic hallmarks of cancer (Figure 1.1). Increased and decreased activity of oncogenic and tumor suppressor pathways, respectively, cooperate to induce the expression of genes promoting survival, proliferation, and other malignant traits. At the same time, the expression of genes opposed to cancer is frequently repressed. Research has shown that the biology and clinical behavior of a tumor is better described by its gene expression pattern than its histological appearance or even tissue of origin (4-7). Regulation of gene expression is mediated by transcription factors, which lie at the interface between signaling events and DNA. Consequently, transcription factors integrate inputs from multiple upstream pathways and function as master regulators of gene expression and cellular phenotype.

Signal transducers and activators of transcription (STAT) proteins are transcription factors with key roles in cancer. The STAT family is conserved from *C. elegans* to vertebrates (8), and in mammals, it comprises seven distinct genes: STAT1-4, STAT5A, STAT5B (often

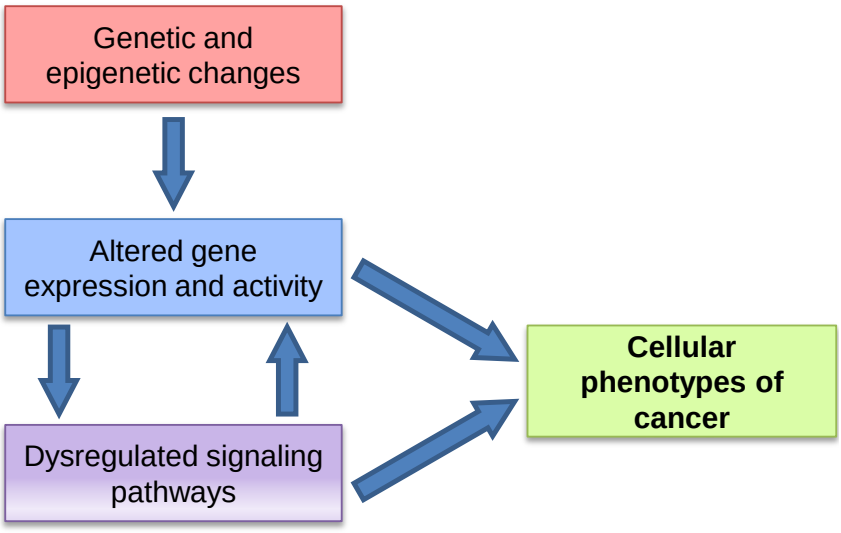

Figure 1.1: Depiction of the pathogenesis of cancer. Underlying genetic and epigenetic changes lead to alterations in the expression level and functional activity of specific genes, which results in dysregulation of key oncogenic and tumor suppressor pathways. In turn, signaling pathways shape the gene expression patterns that promote the defining phenotypes of cancer. Additionally, signaling pathways can directly affect cellular phenotypes, as in the case of modified cellular metabolism.

cited jointly as STAT5), and STAT6. While inactive, STATs reside in the cytoplasm as monomers or in an inactive dimer conformation (9). STAT activation begins with recruitment to specific sites on active receptors or kinases, typically following ligand binding or other signaling events. This interaction occurs between the STAT SH2 domain and phospho-tyrosine residues on the receptor or kinase. Next, the STAT protein is phosphorylated near the C-terminus at a critical, conserved tyrosine residue (Figure 1.2), which is the defining event of STAT activation. Phospho-STATs then dissociate from their receptor or kinase and bind to each other via reciprocal SH2/phospho-tyrosine interactions, forming active homo- or heterodimers (10).

Phospho-STAT dimers undergo nuclear translocation and are resistant to nuclear export (11), thereby accumulating in the nucleus. Nuclear import is mediated by the association of specific importin-α family members with unconventional nuclear localization sequences that are

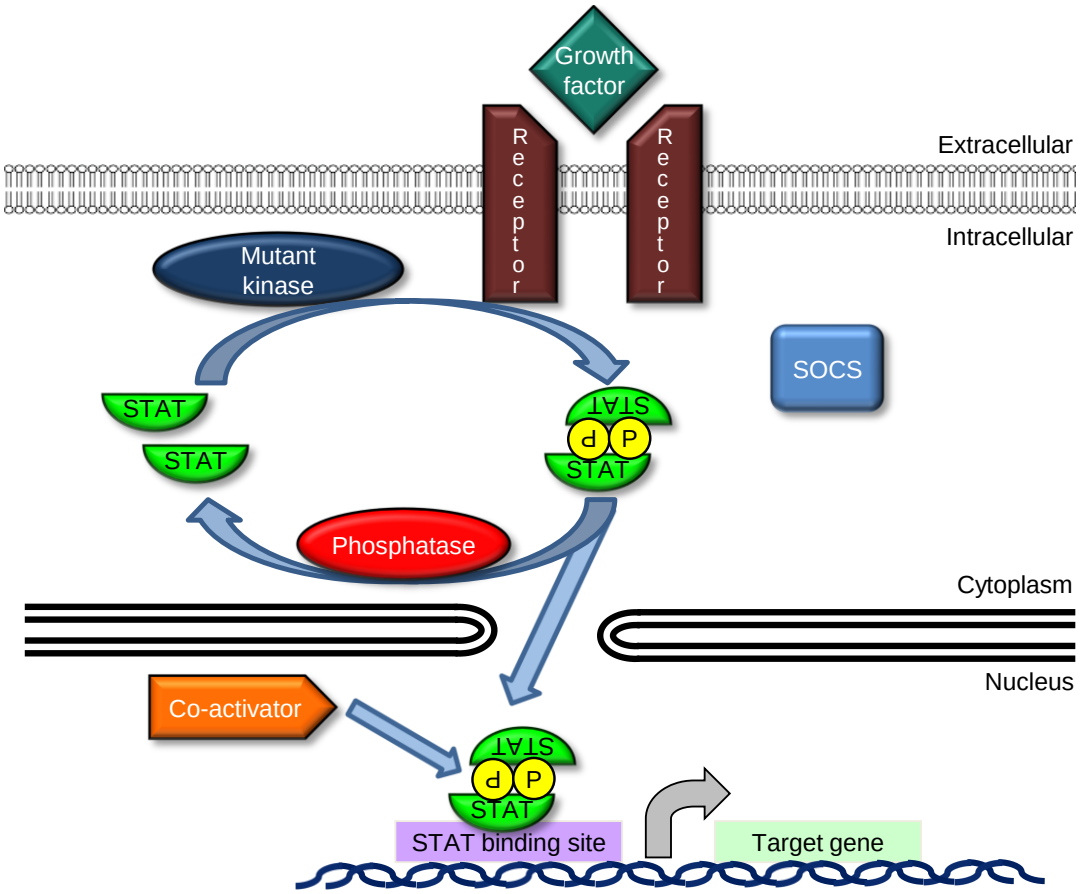

Figure 1.2: Overview of the STAT signaling pathway. While inactive, STATs reside in the cytoplasm. Upon tyrosine phosphorylation by kinases, which may be mutated or aberrantly active in cancer, STATs undergo dimerization, nuclear translocation, and binding to DNA. Transcriptional cofactors are also recruited to promote regulation of target genes.

only active in the context of STAT dimers (11). Once in the nucleus, STATs bind to DNA through the canonical motif $TTCN_{2\text{-}4}GAA$ (10) and recruit transcriptional co-activators to induce the expression of target genes (12). In certain cases, despite being named activators of transcription, STATs can also repress gene expression (13). The transactivation domain is quite divergent between different STAT family members (14), and they regulate overlapping and distinct sets of genes due to specific protein-protein interactions with transcriptional cofactors and DNA sequence determinants outside of the core motif. By this series of steps (Figure 1.2), extracellular signals are propagated to DNA to influence gene expression.

The list of tyrosine kinases that activate STATs is extensive and can be divided into three classes. Receptor-associated tyrosine kinases, specifically the Janus kinase (JAK) family, transduce intracellular signals for receptors that lack intrinsic kinase activity. Such receptors respond to a vast array of cytokines, growth factors, and hormones, including interferons, interleukins, erythropoietin, growth hormone, prolactin, and leptin (15). Although different receptors preferentially associate with particular JAK kinases, the specificity of STAT family member activation is achieved by the structural interaction of STAT SH2 domains with cognate receptors (16-18). Cytoplasmic tyrosine kinases, such as the Src family, also mediate STAT activation (19). Lastly, receptor tyrosine kinases, including EGFR and PDGFR, phosphorylate STATs directly, or in certain contexts act through JAK or Src family members (19).

In addition to tyrosine phosphorylation, STATs are regulated by numerous other post-translational modifications. All STATs except for STAT2 and STAT6 possess a conserved serine residue in the transactivation domain (10). Serine phosphorylation is mediated by kinases such as the MAPK family, mTOR, PKC, and IKKε (20) and is not essential for STAT activation, but contributes to maximal target gene induction. Another modification is ubiquitination, which promotes not only STAT proteasomal degradation but also tyrosine dephosphorylation (10). Two ubiquitin-like modifications, SUMOylation and ISGylation, have been found to modulate STAT activity at certain promoters without affecting protein stability. Finally, acetylation has been reported to facilitate STAT dimerization, DNA binding, and gene expression (10, 21). In general, the effect of these modifications on STAT function and activity is less characterized and more nuanced than the paradigm of tyrosine phosphorylation.

Several mechanisms serve to attenuate STAT signaling. The suppressor of cytokine signaling (SOCS) family consists of 8 proteins, SOCS1-7 and CIS, which are induced by STAT

activation and exert negative feedback at the level of STAT tyrosine phosphorylation. SOCS members bind to and directly inhibit receptors and JAKs, compete with STATs for binding to these proteins, and target signaling components for proteasomal degradation (22). In the nucleus, protein inhibitor of activated STAT (PIAS) proteins block activated STATs from binding to DNA (10). In both the nucleus and cytoplasm, tyrosine phosphatases such as SHP-2 and PTPN2 dephosphorylate STATs (23), resulting in dissociation from DNA and cytoplasmic localization. Phosphatases also act on receptors and kinases to erase phospho-tyrosine markers of activation, thus returning them to an inactive conformation and removing docking sites for STATs.

These inhibitory mechanisms ensure that basal STAT activity is low or absent in normal cells and, upon appropriate stimulation, is rapidly and transiently induced. In normal cells, maximal STAT activation occurs within 30 minutes of onset, after which STAT phosphorylation decays with a half-life of less than 15 minutes (24). By contrast, many cancers harbor constitutive activation of one or more STATs (25). Several mechanisms underlie the constitutive STAT signaling seen in cancer. Until now, STATs themselves were never thought to be somatically mutated during cancer development. Recently, however, acquired STAT3 mutations were discovered in 40% of large granular lymphocytic leukemias, a rare neoplasm (26). The mutations, which are hydrophobic substitutions within the SH2 domain, favor dimerization, persistence of tyrosine phosphorylation, and transcriptional activity.

In all other instances, inappropriate STAT activation in cancer is due to alterations of upstream signaling components or disruption of normal inhibitory mechanisms. First, mutant, fusion, or overexpressed receptors or kinases display overactive signaling and may be immune to negative feedback regulation. Prominent examples include the BCR-ABL fusion in chronic myeloid leukemia and mutant JAK2-V617F in myeloproliferative neoplasms (27). Second,

critical negative regulators of the STAT pathway are frequently downregulated through transcriptional repression, epigenetic silencing, or genomic deletion. This phenomenon has been observed with SOCS and phosphatase genes, which experience hypermethylation in various cancers (28). Third, autocrine or paracrine secretion of growth factors, such as IL-6 (29, 30), often drives constitutive pathway activation, especially in conjunction with loss of negative regulators.

The Role of STAT3 in Cancer

STAT1, STAT3, and STAT5 are activated by many diverse stimuli in numerous settings and exert wide-ranging effects on gene expression and cell behavior. In contrast, STAT2, STAT4, and STAT6 are activated under much more limited conditions and function primarily in the immune system (10). Consequently, STAT1, STAT3, and STAT5 have been most closely linked to roles in cancer, although emerging evidence also implicates STAT6 in certain cases of oncogenesis (31-33). While the actions of STAT1, STAT3, and STAT5 are pleiotropic, STAT1 has generally been viewed as a tumor suppressor and is less often activated in tumors, whereas STAT3 and STAT5 are considered to be oncogenic (34). In particular, STAT3 is constitutively active in a high proportion of nearly all solid and hematological tumor types, suggesting it may be a key event in tumorigenesis (35). Thus, the function of STAT3 has been most extensively investigated in cancer cell biology (Figure 1.3).

An abundance of evidence establishes STAT3 as a central oncogenic mediator. STAT3 is activated by a plethora of oncogenic kinases and growth factors, and it is specifically required for transformation by v-Src (36) and mutant c-Kit (37). Conversely, loss of STAT3 inhibits tumor formation in multiple cell types (35). Moreover, a constitutively-active variant of STAT3, termed

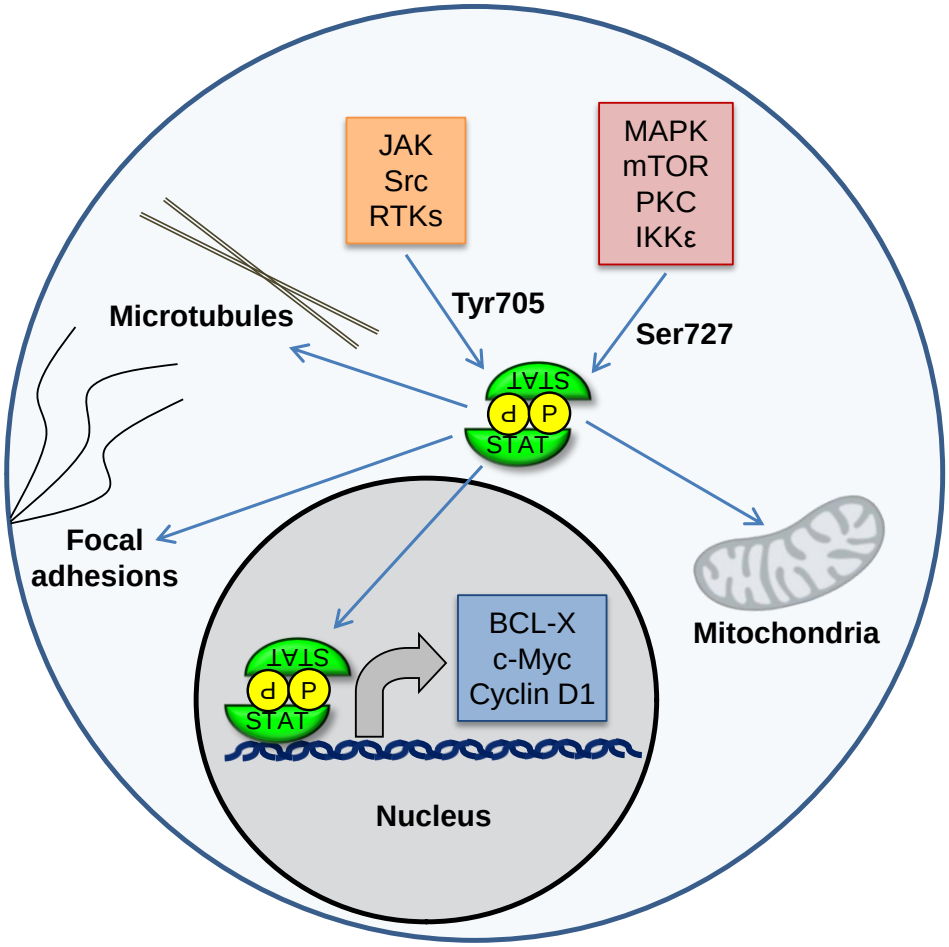

Figure 1.3: Overview of STAT3 interactions with other cellular pathways and compartments. STAT3 is subject to phosphorylation by both tyrosine and serine kinases. Tyrosine phosphorylation is critical to nuclear localization and transcription of tumorigenic target genes, which is the canonical function of STAT3. Additionally, STAT3 can localize at mitochondria to modulate oxidative phosphorylation, which is dependent on STAT3 serine phosphorylation. STAT3 has also been found to associate with focal adhesions and microtubules to affect cancer cell motility in a non-transcriptional manner. RTKs: receptor tyrosine kinases.

STAT3C, is sufficient for neoplastic transformation and induces tumorigenic target genes such as cyclin D1, Bcl-X, and c-Myc (38). STAT3C has cysteine residues introduced near the C-terminus that form intermolecular disulfide bridges, promoting dimerization and transcriptional activity. In addition to transformation and tumor initiation, STAT3 is also critical to tumor maintenance and progression. For example, inhibition of constitutively-active STAT3 in multiple tumor models and cancer cell lines leads to apoptosis (39). The effects of STAT3 are mediated

by the direct regulation of diverse target genes involving all of the hallmarks of cancer (2). Also, the significance of STAT3 in tumor-stromal interactions is increasingly gaining attention.

Uncontrolled proliferation, one of the first cancer hallmarks to be recognized, is advanced by STAT3 at many levels. STAT3 induces cyclin D1 (38, 40), which is critical for G1/S phase transition, as well as cyclins D2/D3/A and the phosphatase cdc25A (41). Genome-wide profiling of STAT3-regulated genes identified Egr1 and JunB as further targets promoting cell cycle entry (35). Also, STAT3 antagonizes the cell cycle inhibitors p21 and p27 by direct transcriptional repression (41) and by upregulating Skp2, which mediates their ubiquitin-mediated degradation (42). STAT3 induction of c-Myc, a pleiotropic protein with key roles in cancer growth and proliferation, is required for v-Src transformation and PDGFR-induced mitogenesis (43). Moreover, the kinases Pim-1 and Pim-2 are STAT3 targets, and ectopic expression of Pim-1 with c-Myc fully rescues loss of cell cycle progression after STAT3 inhibition (44). Finally, STAT3 fosters limitless replicative potential by directly inducing telomerase (45).

STAT3 also enhances cancer cell survival. While STAT3 regulates Bcl-2 and mediates chemotherapy resistance (46, 47), STAT3 regulation of Bcl-X has been better studied. STAT3 is required for Bcl-X expression by EGFR in head and neck squamous cell carcinoma (HNSCC), HER2 in breast cancer, and IL-6 in multiple myeloma (48-51). Mcl-1, a related STAT3 target, collaborates with Bcl-X to resist Fas-mediated cell death, particularly in hematological cancers (50, 52, 53). Survivin is another anti-apoptotic protein induced by STAT3 in various settings, including astrocytoma, breast cancer, gastric cancer, and primary effusion lymphoma (54-57). Inhibiting STAT3 reduces levels of these survival factors and causes apoptosis, which is reversed by their enforced expression, demonstrating the importance of these downstream effectors (51,

56, 57). Additionally, STAT3 transcriptional repression of pro-apoptotic Fas, TNF-α, and p53 facilitates tumor escape from normal death signals (13, 58, 59).

Self-renewal and resistance to apoptosis are traits of cancer stem cells (CSC), and not surprisingly, STAT3 has been linked to the CSC phenotype. In fact, LIF activation of STAT3 is critical to pluripotency in embryonic stem cells (60). The STAT3 target genes KLF4 and BCL6 inhibit differentiation (35), while another STAT3 target, DNA methyltransferase I (61), functions to maintain both hematopoietic and leukemic stem cells (62). CSCs in glioblastoma and breast cancer require STAT3 activation (29, 63) resulting from IL-6 or EGFR (64). Also, trastuzumab resistance in HER2+ breast tumors occurs by IL-6-driven expansion of stem-like cells (65). In other cases, STAT3 activation in CSCs is due to Runx1-mediated silencing of SOCS family members (66). STAT3 additionally promotes CSCs via tumor-stromal interactions. Breast cancer cells secrete factors that activate STAT3 in cancer-associated fibroblasts, which respond by producing CCL2 to induce CSC phenotypes in breast cancer cells (67).

STAT3 activation is associated with aggressive clinical behavior and poor prognosis (68). Interestingly, inhibiting STAT3 can prevent tumor growth in mice without affecting growth of cancer cells *in vitro* (69, 70). The ability to migrate, invade, and eventually metastasize is a malignant hallmark that enables cancer cells to grow and spread *in vivo*. Thus, STAT3 has been found to intimately regulate these processes, and in particular, many matrix metalloproteinases (MMPs) are under transcriptional control of STAT3. For example, STAT3 regulation of MMP-2 promotes invasion and metastasis in melanoma and ovarian cancer cells (70-72), while MMP-7 is critical to pancreatic cancer progression (73). STAT3 and c-Jun cooperatively induce MMP-1 and MMP-10 in bladder cancer cells to increase motility and tumor formation in mice (74).

Moreover, STAT3C transformation of immortalized breast epithelial cells requires MMP-9, whose expression correlates with STAT3 activation in primary breast cancers (75).

Besides MMPs, genes linked to epithelial-mesenchymal transition (EMT) are regulated by STAT3. For instance, STAT3 directly promotes Snail expression while also inducing LIV1, a zinc transporter essential for Snail nuclear localization (76, 77). Twist is another key EMT gene upregulated by STAT3 (78-80). STAT3 mediates EGFR-stimulated Twist expression, EMT, and motility, and levels of Twist correlate with EGFR and STAT3 phosphorylation in primary breast tumors (81). In colorectal carcinoma, STAT3 may promote EMT by inducing ZEB1, a repressor of E-cadherin (82). Transformation of immortalized prostate epithelial cells by STAT3C involves upregulation of integrin β6 and its ligands fibronectin and tenascin C, which produce an EMT phenotype (83). Reciprocally, HER2 interaction with integrin β4 activates STAT3 to cause loss of epithelial adhesion and polarity (84). STAT3 also modulates the cytoskeleton to promote migration through both transcriptional (85) and non-transcriptional mechanisms (86, 87).

Angiogenesis is another process crucial to tumor growth *in vivo* but is not readily assayed *in vitro*. STAT3 induction of MMPs may facilitate angiogenesis (88), in addition to their role in motility. More directly, the pro-angiogenic factor VEGF is a STAT3 target gene. In multiple cancer models, STAT3 regulation of VEGF enhances tumor vascularity, growth, and metastasis *in vivo*; inhibiting STAT3 or VEGF does the opposite (89-91). Interestingly, STAT3 activation in endothelial cells is critical to assuming the angiogenic phenotype (92) and derives from VEGF itself, alongside other factors secreted by both tumor cells and tumor-infiltrating myeloid cells (93). Thus, STAT3 activation in tumor cells spreads to stromal cells, fostering tumor growth from multiple cellular compartments. STAT3 in both tumor and stroma can also modulate VEGF indirectly by upregulating HIF-1α, which stimulates VEGF transcription (94, 95).

In addition, tumor growth *in vivo* requires evading immune destruction. Here, too, the actions of STAT3 in multiple cellular compartments are synergistic, functioning to dampen the immune response and promote tumor tolerance. In both cancer cells and cancer-associated fibroblasts, STAT3 curbs the secretion of chemoattractants and pro-inflammatory cytokines such as TNF-α and IFN-β, while inducing the secretion of immunosuppressive IL-6, IL-10, and TGF-β (96-98). Furthermore, the maturation and function of immunological cells is impaired by STAT3 activation, which can result from STAT3-dependent secretion of paracrine factors by tumor cells (99, 100). Increased STAT3 activity in antigen-presenting cells promotes anergy, whereas inhibition of STAT3 leads to priming of CD4+ T cells to otherwise tolerogenic stimuli (101). Similarly, targeted disruption of STAT3 in hematopoietic cells elicits innate and adaptive anti-tumor responses and reduces formation of regulatory T cells (102).

The interplay between the immune system and cancer is complex, and STAT3 drives not only immune evasion, but also appropriation of inflammatory signals for tumor initiation and progression. For example, STAT3 activation in tumor-associated myeloid cells facilitates reciprocal STAT3 activation in tumor cells, xenograft growth in mice, and priming of pre-metastatic niches for colonization (103, 104). Also, many cancers are characterized by chronic inflammation. In Kras-driven models of pancreatic cancer, STAT3 signaling upregulates chemokines to recruit infiltrating immune cells, which in turn secrete factors that act on cancer cells to further neoplastic development (73, 105). Furthermore, paracrine activation of STAT3 in tumor-initiating cells by myeloid cell-derived IL-6 is a crucial event in models of inflammatory colorectal cancer (106). In this context, STAT3 ablation leaves inflammation intact, but abrogates its ability to promote cancer development (107). Thus, STAT3 mediates substantial oncogenic crosstalk within the tumor microenvironment.

Recently, metabolic reprogramming has emerged as a significant hallmark and driver of cancer. Whereas STAT3 tyrosine phosphorylation is required for v-Src transformation, STAT3 serine phosphorylation is required for Ras-mediated transformation and, unexpectedly, causes STAT3 to localize to the mitochondria (108). Mitochondrial STAT3 supports oxidative phosphorylation and ATP production. However, STAT3 can also boost aerobic glycolysis and reduce mitochondrial respiration, partly through HIF-1α upregulation (109). The specific effects of STAT3 may depend on the underlying driver mutations and associated metabolic context. For example, mutant JAK2-V617F induces GLUT1 and PFK2 through STAT5 (110); it is unknown if STAT3 may do the same. Interestingly, pyruvate kinase M2, which is the isoform expressed preferentially in proliferating cells, functions as a novel tyrosine kinase for STAT3 (111). This further illustrates the crosstalk between STAT3 and cancer metabolism.

Functional Relationships Between STATs and MicroRNAs

MicroRNAs are short (18-25nt) non-coding RNAs conserved among eukaryotes. About 30% of miRNAs are intergenic and undergo transcription from their own promoters as a primary transcript (pri-miRNA). The remaining miRNAs are located within introns of protein-coding genes (112). Drosha cleavage or mRNA splicing, respectively, liberates a stem-loop intermediate (pre-miRNA) that is exported to the cytoplasm, where it undergoes a second cleavage by Dicer to generate an RNA duplex with short 3' overhangs (Figure 1.4). One strand becomes the mature miRNA (guide strand) by preferential loading into the RNA-induced silencing complex (RISC) (113). The complementary strand (anti-guide, passenger, or minor strand) is typically degraded, but may also experience RISC loading under certain conditions (114). Asymmetric strand selection is mediated by the thermodynamic attributes of the duplex ends (115).

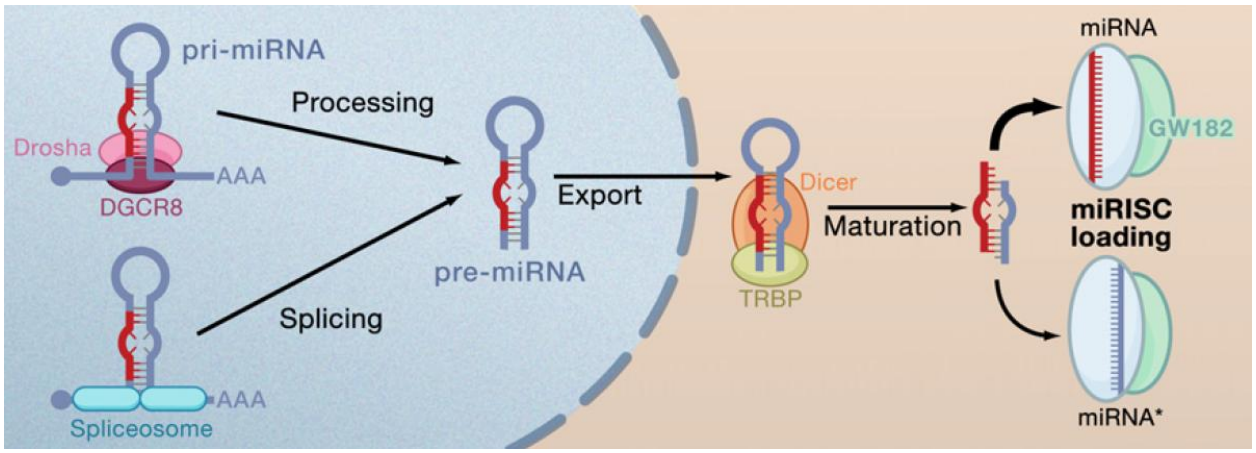

Figure 1.4: Overview of microRNA biogenesis in metazoans. MicroRNAs may be transcribed from their own promoters (as pri-miRNA) or lie within introns of protein-coding genes. The pre-miRNA is formed by Drosha cleavage of pri-miRNAs or splicing of intronic miRNAs. After nuclear export, additional cleavage by Dicer yields a duplex. Each strand may then be loaded into RISC, but usually one is preferred over the other. The less commonly-loaded strand is designated miRNA*. Image source: (116)

The RISC recognizes specific mRNAs by sequence complementarity of the miRNA seed region (positions 2-8) with sites in target mRNAs, most often in the 3' UTR. This base-pairing is necessary but often not sufficient for target recognition, and additional contextual cues may be required (117, 118). RISC-bound mRNAs are translationally repressed, destabilized by de-adenylation, or both. Remarkably, up to 90% of human genes appear to be miRNA targets, underscoring the significance and extent of this mode of post-transcriptional regulation (119, 120). Also, each miRNA typically binds multiple targets, and one target may be regulated by multiple miRNAs. As of early 2013, over 1500 miRNAs have been identified in humans, thus outnumbering kinases by a factor of two to three. Accordingly, miRNAs have been implicated in numerous processes in development, physiology, and disease (121).

Not surprisingly, miRNAs are recognized to modulate key aspects of tumor biology, and a large number reside in fragile sites that are commonly deleted or amplified in cancer (122). As negative regulators of protein-coding genes, miRNAs targeting tumor suppressors are deemed

oncogenic, whereas those targeting oncogenes function as tumor suppressors. For example, c-Myc and Ras are targets of the let-7 family. Its members are often downregulated in tumors, and their reintroduction inhibits proliferation, tumorigenesis, and metastasis. By contrast, miR-21 is often overexpressed, and a key target is the tumor suppressor PTEN. Inhibiting miR-21 via antisense oligonucleotides reduces the growth, migration, and invasion of cancer cells (123). However, context is critical: a miRNA can be oncogenic in one setting but tumor suppressive in another, depending on which targets are present (123).

Over the past few years, significant functional interactions between STATs and miRNAs have become recognized. While genome-wide identification of STAT-regulated mRNAs has been reported (124), an analogous study of miRNAs is lacking. Thus, less is known about STAT-regulated miRNAs than mRNAs. Nonetheless, for multiple STATs, cancer-related miRNAs have been discovered as direct target genes. STAT1 has long been regarded as a tumor suppressor, and consistent with this view, STAT1 represses miR-221 (125), an oncogenic miRNA that targets PTEN and p27. Moreover, IFN-γ activation of STAT1 upregulates the miR-29 family, which targets CDK6 and mediates growth inhibition in melanoma (126). In hematological cancers, the pro-tumorigenic role of STAT5 is well-documented. Downregulation of miR-15/16 by STAT5 relieves Bcl-2 from their suppression, resulting in higher Bcl-2 levels (127).

Research has shown that the oncogenic effects of STAT3 are partially mediated through miRNAs. In particular, miR-21 is a cancer-promoting miRNA that has been extensively studied. STAT3 regulation of miR-21 was first demonstrated in multiple myeloma, in which it is induced by IL-6. Enforced miR-21 expression inhibits apoptosis after IL-6 withdrawal (128). Likewise, STAT3-driven upregulation of miR-21 protects cells from apoptosis after interferon stimulation (129). Furthermore, STAT3 induction of miR-21 and miR-181b causes repression of PTEN and

CYLD, respectively, facilitating NF-κB activation, IL-6 production, and maintenance of cellular transformation (130). However, miR-21 expression is inhibited by STAT3 in glioma cells upon IFN-β treatment (131). The opposing results highlight the significant effects of cellular context on STAT-regulated gene expression.

Another prominent STAT3 target is the miR-17/92 cluster (132), which consists of 6 miRNAs transcribed as one polycistron. The cluster is also under transcriptional control of c-Myc, and its targets include Bim, p21, and PTEN (133-136). Accordingly, the miR-17/92 cluster was first identified as an oncogene. Its induction by STAT3 confers resistance to MEK inhibitors via miR-17 repression of Bim (137), while miR-92 repression of VHL stabilizes HIF-1α and induces VEGF in synergy with STAT3 (138). Interestingly, some targets of the miR-17/92 cluster lie within the STAT3 pathway itself, providing for both positive and negative feedback regulation. For instance, STAT3 activity is increased via miR-18a repression of PIAS3 (139, 140) and miR-19a/b repression of SOCS1 (141). Conversely, STAT3 itself is a direct target of multiple members of the miR-17/92 cluster (142-144), and miR-20b targets not only STAT3 but also HIF-1α, resulting in diminished VEGF expression (145).

In addition, several other STAT3 miRNA targets have been discovered which, like the miR-17/92 cluster, also modulate STAT3 activity. In a model of hepatocellular carcinogenesis, STAT3 induces miR-24 and miR-629 to repress HNF4α and maintain constitutive IL-6/STAT3 signaling (146). Also in hepatocellular carcinoma cells, IL-6 is targeted by miR-26a, leading to decreased STAT3 activation, tumor growth, and metastasis in mice (147). Interestingly, STAT3 directly represses miR-26a (148), and this potentially contributes to persistence of IL-6-driven STAT3 activation. By contrast, STAT3 regulation of other miRNAs appears to act as negative feedback mechanisms. For instance, STAT3 represses miR-204 and induces miR-125b, which

target the phosphatase SHP2 and STAT3 itself, respectively (149, 150). Therefore, STAT3 may regulate its own activity through miRNA-mediated feedback loops.

A number of miRNAs that do not appear to be under STAT transcriptional control have also been shown to modulate STAT function in a variety of ways. The most straightforward relationship is direct miRNA-mediated repression of STATs themselves, and several miRNAs not already mentioned are known to act in this fashion. For example, STAT5A is a target of miR-222 (151), STAT1 is a target of miR-145 and miR-146a (152, 153), and STAT3 is a target of miR-223 and let-7a (154, 155). In certain instances, such interactions have been demonstrated to affect specific aspects of cancer. As illustration, miR-124 targeting of STAT3 promotes T cell clearance of glioma (156). Additionally, miR-337-3p targeting of STAT3 mediates sensitivity to taxanes in non-small cell lung cancers (157).

More broadly, though, miRNAs can affect STAT signaling by targeting genes that activate or inhibit the STAT pathway, such as upstream kinases or negative regulators. Since the set of kinases that act upon STATs is expansive, the class of miRNAs capable of modulating STAT activity through kinase regulation is likely to be even larger. However, a few cases deserve specific mention. Multiple Src family members are targets of miR-205, which consequently has been shown to inhibit STAT3 phosphorylation (158). Furthermore, miR-135a represses JAK2 (159). The related miR-135b is a transcriptional target of STAT3 (160) and may also repress JAK2 due to sharing the same seed region as miR-135a, suggesting a possible route of negative feedback for JAK2-dependent STAT3 activation. Additional biologically significant examples involving miRNAs and STAT-associated kinases are likely to emerge.

Outside of kinases, multiple SOCS family members are miRNA targets. For instance, miR-203 represses SOCS3 to promote STAT3 phosphorylation (161). Inhibition of SOCS1 by

miR-155, which is overexpressed in many cancers, increases activation of both STAT1 and STAT3 (162) and promotes STAT3-driven breast tumor growth in mice (163). Importantly, miR-155 is upregulated by IL-6, IFN-γ, and other inflammatory factors (163) and is a direct target of at least STAT1 (164), suggesting a potential positive feedback relationship. Lastly, miR-9 targets SOCS5 to increase phosphorylation of STAT1 and STAT3 (165). Interestingly, in this study, miR-9 derived from tumor cells was delivered by microvesicles to endothelial cells and mediated their STAT-dependent migration and angiogenesis. However, in other settings, miR-9 has been found to reduce STAT3 phosphorylation (166).

In summary, the functional relationships between STATs and miRNAs are reflective of the fundamental nature of STATs in cancer biology. Several recurring themes can be viewed as organizing principles. Like STATs and miRNAs individually, their interactions influence a broad range of biological processes and phenotypes. Additionally, feedback loops are widespread and serve as key regulatory modules. Finally, the significance of cellular context and intercellular communication is increasingly being recognized and deserves further investigation.

Targeting the STAT3 Pathway for Cancer Therapy

Multiple arguments underlie the rationale for targeting the STAT3 pathway as cancer therapy. The critical oncogenic role of STAT3 in human tumors, as demonstrated by a wealth of preclinical and clinical data (167), make it an attractive target for pharmacological intervention. Moreover, for several reasons, inhibiting STAT3 provides a means of selectively affecting malignant and not normal cells. STAT3 activation is transient and dispensable in normal cells (35), and germline loss of STAT3 function is compatible with human development and survival (168). By contrast, cancer cells are specifically addicted to persistently activated STAT3 for

survival, proliferation, and other cancer hallmarks. Consequently, inhibiting aberrant STAT3 activation in cancer is a promising therapeutic strategy. However, despite extensive research, clinically available therapies to target STAT3 remain extremely limited.

The multistep process of STAT activation theoretically affords many opportunities for pharmacological modulation (Figure 1.1). However, the most straightforward drug targets are kinases (Figure 1.5), which possess binding pockets amenable to small molecule inhibition. Due to the crucial role of JAKs in the STAT pathway, many JAK inhibitors have been developed for preclinical use, and some natural products found to inhibit STAT3 appear to be JAK inhibitors (169, 170). As of 2013, the only FDA-approved drug to target STATs in cancer is ruxolitinib, a recent JAK inhibitor (30), though laboratory data also suggest the utility of gefitinib and dasatinib to inhibit STAT3 activated by EGFR and Src, respectively (171, 172). Moreover, tocilizumab is a monoclonal antibody to IL-6 receptor used clinically to treat autoimmune diseases. However, its potential as a cancer treatment has not been explored.

Unfortunately, the clinical efficacy of single-pathway kinase inhibitors has mostly been modest and transitory, perhaps due to functional redundancy of other signaling pathways or emergence of resistance mutations. Another possibility is concurrent or compensatory STAT activation by kinases that are not blocked by the drug. For example, the effect of dasatinib on STAT3 phosphorylation is short-lived because cells adapt to Src inhibition by increasing JAK activity (172). Thus, therapies to target STAT3 downstream of kinase activation may be useful, since a single drug could inhibit STAT3 regardless of how it is activated. One strategy is to increase the activity of endogenous negative regulators, such as phosphatases or SOCS family members, and a SOCS1 peptide mimetic has been reported (173). However, aside from the use

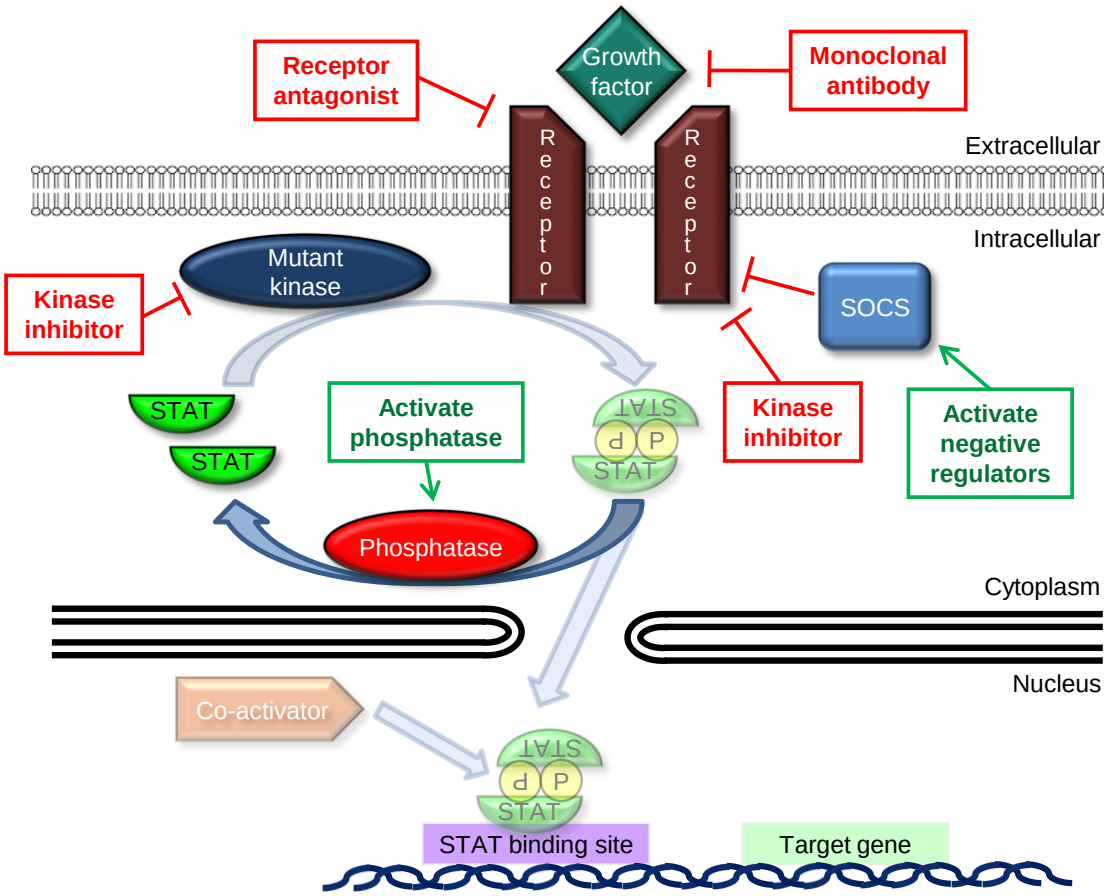

Figure 1.5: Strategies to inhibit the STAT pathway at the level of tyrosine phosphorylation. Kinase inhibitors, antagonists of receptors or their ligands, and SOCS proteins target upstream mechanisms of phosphorylation. By comparison, phosphatases diminish STAT phosphorylation after it has already occurred.

of specific drugs to reverse epigenetic silencing, enhancing protein function by small molecules is challenging.

Instead, much research has focused on inhibiting STAT3 directly. The STAT SH2 domain mediates critical interactions with kinases, receptors, and other STATs. Targeting the SH2 domain may affect STAT phosphorylation, dimerization, or both, and has therefore been pursued extensively. Phospho-peptides and peptidomimetics have been developed to inhibit the STAT3 SH2 domain by mimicking the phospho-tyrosine docking sites on STAT3 itself, EGFR, gp130, and other cytokine receptors (167). Despite high SH2 domain conservation, moderate

selectivity was achieved for STAT3 over STAT1 homodimers (174). However, this approach is hampered by poor cell permeability, low potency in the mid-micromolar range, and metabolic instability (167, 174). Consequently, numerous efforts have been made to antagonize the STAT3 SH2 domain using small molecules.

Since the crystal structure of the STAT3 dimer has been determined (175), several groups have used computational docking to screen for potential small molecule SH2 domain inhibitors *in silico*. STA-21 and S3I-201 were identified in this manner (176, 177). Biochemical screening assays have also been used. Stattic was discovered as a compound that inhibited STAT3 binding to a fluorescein-labeled phospho-peptide fragment of gp130 (178). It was subsequently found to bind to the STAT3 SH2 domain, causing decreased phosphorylation and dimerization (178). These drugs generally operate at mid- to low micromolar concentrations, but analogues have been created with potencies in the low micromolar or even nanomolar range (169). Furthermore, a number of natural products identified as potential STAT3 inhibitors mediate their effects through the SH2 domain (169).

Even after STAT3 phosphorylation and dimerization, STAT3 biological activity may be targeted in several ways (Figure 1.6). Inhibiting the step of nuclear translocation has been considered, but drugs specifically affecting STAT3 nuclear import have yet to be identified (167). STAT3 can also be prevented from binding to its cognate sites in the genome. This is the basis for using double-stranded DNA oligonucleotides as decoys to titrate STAT3 away from endogenous DNA (179, 180). While delivery and stability remain problematic, covalent linkage of both duplex ends confers resistance to degradation, and intratumoral delivery to HNSCC patients in a human Phase 0 trial showed downregulation of STAT3 target genes (181). Drugs

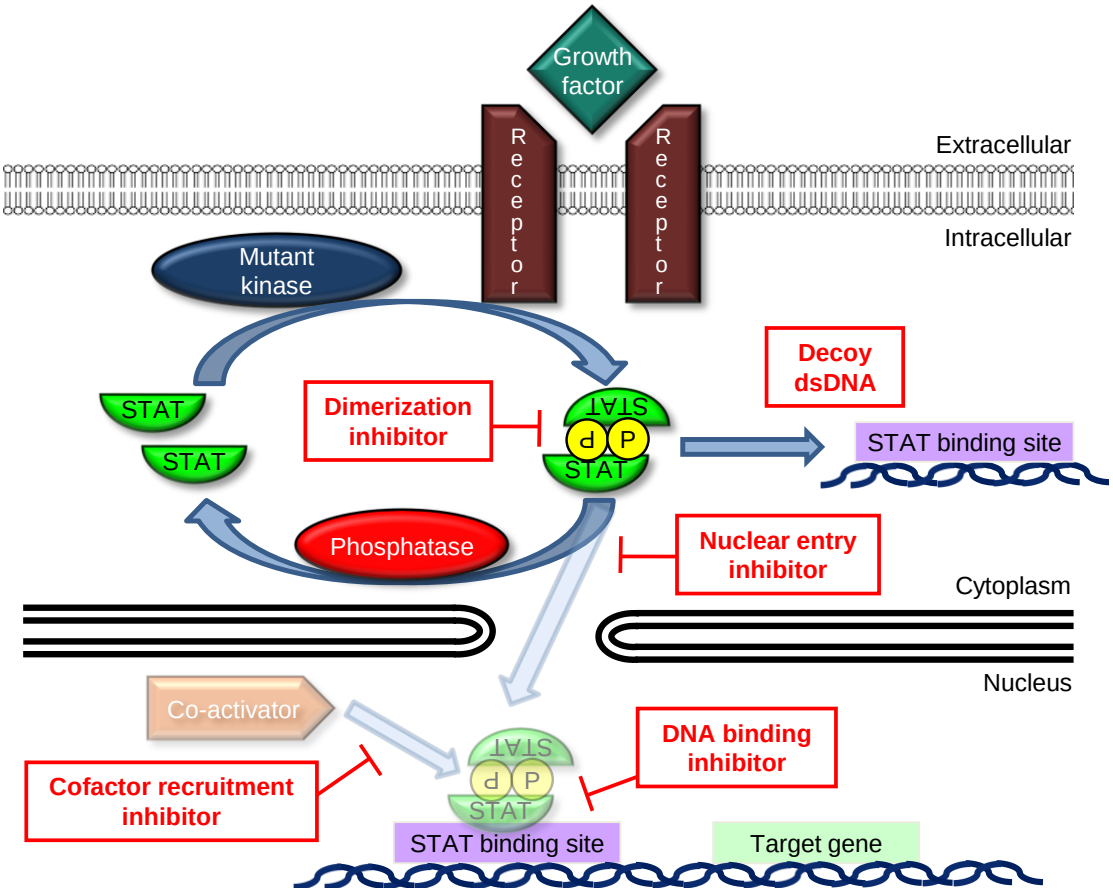

Figure 1.6: Strategies to inhibit the STAT pathway that do not directly affect STAT phosphorylation. These include dimerization inhibitors, nuclear entry inhibitors, and oligonucleotide decoys containing STAT binding sites. Within the nucleus, drugs could inhibit STAT recruitment of required cofactors or STAT DNA binding.

may also directly inhibit STAT3 binding to DNA, as in the case of platinum compounds (182) and the investigational agent flavopiridol (183).

A fruitful approach to uncover novel STAT3 inhibitors is the use of cell-based screens in which a luciferase reporter gene is under the control of STAT3 activity. Simultaneously counter-screening with a non-STAT3-dependent reporter helps to rule out nonspecific toxicity. The primary advantage of this approach is that it allows unbiased discovery of compounds that may act at any step of the STAT3 pathway, from phosphorylation to gene expression. When this strategy was applied to chemical libraries, it identified pimozide, pyrimethamine, and

nifuroxazide as STAT3 inhibitors (184-186). Notably, the first two are FDA-approved drugs. Whereas nifuroxazide appears to be a JAK inhibitor, how the other drugs inhibit STAT3 is not currently understood. Therefore, the large mechanistic landscape open to drugs identified in this manner can be both a strength and a shortcoming.

Importantly, most of the compounds being investigated as STAT3 inhibitors have been shown to specifically block the growth of cancer cells with constitutively activated STAT3, but not cells lacking STAT3 activation. This supports the prospect of targeting STAT3 in human cancers. Also, several components of the STAT3 pathway are currently understudied, and thus far, they are not known to be the subject of pharmacological modulation. Examples include STAT3 acetylation and recruitment of transcriptional cofactors. Conceivably, some of these processes may be affected by compounds that inhibit STAT3 activity but whose mechanisms of action remain uncharacterized. Finally, research has demonstrated that non-kinase and kinase inhibitors can be combined to achieve a synergistic effect (184, 187), which represents a growing paradigm in targeted cancer therapy.

CHAPTER 2:

STAT3-Regulated MicroRNA-146b Opposes NF-κB and Inhibits IL-6/STAT3-Driven Cancer Phenotypes

INTRODUCTION

Signal transducer and activator of transcription 3 (STAT3) is a key transcription factor in cancer pathogenesis (35). STAT3 activation is transient and tightly-controlled in normal cells, but is often constitutively activated in numerous tumor types to drive target genes regulating growth, survival, invasion, and angiogenesis. A major source of STAT3 activation in malignancy is the cytokine IL-6 (170), which signals through a complex of IL-6Rα and gp130 to activate Janus kinases (JAKs) and induce phosphorylation of STAT3. The importance of IL-6-driven STAT3 activation has been demonstrated in multiple tumor types, including breast, lung, liver, prostate, pancreatic, colon, head and neck, multiple myeloma, and melanoma (69, 188). The source of IL-6 can be paracrine—derived from non-neoplastic stromal or inflammatory cells—or autocrine, produced by tumor cells (189).

Specifically, NF-κB-dependent expression of IL-6 (190) is a common and significant autocrine pathway in cancer. For example, NF-κB can trigger an epigenetic switch leading to neoplastic transformation through induction of IL-6 and STAT3 activation (130, 191). Additionally, the signaling cascade of NF-κB, IL-6, and STAT3 promotes growth, survival, and chemotherapy resistance in breast cancer (192, 193), androgen-independent prostate cancer (194, 195), angiosarcoma (196), and colitis-associated cancer (106, 197). Therefore, NF-κB-dependent IL-6 is a significant driver of STAT3 activation and STAT3-dependent cellular phenotypes. However, the genetic circuits that control this process in physiological and disease states have yet to be elucidated.

While many protein-coding target genes of STAT3 have been characterized, relatively little is known about STAT3 microRNA target genes. MicroRNAs are short, non-coding RNAs

that regulate messenger RNAs through translational inhibition and transcript degradation (117), and as with STAT3, have been found to influence virtually all aspects of tumor biology. Given the functional importance of both STAT3 and miRNAs in cancer, the role of STAT3 as a transcription factor, and the dearth of known STAT3 miRNA targets, we focused on identifying novel STAT3-regulated miRNAs with relevance to cancer. Here, we report the discovery of miR-146b as a novel STAT3 target and its role in a feedback circuit involving STAT3, NF-κB, and IL-6 with significance in human cancer.

Attributions

Mouse mammary tissue and related western blot data (Figure 2.3A) and beta-casein expression data (Figure 2.3B) were supplied by Dr. Vida Vafaizadeh and Professor Bernd Groner (Georg-Speyer-Haus, Institute for Biomedical Research; Frankfurt, Germany). Phospho-STAT3 immunohistochemical staining and miR-146b expression data in primary human breast cancers (Figure 2.12E) were supplied by Dr. Nicolai J. Birkbak and Professor Andrea L. Richardson (Departments of Pathology, Brigham and Women's Hospital and Harvard Medical School; Boston MA, USA).

RESULTS

A Genome-Wide Screen for STAT3-Regulated MicroRNAs Reveals MiR-146b as a Novel STAT Target

To discover novel STAT3-regulated miRNAs, we generated a cellular system in which STAT3C, a constitutively-active mutant form of STAT3 (38), is inducibly regulated by doxycycline. Unlike kinase or cytokine-based signaling, which may also activate other pathways, this strategy enabled specific and focused activation of STAT3. We selected MCF-10A cells, an immortalized non-tumorigenic breast epithelial cell line that lacks basal STAT3 activation, because introducing STAT3C is sufficient for neoplastic transformation (75). Therefore, we reasoned that MCF-10A cells would be especially informative for miRNAs germane to STAT3 function and activity. The engineered MCF-10A cells responded robustly to doxycycline treatment with induction of STAT3C protein and STAT3 target genes (Figure 2.1A-B).

Screening for differentially-expressed miRNAs following STAT3C induction (Figure 2.1C) revealed 12 with a change of at least 2-fold (Figure 2.2A). These 12 miRNAs were further assessed by qRT-PCR, which validated the upregulation of 5 miRNAs, including miR-21, an established STAT target (128). To distinguish between direct and indirect targets, we analyzed the miRNA primary transcripts for induction by IL-6-mediated STAT3 activation while new protein synthesis was blocked (Figure 2.1D). This revealed miR-146b as the single novel direct miRNA target identified from the screen.

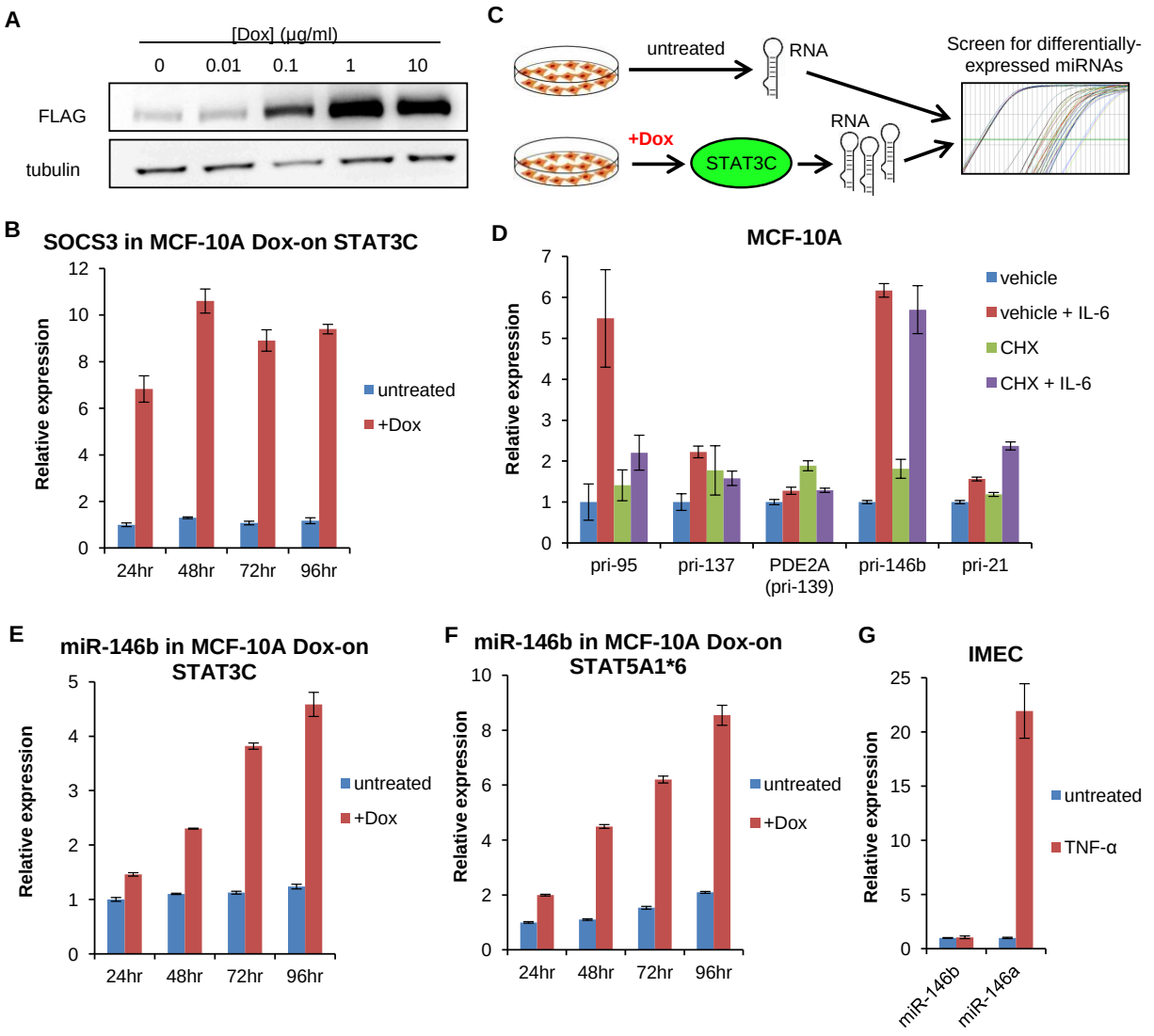

Figure 2.1: Characterization and use of doxycycline-inducible cell systems for miRNA screening and analysis of miR-146b regulation. (A) Induction of STAT3C (FLAG-tagged) in doxycycline-inducible STAT3C cells after 24hr. (B) Induction of SOCS3, a STAT3 target gene, in STAT3C-inducible cells after treatment with doxycycline (2μg/ml) for 24-96hr. (C) Screening strategy to identify STAT3-regulated miRNAs. (D) The protein synthesis inhibitor cycloheximide distinguishes between direct and indirect STAT targets. MCF-10A cells were pre-treated with vehicle or cycloheximide (2μg/ml) for 1 hour, then stimulated with IL-6 (20ng/ml) for 2 hours. Primary transcripts of validated miRNA hits from the screen were analyzed by qRT-PCR. (E-F) Doxycycline-inducible STAT3C and STAT5A1*6 cells demonstrate STAT activity is sufficient to induce miR-146b. (G) MiR-146a, but not miR-146b, is responsive to TNF-α in immortalized mammary epithelial cells (IMEC) treated with TNF-α (10ng/ml) for 48hr.

Molecular Regulation of MiR-146b by STATs

The system of inducible STAT3C indicates STAT3 activation alone is sufficient to induce miR-146b; a similar result was obtained with inducible constitutively-active STAT5 (STAT5A1*6) (Figure 2.1E-F). Furthermore, miR-146b was induced by cytokines that activate STAT3 (IL-6) or STAT1 (IFN-γ) (Figure 2.2B), and cytokine-stimulated induction of miR-146b was abrogated by dominant-negative STAT constructs, demonstrating that STAT transcriptional activity is necessary in this context (Figure 2.2C). Cytokine-stimulated STAT5 activation was not evaluated because MCF-10A cells lack prolactin receptor (Neilson et al., 2007 and data not shown) .

Next, we compared the regulation of miR-146b with that of miR-146a. The two miR-146 isoforms share 91% sequence identity, but reside at distinct genomic loci. Whereas miR-146a is a well-characterized NF-κB target (199), it is not known if NF-κB regulates miR-146b. In MCF-10A cells, STAT activation upregulated miR-146b but not miR-146a, while NF-κB activation via TNF-α showed the opposite pattern (Figure 2.2D). Also, TNF-α induced only miR-146a and not miR-146b in immortalized mammary epithelial cells (IMEC) (Figure 2.1G). Thus, miR-146a and miR-146b are subject to divergent regulatory control, and miR-146b is a target of STAT but not NF-κB activity.

To elucidate how STATs regulate miR-146b at a molecular level, we first analyzed the 3kb genomic region upstream of miR-146b, which was found to contain two consensus STAT binding motifs in islands of high phylogenetic conservation (Figure 2.2E). When this 3kb region was inserted upstream of a luciferase reporter, it conferred responsiveness to cytokine treatment and STAT3C (Figure 2.2F). Mutagenesis of either consensus STAT site inhibited induction of the luciferase reporter, thus establishing both sites as functional. Additionally, electrophoretic mobility shift assay (EMSA) demonstrated direct binding of IL-6-activated STAT3 to the distal

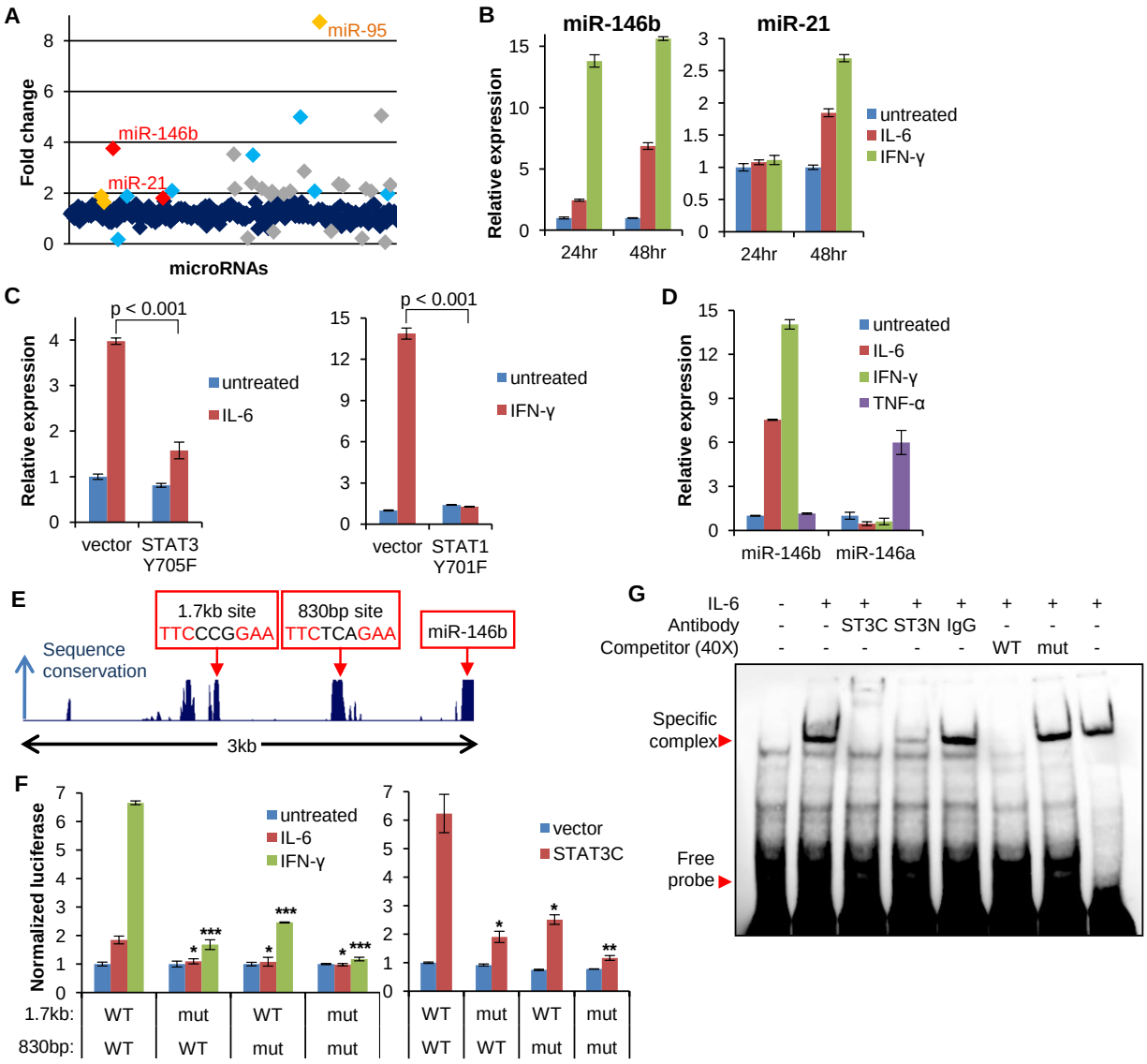

Figure 2.2: STAT family members directly regulate miR-146b expression. (A) Results of genome-wide screen for STAT3-dependent miRNAs. Red and orange refer to direct and indirect STAT targets, respectively; light blue hits did not pass qRT-PCR validation. Gray indicates low-confidence hits not evaluated by qRT-PCR due to high Ct value (> 30) or lack of statistical significance. (B) IL-6 or IFN-γ (20ng/ml) treatment of MCF-10A cells upregulates miR-146b. (C) Transduction of dominant-negative STAT constructs prevents miR-146b induction in MCF-10A cells treated with cytokine for 48hr. (D) STAT activation induces miR-146b and not miR-146a in MCF-10A cells treated with cytokine for 48hr. (E) Schematic of the miR-146b promoter region (3kb upstream) with consensus STAT binding motifs defined as $TTCN_{2\text{-}4}GAA$. (F) Both consensus STAT binding sites are functional. Luciferase reporters were constructed harboring the miR-146b promoter region with wild-type sequence or with mutations (TT→AA) introduced at either or both consensus STAT site(s). Luciferase activity was measured 6hr after cytokine treatment in wild-type MCF-10A (left) or 24hr post-transfection in MCF-10A transduced with STAT3C (right). P-values (*, $p < 0.05$; **, $p < 0.01$; ***, $p < 0.001$) are shown for the induction of mutant constructs relative to that of fully wild-type construct under the same condition.

Figure 2.2 (Continued)

(G) STAT3 binds directly to an oligonucleotide probe centered on the 1.7kb STAT site (lanes 1-7) by EMSA using nuclear extract from MCF-10A cells stimulated by IL-6 for 15 min. Separate N-terminal or C-terminal antibodies to STAT3 were used to disrupt the specific complex. Unlabeled competitor probes were used at 40X excess. Lane 8 utilizes Region B probe, a control known to bind STAT3 (200).

site (Figure 2.2G). STAT3 binding to the proximal site, which lies in a highly GC-rich region, was not detected by EMSA, perhaps because of lower affinity or requirement of additional *cis* elements.

STAT Activation Induces MiR-146b in Non-transformed But Not Cancer Cells

To investigate the regulation of miR-146b in normal physiology, we examined mouse mammary epithelium at various developmental stages, due to well-characterized STAT activation in this setting and the tissue origin of MCF-10A cells. Prominent induction of miR-146b, but not miR-146a, occurred throughout late pregnancy, lactation, and involution (Figure 2.3A), paralleling recognized patterns of STAT phosphorylation and target gene expression (Figure 2.3B). By contrast, a panel of breast cancer cell lines with constitutive STAT3 activation (29) did not have increased miR-146b levels relative to unstimulated MCF-10A cells (Figure 2.3C).

Next, we analyzed a wide range of non-transformed and cancer cell lines lacking basal STAT activation for miR-146b induction upon cytokine treatment (Figure 2.4 and Supplemental Figure 1). Interestingly, miR-146b responsiveness was restricted almost entirely to the non-tumorigenic and non-transformed cell lines. This indicates STAT regulation of miR-146b is highly context-dependent, varying by cell line and cellular state.

To explain the striking disparity of miR-146b induction among different cells, we hypothesized that STAT regulation of miR-146b was modulated by additional factors. We investigated two possibilities: epigenetic regulation and participation of other signaling pathways.

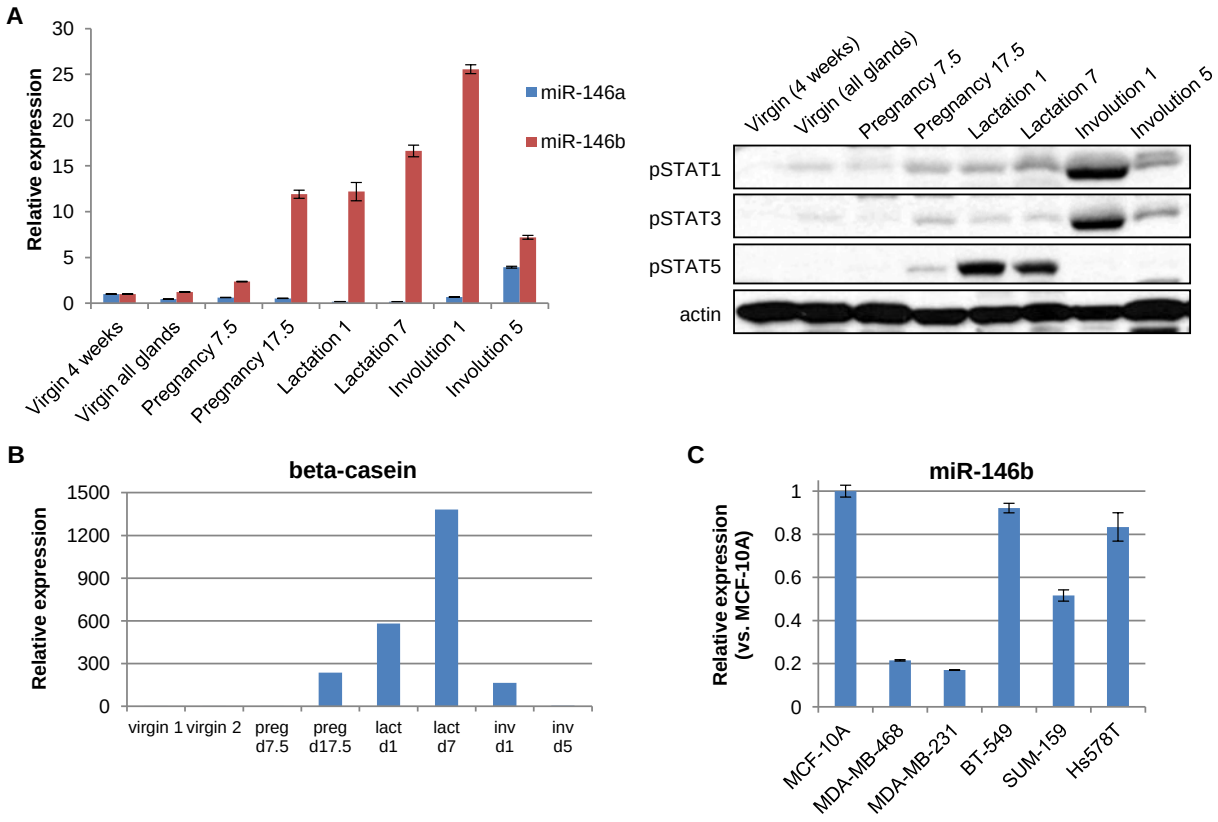

Figure 2.3: Analysis of STAT activity and miR-146b expression in physiology and cancer. (A) Mouse mammary epithelial tissue from the indicated developmental stages was analyzed for expression of miR-146a and -146b relative to virgin 4 weeks (left) and for tyrosine phosphorylation of STAT1, STAT3, STAT5 (right). (B) Expression of the STAT5 target gene beta-casein was measured in the same samples as in panel A. Similar results were obtained with the STAT3 target gene SOCS3 (data not shown). (C) MiR-146b expression was measured in 5 breast cancer cell lines with constitutively-active STAT3 (29) and graphed relative to unstimulated MCF-10A cells. U6 snRNA was used to normalize between different cell lines.

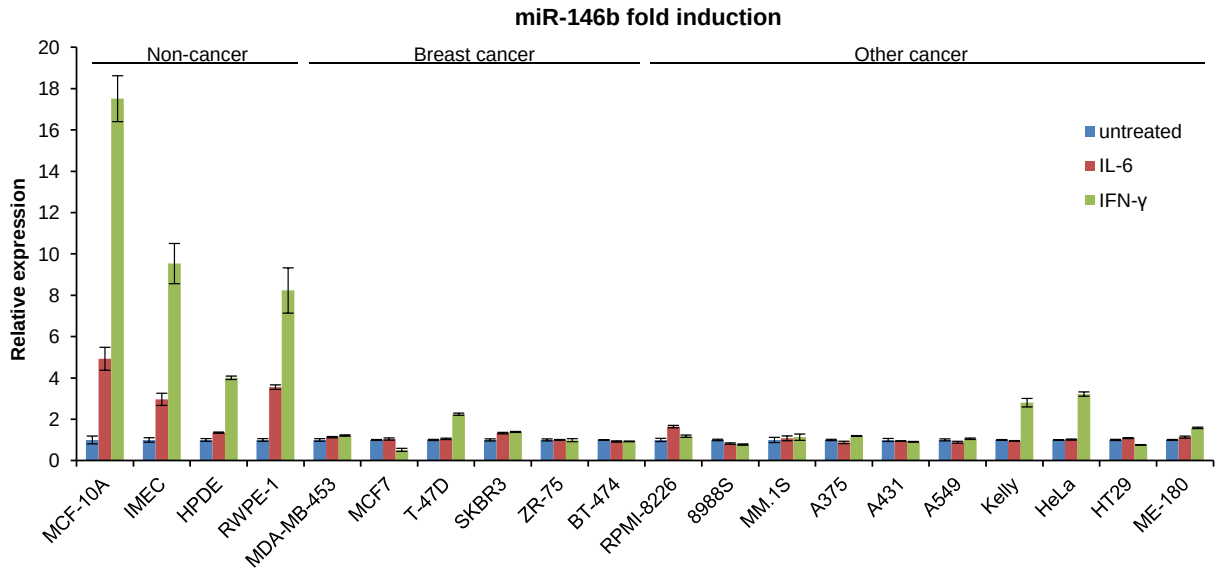

Figure 2.4: STAT activation preferentially induces miR-146b in non-transformed cells compared to cancer cells. The induction of miR-146b in these cell lines, which lack basal STAT activation, was measured after 48hr cytokine treatment. Western blot was performed to confirm STAT activation by cytokine treatment (Supplemental Figure 1 and data not shown).

DNA Methylation Inhibits Mir-146b Expression *In Vitro* and *In Vivo*

Given the role of DNA methylation in suppressing gene expression in tumor cells, we asked whether methylation inhibits STAT3 activity at the miR-146b promoter. To address this possibility, we first treated the miR-146b luciferase reporter with a CpG methyltransferase. Methylation of this construct decreased its responsiveness to STAT3C by 70% (Figure 2.5A). Next, we examined the effect of methylation on endogenous miR-146b expression in breast cancer cell lines with JAK-dependent constitutive STAT3 activation (29). Treatment of these cells with the demethylating agent 5-azacytidine induced both mature miR-146b and its primary transcript (Figure 2.5B). Importantly, the induction was negated by co-treatment with a JAK inhibitor, demonstrating that both demethylation and STAT3 activity were necessary. Additionally, this pattern mirrored that of SOCS3 (Figure 2.6B), which is a STAT3-dependent negative regulator frequently hypermethylated in cancer (35).

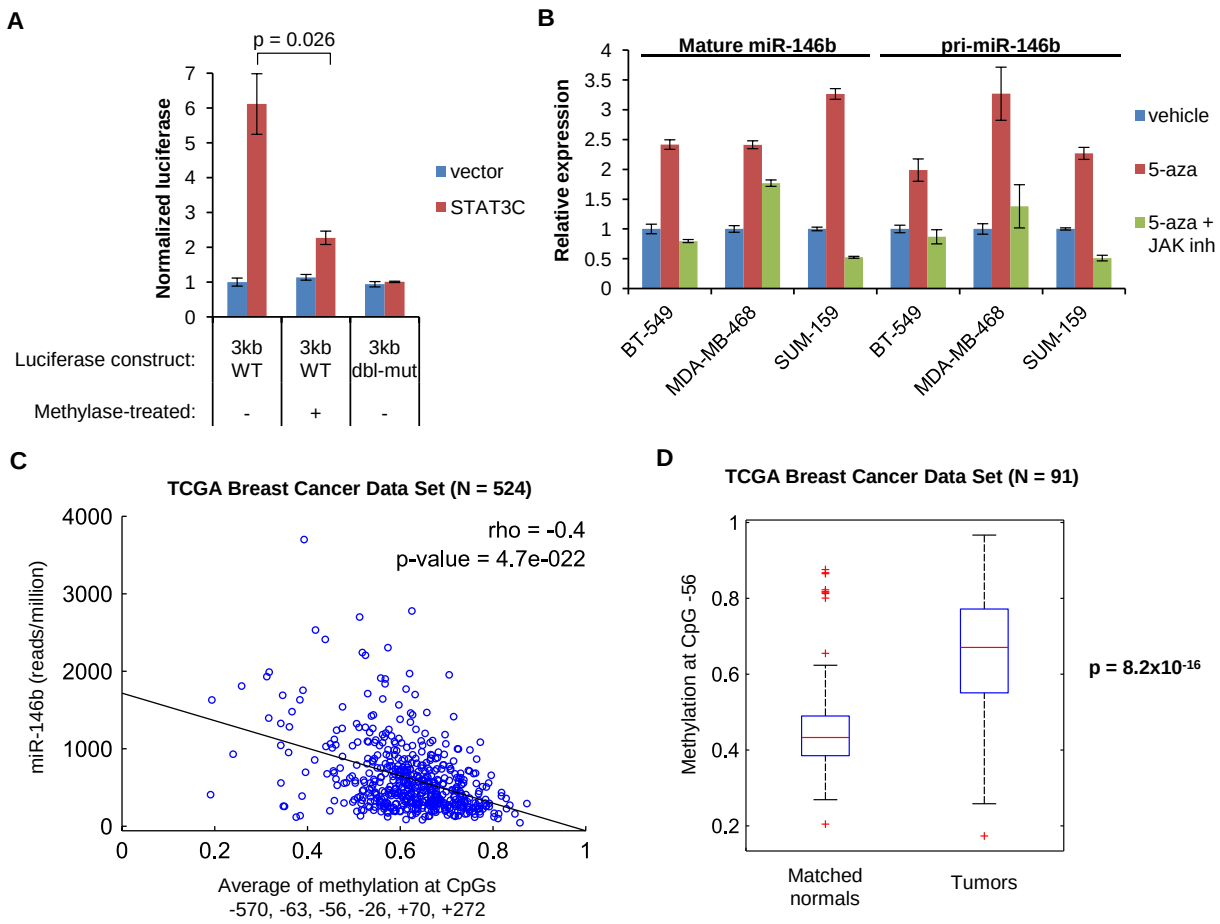

Figure 2.5: DNA methylation counteracts STAT3 activity at the miR-146b promoter and inhibits miR-146b expression *in vitro* and *in vivo*. (A) Luciferase activity of the miR-146b reporter construct, assessed 24hr post-transfection in MCF-10A transduced with STAT3C, was inhibited by prior treatment with SssI methylase. Methylation was confirmed by protection of plasmid from HpaII digestion (Figure 2.6A). (B) Expression of primary and mature miR-146b increased in breast cancer cells with constitutive STAT3 activation after demethylation by 5-azacytidine, but not in combination with JAK inhibitor. (C) Correlation of miR-146b expression and miR-146b promoter CpG methylation in 524 breast cancer samples from The Cancer Genome Atlas (TCGA) (Pearson and least-squares regression line). (D) MiR-146b promoter methylation was increased in TCGA breast cancer samples compared to corresponding matched normal breast tissue; N = 91 (rank-sum test).

To extend these findings to primary tumors, we utilized The Cancer Genome Atlas (TCGA). This database contains over 500 breast cancer samples with methylation of 485,000 CpGs measured at single-nucleotide resolution. Methylation at the 6 CpGs closest to miR-146b was strongly inversely correlated with expression of miR-146b (Figure 2.5C and 2.6C), but not

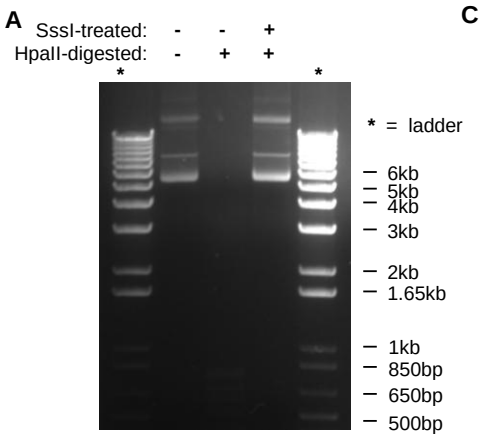

C

BP to miR-146b stem-loop	rho	p-value	BP to miR-146b stem-loop	rho	p-value
-8033	-0.05	0.2351	-2906	-0.16	0.0003
-4303	-0.14	0.0018	-2534	-0.16	0.0005
-4116	-0.15	0.0008	-1426	0.02	0.6190
-4030	-0.07	0.1175	-898	-0.20	1.23×10^{-5}
-3950	-0.01	0.8732	-570	-0.32	6.94×10^{-13}
-3832	-0.14	0.0018	-63	-0.35	3.83×10^{-15}
-3807	-0.12	0.0066	-56	-0.37	2.01×10^{-17}
-3790	-0.15	0.0008	-26	-0.32	8.34×10^{-13}
-3777	-0.13	0.0046	+70	-0.36	2.07×10^{-16}
-3762	-0.14	0.0015	+272	-0.31	3.38×10^{-12}
-3750	0.00	0.9590	+10070	-0.02	0.6794

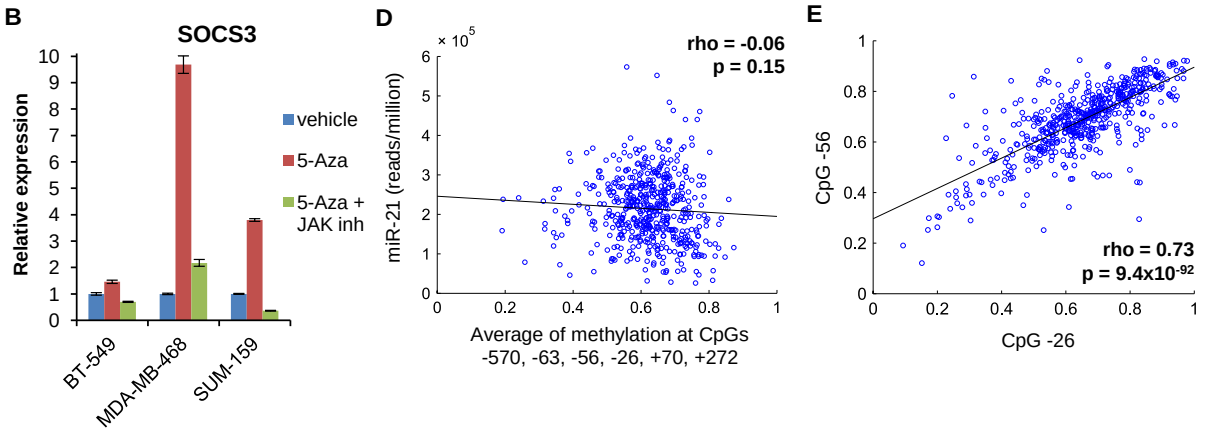

Figure 2.6: Further characterization of miR-146b and role of methylation. (A) SssI-treated plasmid DNA was resistant to digestion by methylation-sensitive HpaII restriction enzyme. (B) Experiment performed as in Figure 2.5B, but with analysis of SOCS3 expression. (C) Correlation between miR-146b expression and extent of CpG methylation at 22 CpGs within 10kb of miR-146b interrogated by Illumina 450k profiling in TCGA. Sites highlighted in blue indicate a highly significant inverse correlation. (D) Lack of correlation between CpG methylation at the miR-146b locus and miR-21 expression. (E) Strong positive correlation between CpG sites near miR-146b, indicating coordinate regulation in this region.

miR-21, an irrelevant STAT3 target (Figure 2.6D). Also, methylation among the 6 sites was highly correlated with one another (Figure 2.6E), indicating that they are coordinately regulated. Lastly, methylation of miR-146b was significantly higher in tumors relative to matched normal breast tissue (Figure 2.5D), supporting the role of miR-146b as a negative regulator and tumor suppressor.

Interestingly, 5-azacytidine treatment of cancer cell lines lacking STAT activation did not confer inducibility of miR-146b upon cytokine stimulation (data not shown). Therefore, we hypothesized that other mechanisms could modulate STAT regulation of miR-146b.

STAT Regulation of MiR-146b Is Potentiated by the MAPK Pathway

For several reasons, we hypothesized that MAPK signaling could modulate STAT regulation of miR-146b. First, the MAPK pathway is known to regulate miR-146b via direct binding of c-fos to the miR-146b promoter at a site about 600bp upstream of the distal STAT site (201). Second, MCF-10A cells, which show robust induction of miR-146b upon STAT activation, are grown in media containing epidermal growth factor (EGF) and insulin, both of which can activate MAPK.

Interestingly, treatment with EGF or insulin rendered miR-146b much more responsive to cytokine stimulation and STAT activation in cells that normally exhibit little or no miR-146b induction (Figure 2.7A). By contrast, induction of other STAT3 target genes, such as SOCS3 and STAT3 itself, was not enhanced (Figure 2.7B). Similarly, EGF specifically potentiated the induction of the miR-146b luciferase reporter, while induction of an unrelated STAT3-responsive reporter, m67 luciferase, was unaltered (Figure 2.7C).

To understand the mechanism of potentiation, we analyzed the phosphorylation of STAT3 and MAPK following IL-6 stimulation. When EGF or insulin was present, MAPK activation was much more prominent and sustained, while there was no change in the tyrosine or serine phosphorylation of STAT3 (Figure 2.7D). Furthermore, the MEK inhibitor U0126 abrogated EGF potentiation of miR-146b induction, while the PI3K inhibitor LY294002 had no

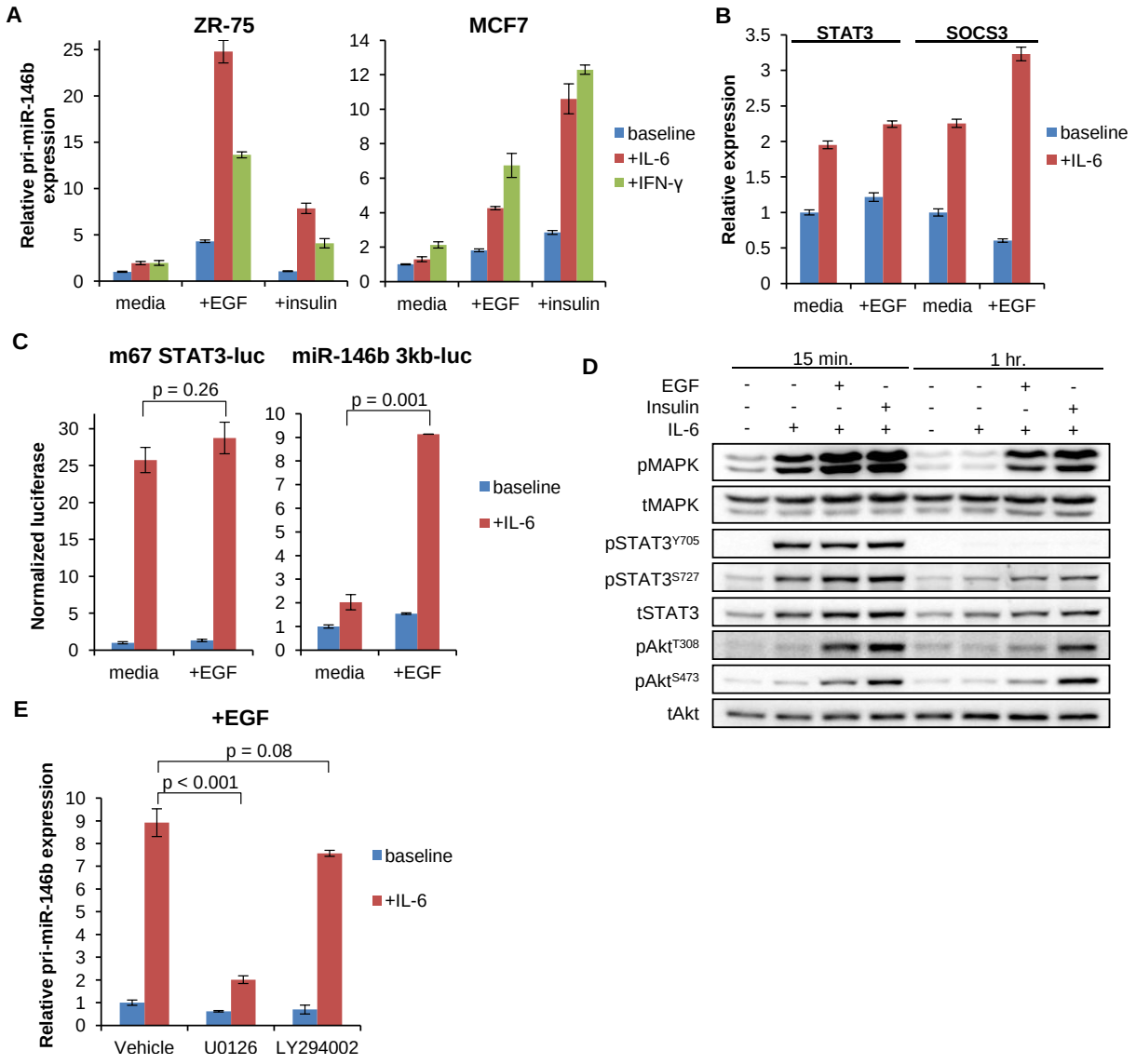

Figure 2.7: STAT regulation of miR-146b is potentiated by the MAPK pathway. (A) Expression of miR-146b primary transcript in ZR-75 and MCF7 breast cancer cell lines following 3hr treatment with IL-6 or IFN-γ (20ng/ml), in base media only or with addition of EGF (100ng/ml) or insulin (10µg/ml). (B) Expression of STAT3 target genes in ZR-75 cells following 3hr treatment with IL-6 in base media only or with addition of EGF. (C) Luciferase activity of a canonical STAT3 reporter construct (m67, left) or miR-146b reporter construct (right) in ZR-75 cells after 6hr IL-6 stimulation in base media only or with addition of EGF. (D) Immunoblot of ZR-75 cells, untreated or treated with IL-6, alone or in combination with EGF or insulin, for 15 minutes and 1 hour. (E) Expression of miR-146b primary transcript in ZR-75 cells pre-treated for 1 hour with the indicated inhibitors, then treated with EGF ± IL-6.

effect (Figure 2.7E). These data establish the MAPK pathway as a potentiator of STAT regulation of miR-146b.

MiR-146b Opposes NF-κB to Inhibit Autocrine IL-6-Dependent STAT3 Activity

Having characterized the STAT3-dependent regulation of miR-146b, we next considered the biological significance of miR-146b as a STAT3 target gene. It is known that miR-146b targets TRAF6 and IRAK1, which serve to activate NF-κB (199). Accordingly, transfection of a miR-146b mimic repressed TRAF6 and IRAK1 across multiple breast cancer cell lines (Figure 2.8C and 2.9A). To determine whether induction of endogenous miR-146b could have the same effect, MCF-10A cells were treated with IL-6 or IFN-γ, which also led to repression of TRAF6 and IRAK1 (Figure 2.9B). This effect was blunted by transfection of a miR-146b inhibitor, showing that it was dependent on induction of miR-146b. Thus, STAT-mediated upregulation of endogenous miR-146b was able to recapitulate the effects of miR-146b mimic.

Since IRAK1 and TRAF6 are upstream of NF-κB, we next examined the effect of miR-146b on NF-κB activity in several breast cancer cell lines with constitutively-active NF-κB. The miR-146b mimic caused marked downregulation of all NF-κB target genes tested (Figure 2.8A), indicating substantially suppressed NF-κB activity. Among the downregulated genes is IL-6, which can activate STAT3 in an autocrine fashion. Therefore, we hypothesized that miR-146b functions to inhibit NF-κB-dependent IL-6 expression, leading to dampened STAT3 activity.

We first determined if STAT3 activation results from NF-κB-dependent IL-6 expression by using siRNA to knock down IL-6 or the NF-κB subunit RelA in SUM-159 cells. Both siRNAs reduced IL-6 expression, STAT3 tyrosine phosphorylation, and STAT3 target gene expression (Figure 2.8B). STAT3 tyrosine phosphorylation was also abolished by treatment with

a pharmacological JAK inhibitor or a neutralizing antibody to IL-6 (Figure 2.8C), further underscoring the role of autocrine IL-6 in activating STAT3.

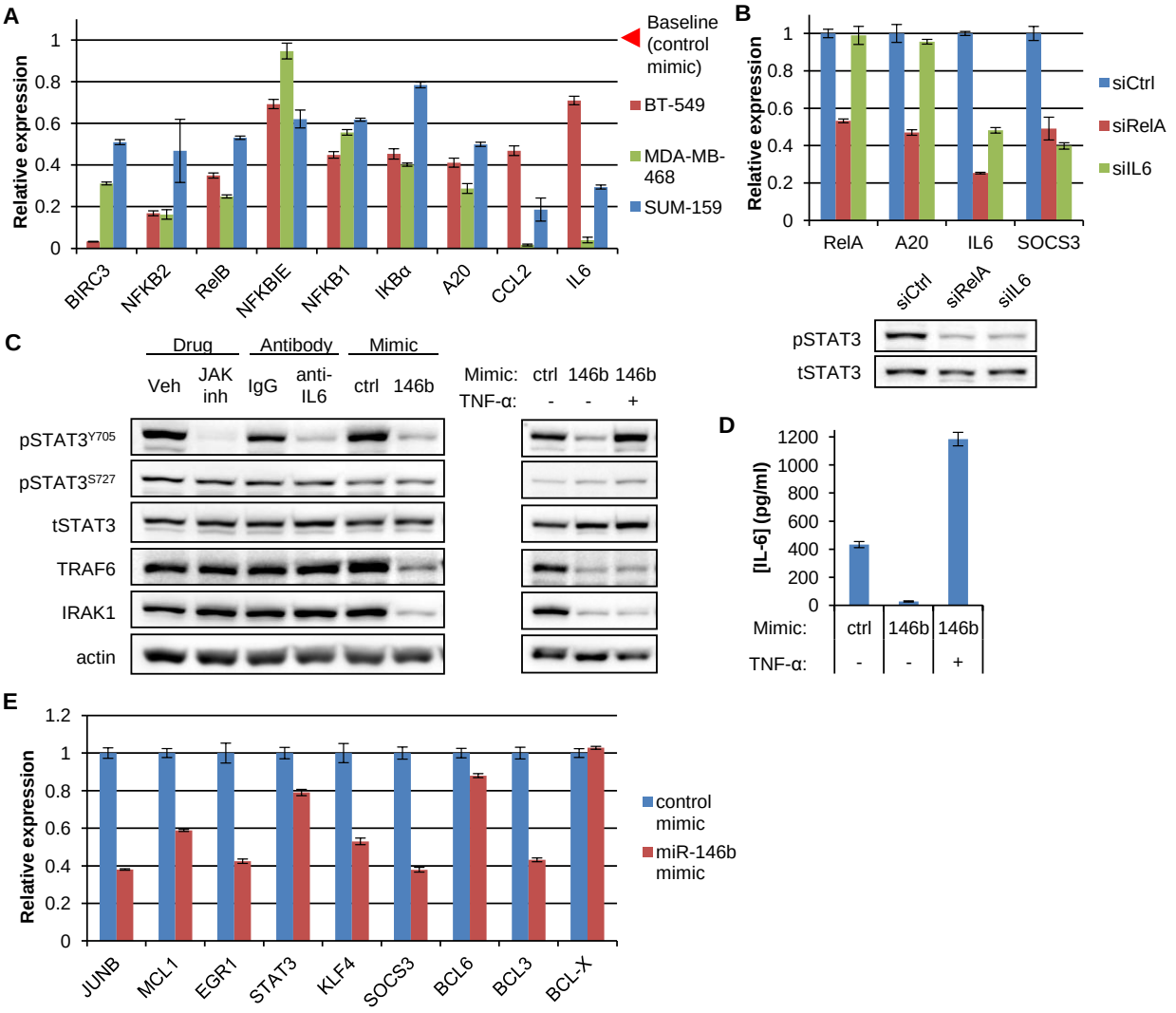

Figure 2.8: MiR-146b inhibits NF-κB-dependent IL-6 expression and autocrine IL-6-dependent STAT3 activation. (A) NF-κB target gene expression was depressed in 3 breast cancer cell lines after miR-146b mimic transfection (72hr) relative to control mimic in each respective cell line. (B) IL-6 expression and STAT3 activation are dependent on NF-κB. Gene expression and STAT3 phosphorylation (Tyr705 immunoblot) were assessed in SUM-159 cells 72hr after transfection with the indicated siRNA constructs. (C) Left: Phospho-STAT3 was diminished in SUM-159 cells treated with JAK inhibitor (2hr), IL-6 neutralizing antibody (6hr), or miR-146b mimic transfection (72hr). Right: In cells transfected with miR-146b mimic, phospho-STAT3 was rescued by simultaneous treatment with TNF-α (5ng/ml). (D) MiR-146b mimic inhibits IL-6 secretion into conditioned medium measured by ELISA (mean ± SD). (E) Diminished expression of STAT3 target genes in SUM-159 cells 72hr after transfection with miR-146b mimic.

Importantly, miR-146b mimic inhibited autocrine IL-6 protein secretion, STAT3 tyrosine phosphorylation, and expression of a large panel of STAT3 target genes (Figure 2.8C-E). Alternative activation of NF-κB by TNF-α, which is independent of TRAF6 and IRAK1, reversed all of these effects (Figure 2.8C-D and 2.9C). These findings establish the role of miR-146b as an inhibitor of NF-κB-dependent STAT3 activity.

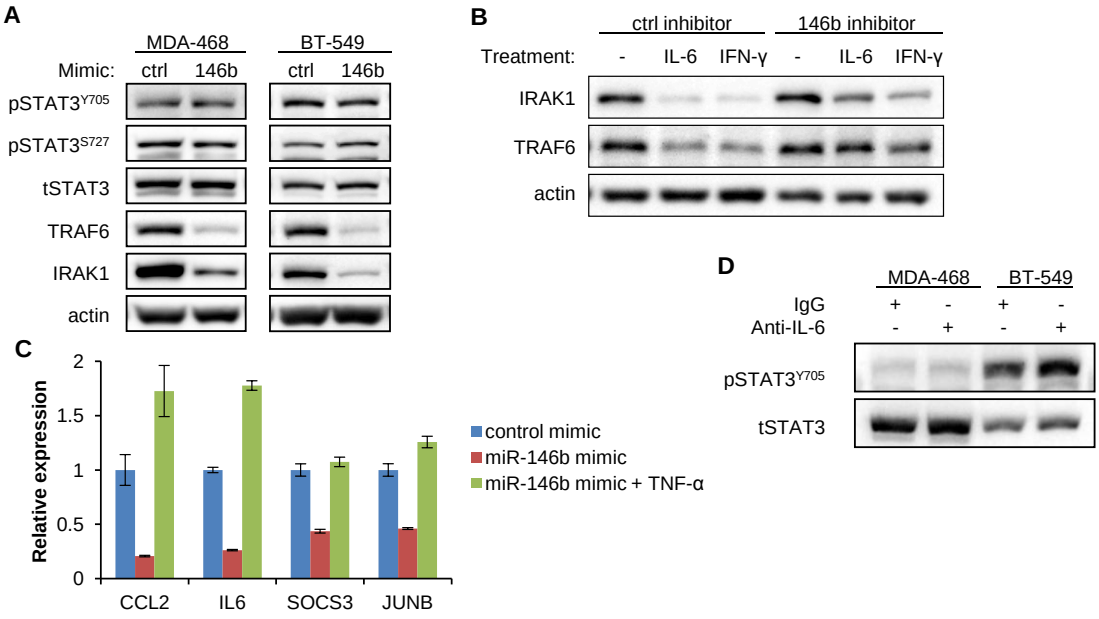

Figure 2.9: Further characterization of effects of miR-146b and IL-6 neutralizing antibody on IRAK1, TRAF6, and STAT3. (A) MDA-MB-468 and BT-549 cells have constitutively-active STAT3. TRAF6 and IRAK1 protein, but not phospho-STAT3, were inhibited by miR-146b mimic (25nM for 72hr). (B) STAT-mediated upregulation of endogenous miR-146b is sufficient to repress IRAK1 and TRAF6. MCF-10A cells were transfected overnight with control or miR-146b inhibitor, then treated with IL-6 or IFN-γ for 72hr to induce miR-146b. (C) TNF-α rescues the decreased expression of NF-κB and STAT3 target genes in SUM-159 cells after transfection with miR-146b mimic. (D) In MDA-MB-468 and BT-549 cells, constitutive STAT3 phosphorylation is not affected by IL-6 neutralizing antibody.

In MDA-MB-468 and BT-549 cells, STAT3 phosphorylation was unaffected by IL-6 neutralizing antibody (Figure 2.9D), and IL-6 mRNA was substantially lower than in SUM-159 (data not shown); correspondingly, miR-146b mimic did not inhibit their level of STAT3

phosphorylation (Figure 2.9A). Thus, further characterization of miR-146b on STAT3-related phenotypes was focused in SUM-159 cells.

MiR-146b Inhibits IL-6/STAT3-Driven Migration, Invasion, and Mesenchymal Phenotype of Tumor Cells

Given that miR-146b inhibits autocrine IL-6-dependent STAT3 activity, we next asked: what are its functional effects in cancer cells? It is known that miR-146b decreases migration and invasion *in vitro* and metastasis *in vivo* (202-204). Conversely, STAT3 promotes migration and invasion (35). Therefore, we hypothesized that miR-146b inhibition of cell motility was at least partly mediated through suppression of IL-6-induced STAT3 activation.

In SUM-159 cells, miR-146b mimic caused striking defects in migration and invasion (Figure 2.10A-D) without substantially affecting cell viability (Figure 2.10F). To determine if these effects were specifically due to inhibition of STAT3 activity, STAT3C was introduced into cells to maintain STAT3 signaling independent of autocrine IL-6. Importantly, STAT3C rescued the miR-146b-induced motility defects by roughly 50%, indicating that the phenotype was substantially attributable to suppression of autocrine IL-6-mediated STAT3 activity.

Cell motility is associated with epithelial-to-mesenchymal transition (EMT), which is also promoted by STAT3 (82). Thus, we hypothesized that miR-146b inhibits the mesenchymal phenotype of SUM-159 cells. Indeed, miR-146b caused marked morphological changes (Figure 2.10E): individual cells became less spindle-shaped and more epithelial in appearance, while the overall population appeared more clustered, with increased cell-cell contacts. In addition, miR-146b caused gene expression changes consistent with transition to a more epithelial state (Figure 2.10G). Importantly, STAT3C opposed the morphological effects and some of the gene

expression changes of miR-146b. Overall, our data show that miR-146b inhibits IL-6/STAT3-driven migration, invasion, and EMT of cancer cells.

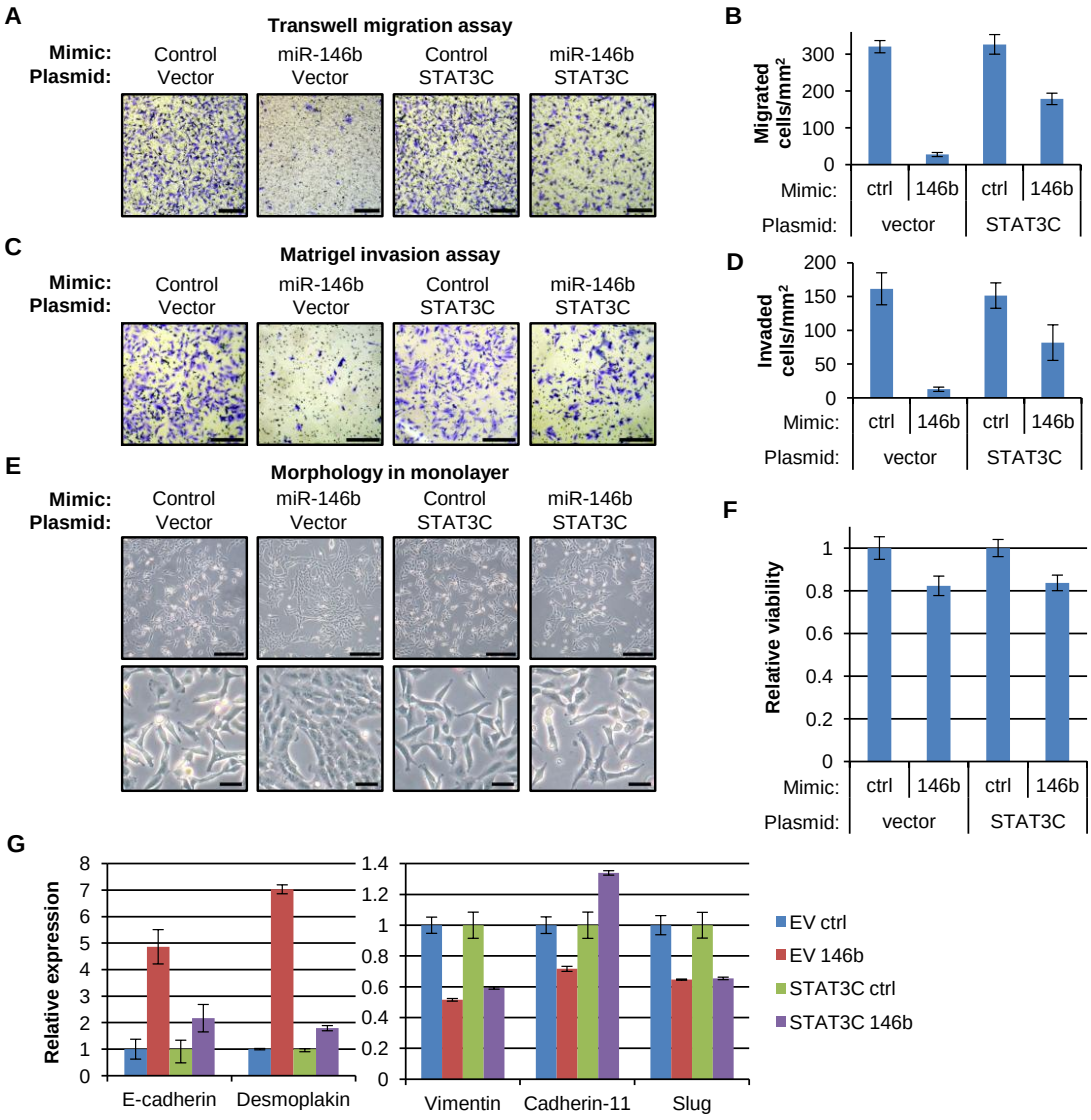

Figure 2.10: MiR-146b inhibits IL-6/STAT3-driven migration, invasion, and mesenchymal phenotype of cancer cells. (A-B) MiR-146b mimic inhibits transwell migration of SUM-159 cells, which is rescued by transduction of STAT3C. Scale bar, 250μm. (C-D) Experiment as in panels A-B but with Matrigel invasion assays. Scale bar, 250μm. (E) MiR-146b mimic confers epithelial morphology to SUM-159 cells, which is reversed by STAT3C. Scale bar, 250μm (upper) and 50μm (lower). (F) MiR-146b mimic did not substantially affect cell viability when cell motility was assayed, which was 48hr after transfection. (G) Expression of epithelial and mesenchymal markers in SUM-159 cells 72hr after mimic transfection.

JAK Inhibition and MiR-146b Repletion Have a Combinatorial Effect on Tumor Viability

JAK inhibitors are in investigational or clinical use for treating malignancies with constitutive STAT activation, including IL-6-dependent STAT3 activation (205). Treating SUM-159 cells with a pharmacological JAK inhibitor decreased their viability. However, by shutting off STAT3, JAK inhibition also substantially reduced expression of miR-146b (Figure 2.11A). Therefore, we hypothesized that JAK inhibition and miR-146b repletion together could exert a combinatorial effect on tumor viability. Indeed, the combination treatment had a greater effect than either agent alone (Figure 2.11B), perhaps because JAK inhibition by itself causes downregulation of STAT3-dependent negative regulators, such as miR-146b.

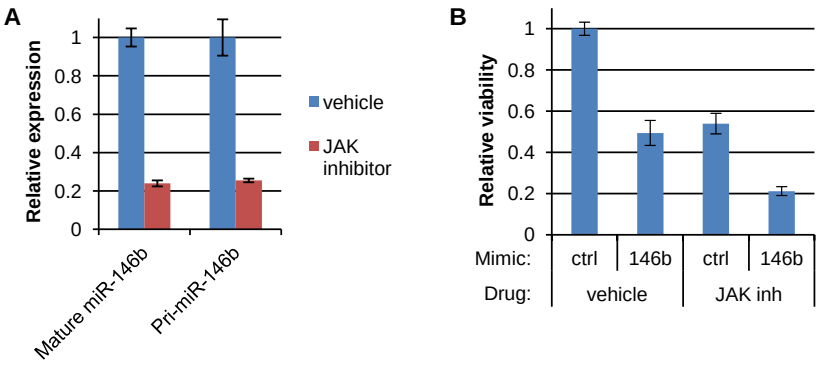

Figure 2.11: Effects of pharmacological JAK inhibition and miR-146b mimic, separately and in combination, on cancer cell viability. (A) JAK inhibition downregulates miR-146b in cells with constitutively-active STAT3. SUM-159 cells were treated with JAK inhibitor 1 (1μM) for 72hr. (B) Viability of SUM-159 cells treated with JAK inhibitor 1 (500nM), transfected with miR-146b mimic, or both after 96hr.

In Primary Breast Cancers, MiR-146b Level Correlates with Molecular Subtype, Patient Survival, and Degree of STAT3 Phosphorylation

Our data suggest that miR-146b forms a negative feedback circuit connecting STAT3 activation to decreased NF-κB activity and IL-6 production, thereby regulating STAT3 activation (Figure 2.12A). In breast cancer, ER negative tumors, including triple negative or basal-like

tumors, are most likely to have IL-6/STAT3 signaling (29, 206). This is consistent with the finding that IL-6 activation of STAT3 directly represses ERα (207) and the classification of SUM-159 cells as triple negative. In the TCGA cohort, ER negative and triple negative tumors displayed elevated IL-6 expression compared to other molecular subtypes (Figure 2.12B and 2.13A). Additionally, IL-6 expression was strongly correlated with expression of multiple NF-κB target genes (Figure 2.13B), suggesting that IL-6 expression in primary tumors is driven by NF-κB.

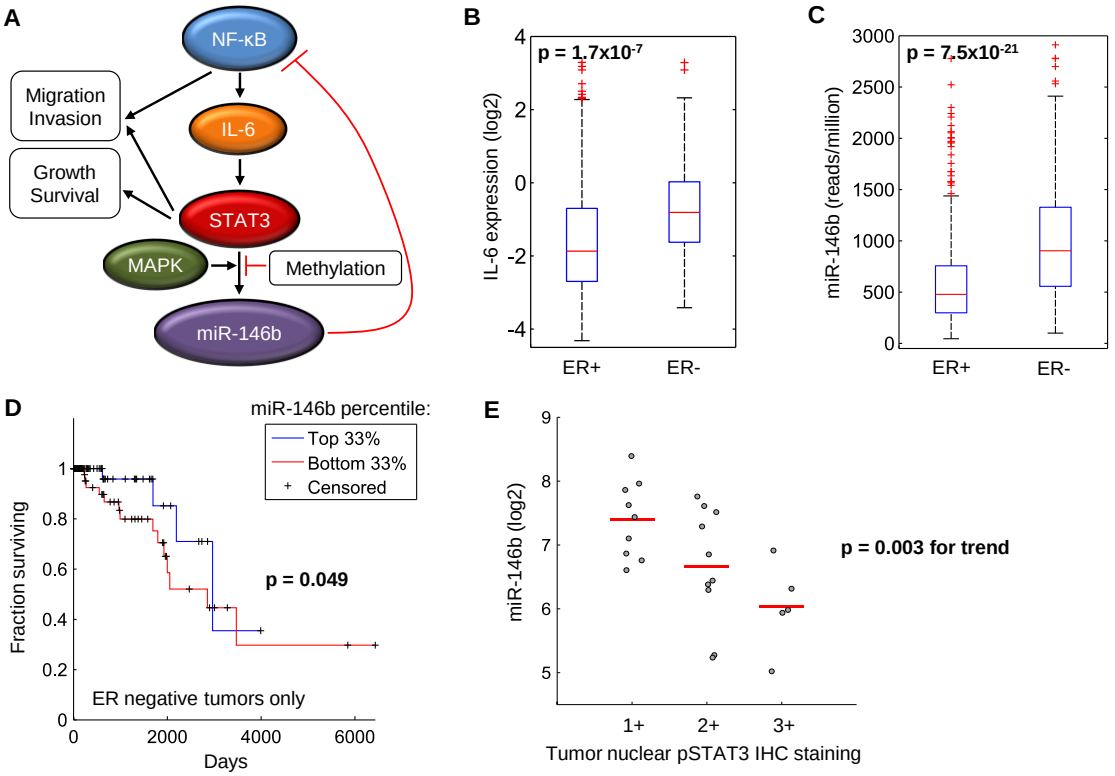

Figure 2.12: Significance of STAT3 regulation of miR-146b in human breast cancers. (A) Schematic of the proposed regulatory circuit integrating STAT3, miR-146b, NF-κB, and IL-6. (B-C) IL-6 and miR-146b expression in TCGA breast cancer samples according to ER status (rank-sum test). (D) Improved Kaplan-Meier survival curve of top tertile versus bottom tertile of miR-146b expression (read count per sample) in TCGA patients with ER negative breast cancer (log-rank test). (E) Inverse relationship of miR-146b expression and degree of STAT3 phosphorylation in invasive breast tumor specimens (N = 24) (Pearson correlation).

Interestingly, miR-146b expression was increased in ER negative and triple negative tumors compared to other breast cancer subtypes (Figure 2.12C and 2.13C), suggesting the transcriptional regulation of miR-146b is linked to the presence of STAT3 activation in primary tumors. To determine the clinical significance of miR-146b, we examined patient survival

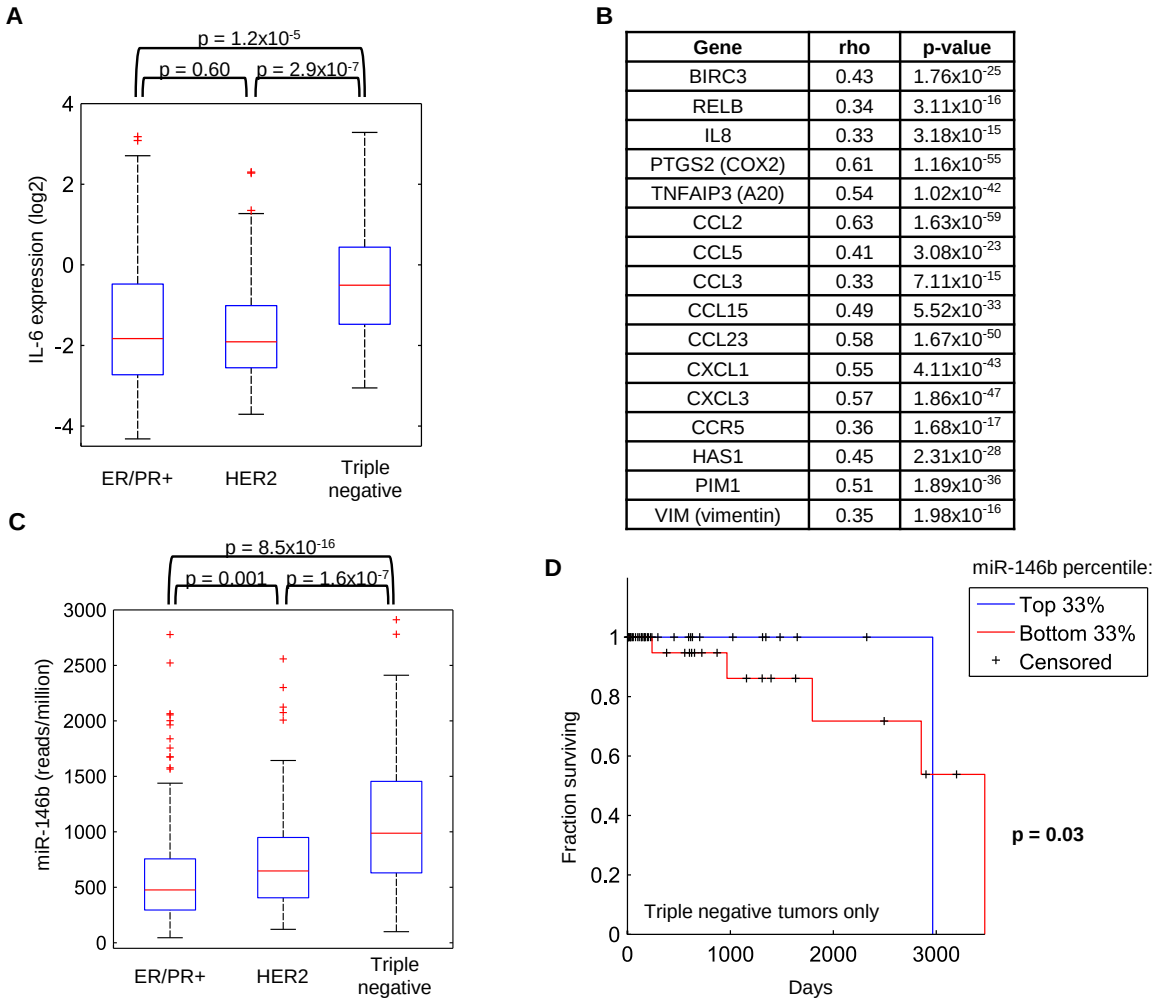

Gene	rho	p-value
BIRC3	0.43	1.76×10^{-25}
RELB	0.34	3.11×10^{-16}
IL8	0.33	3.18×10^{-15}
PTGS2 (COX2)	0.61	1.16×10^{-55}
TNFAIP3 (A20)	0.54	1.02×10^{-42}
CCL2	0.63	1.63×10^{-59}
CCL5	0.41	3.08×10^{-23}
CCL3	0.33	7.11×10^{-15}
CCL15	0.49	5.52×10^{-33}
CCL23	0.58	1.67×10^{-50}
CXCL1	0.55	4.11×10^{-43}
CXCL3	0.57	1.86×10^{-47}
CCR5	0.36	1.68×10^{-17}
HAS1	0.45	2.31×10^{-28}
PIM1	0.51	1.89×10^{-36}
VIM (vimentin)	0.35	1.98×10^{-16}

Figure 2.13: In the TCGA breast cancer cohort, levels of IL-6 and miR-146b are higher in triple negative breast cancers compared to other molecular subtypes, and higher absolute miR-146b levels are associated with longer survival in the subset of triple negative breast cancers. (A) Analysis performed as in Figure 2.12B, but comparing triple negative breast cancers to other molecular subtypes. (B) Positive correlation of IL-6 expression with the indicated NF-κB target genes across all breast tumors. (C) Analysis performed as in Figure 2.12C, but comparing triple negative breast cancers to other molecular subtypes. (D) Analysis performed as in Figure 2.12D, but in the specific subset of triple negative breast cancers.

according to miR-146b expression. Higher levels of miR-146b were associated with superior overall survival in the subset of patients with ER negative (Figure 2.12D) or triple negative tumors (Figure 2.13D), but not in other subtypes or across all tumors.

The survival association of miR-146b specifically in tumor subtypes linked to IL-6/STAT3 signaling suggested that the impact of miR-146b in human cancer may be exerted mainly through modulation of STAT3, similar to our findings in SUM-159 cells. To investigate this possibility, we studied a cohort of invasive breast cancers demonstrated to have tyrosine-phosphorylated STAT3 in the nucleus by immunohistochemistry. Interestingly, miR-146b expression was highest in tumors with low-level STAT3 phosphorylation and decreased with increasing intensity of phospho-STAT3 staining (Figure 2.12E). Thus, miR-146b may modulate STAT3 phosphorylation *in vivo*, become subverted in tumors with high-level STAT3 activation, or both, further supporting the functional interplay between miR-146b and STAT3 in primary tumors.

DISCUSSION

This work represents the first genome-wide survey of miRNA expression changes associated with specific and focused activation of STAT3, which was achieved using inducible expression of STAT3C. Although several STAT3 miRNA targets have been reported in the literature, miR-21 was the only previous target to be identified in our screen. This suggests that the miRNA targets of STAT3 are highly context-dependent, varying according to differences in epigenetic marks and chromatin structure, expression of transcriptional cofactors, activity of other signaling pathways, and time point. Likewise, induction of miR-146b was concentrated almost exclusively in non-tumorigenic and non-transformed cells (Figure 2.4).

Generally, miR-146b has emerged as a negative regulator of cancer processes. The same is true of miR-146a. Although STATs do not regulate miR-146a, it shares overlapping targets with miR-146b owing to an identical seed region. Thus, functional effects for miR-146b may be inferred from studies of miR-146a. In the context of breast cancer, both miR-146 isoforms decrease tumor cell motility by targeting IRAK1 and TRAF6 to inhibit NF-κB (202). Moreover, miR-146a and miR-146b inhibit metastasis of breast cancer cells *in vivo* (203). Similar tumor suppressor effects have also been demonstrated in glioblastoma (204, 208), pancreatic cancer (209), gastric cancer (210), and androgen-independent prostate cancer (211, 212). These studies have identified MMP16, EGFR, and ROCK1 as additional mRNA targets of miR-146a and miR-146b.

Despite these functional data, the transcriptional regulation of miR-146b has remained poorly understood. Up until now, c-fos was the only factor characterized to regulate miR-146b at a molecular level (201). Unlike nearly all other known STAT3 targets, miR-146b is a tumor suppressor, and its regulation by STAT3 may seem surprising since STAT3 is generally regarded

as oncogenic. However, several precedents exist for other STAT3-induced negative regulators. A classic example of negative feedback is SOCS3, which inhibits cytokine and growth factor signaling, thereby dampening STAT3 activation. Additionally, STAT3 can induce miR-125b and the miR-17/92 cluster, which can target STAT3 itself (132, 144, 149).

Intriguingly, these factors and miR-146b share the common property of inhibiting STAT3 activity, either directly or indirectly. Thus, STAT3-dependent negative regulators of STAT3 itself may be central to the proper temporal control of STAT3 activity, which in turn is crucial to prevent normal STAT3 activation from becoming an oncogenic event. Since the dysregulation of negative regulators can shift the net effect of pathway activation toward oncogenicity, understanding the negative regulators, such as miR-146b, is crucial to fully understanding the role of STAT3 in cancer pathogenesis.

Similar to SOCS3, miR-146b is a STAT3-regulated feedback inhibitor prone to hypermethylation in tumors, supporting its role as a tumor suppressor *in vivo*. Suppression of SOCS3 expression in cancer contributes to the constitutive nature of STAT3 activation, which is transient and tightly regulated in normal cells (35). Thus, the same paradigm for SOCS3 may also hold true for miR-146b. Despite increased promoter methylation, miR-146b expression was not significantly reduced in tumors relative to normal tissue (data not shown). This may be due to activation of pathways in cancer cells that upregulate miR-146b, such as STAT3 and MAPK, which act in opposition to methylation-related downregulation.

STAT regulation of miR-146b, but not other STAT targets, is potentiated by MAPK signaling. Since c-fos mediates MAPK regulation of miR-146b (201), MAPK potentiation is also likely due to c-fos or related family members, which may act as pioneer factors for this region of chromatin. Analysis of Fos and Jun family member expression in the TCGA data set revealed a

significant positive correlation between miR-146b and *FOSL1* (rho = 0.29, $p = 3.5x10^{-11}$). Of note, insulin differs from EGF in a few respects: unlike EGF, its effect is blocked by PI3K inhibition, and it also activates PI3K/Akt with higher magnitude and duration (Figure 2.7D). Therefore, FOSL1 and PI3K/Akt signaling may be additional mechanisms of miR-146b regulation.

The relationship between STAT3 and NF-κB is complex, and many modes of crosstalk have been demonstrated (213, 214). For example, STAT3 is known to positively regulate NF-κB by promoting p300-dependent acetylation of RelA, which increases nuclear retention (215). In the present study, our results show miR-146b to be a novel mediator of inhibitory crosstalk between STAT3 and NF-κB. We posit that STAT3 regulation of miR-146b normally prevents unchecked STAT3 activation from taking hold in the setting of cell-autonomous NF-κB and IL-6 signaling. However, in cancer, this negative feedback mechanism is at least partially subverted, permitting the growth and progression of tumors dependent on the NF-κB/IL-6/STAT3 pathway.

Multiple lines of evidence support this model. First, STAT3 and NF-κB are frequently co-activated in tumors (215), and NF-κB-dependent IL-6 is a major driver of STAT3 activation in cancer. Second, miR-146b is readily inducible in non-transformed but not cancer cells. Third, miR-146b is repressed by promoter methylation, which is increased in tumor samples compared to normal tissue. Fourth, miR-146b inhibits multiple tumorigenic phenotypes in cancer cells with activation of the NF-κB/IL-6/STAT3 pathway. Fifth, higher miR-146b expression is associated with reduced STAT3 phosphorylation in primary tumors and improved patient survival.

While our work involved mostly models of breast cancer, the high interdependence between STAT3 and NF-κB suggests a broad role for miR-146b as a key STAT3-regulated tumor suppressor. For example, persistent activation of NF-κB and STAT3 via IL-6 can trigger

neoplastic transformation (191). Thus, STAT3 induction of miR-146b may be a feedback inhibitor of NF-κB-mediated tumorigenesis. In other cases, STAT3 activation is the primary event and facilitates oncogenic NF-κB activation (207, 216). In this context, concomitant miR-146b induction may ensure NF-κB activity does not cross the oncogenic threshold. This network motif is an incoherent feed-forward loop, which reduces biological noise and is especially suited to miRNA mediators (217).

Additionally, the NF-κB/IL-6/STAT3 signaling cascade is active and crucial in multiple tumor types, implicating a tumor suppressor role for miR-146b in these situations as well. One prominent example is colitis-associated cancer (CAC) (106, 197). STAT3 activation is an important early event in CAC development (106, 107). Interestingly, miR-146b is upregulated in the transition from normal tissue to dysplasia, but downregulated as dysplasia progresses to CAC (218). This suggests miR-146b is competently induced by activated STAT3 in early lesions, but becomes dysregulated during CAC progression, which may facilitate tumor growth.

NF-κB, IL-6, and STAT3 are important to breast cancer biology (29, 219); thus, miR-146b and the regulatory circuit linking these factors are likely to be significant in human cancer. First, a tumor suppressor role for miR-146b in primary tumors is supported by our finding of miR-146b promoter hypermethylation in that setting. Second, miR-146b expression was positively associated with patient survival in tumors linked to IL-6/STAT3 signaling, which agrees with our functional studies in SUM-159 cells. Third, miR-146b expression was lowest in tumors with the highest level of phosphorylated nuclear STAT3, indicating it may become subverted in those cells. Therefore, multiple lines of evidence from human tumors indicate that miR-146b functionally interacts with STAT3 in a clinically significant manner.

While delivery of miR-146b in humans is not yet clinically feasible, alternate strategies to achieve a similar goal include upregulation of endogenous miR-146b using demethylating agents or developing small molecules to target the key, potentially druggable targets of miR-146b, such as IRAK1. Our work suggests that therapies to inhibit JAK/STAT signaling and reconstitute miR-146b activity may be combined for enhanced clinical benefit, particularly for triple-negative breast cancers, which have relatively poor prognosis and limited treatment options.

Accumulated evidence has shown that inflammation can promote cancer (220), yet this is still a rare event. Clearly, for inflammation to switch from being benign to oncogenic, specific genetic and epigenetic perturbations must occur. Our study elucidates a negative feedback circuit involving STAT3, miR-146b, NF-κB, and IL-6 with significance to human cancer and clinical outcomes, thus adding to our understanding of how inflammatory networks are regulated in normal and neoplastic tissue.

MATERIALS AND METHODS

Cell Lines and Tissue Culture

MCF-10A cells were obtained from ATCC and cultured as previously described (221). RWPE-1 cells were obtained from ATCC and cultured in Keratinocyte Serum-Free Medium (Invitrogen). BT-474 cells were obtained from ATCC and cultured in RPMI-1640 + 10% FBS. Immortalized mammary epithelial cells (IMEC) were a kind gift of Dr. Myles Brown and grown as previously described (222). Immortalized human pancreatic duct epithelial cells (HPDE) were a kind gift of Dr. Ming Tsao and cultured as previously described (223). SUM-159 cells were a kind gift of Dr. Kornelia Polyak and grown in a 1:1 mix of DMEM/F12 + 10% FBS and Mammary Epithelial Cell Growth Medium (Lonza). T-47D, SKBR3, MCF7, MDA-MB-468, BT-549, and RPMI-8226 cells were obtained and cultured as previously reported (186, 224, 225). All other cell lines were graciously provided by the investigators and grown as indicated in Table 2.1. All cells were maintained in a humidified incubator at 37°C with 5% CO_2.

Table 2.1: Source and growth media of cell lines used in this study

Cell Line	Investigator	Growth Media
8988S	Dr. Ronald Depinho	DMEM+10% FBS
MDA-MB-453	Dr. Lindsay Harris	RPMI-1640+10% FBS
ZR-75	Dr. Lindsay Harris	DMEM+10% FBS
MM.1S	Dr. Kenneth Anderson	RPMI-1640+10% FBS
A431	Dr. Martin Hemler	DMEM+10% FBS
A375	Dr. James Mier	RPMI-1640+10% FBS
A549	Dr. Pasi Janne	RPMI-1640+10% FBS
Kelly	Dr. Rani George	RPMI-1640+10% FBS
HeLa	Dr. Ronny Drapkin	DMEM+10% FBS
HT29	Dr. David Pellman	McCoy's 5A+10% FBS
ME-180	Dr. Miriam Barshak	RPMI-1640+10% FBS

Generation of MCF-10A and SUM-159 cells with constitutive expression of STAT3C was achieved by retroviral transduction with pLNCX2 (Clontech) containing STAT3C-FLAG insert. MCF-10A cells expressing dominant-negative STAT3 were generated by transduction with pLNCX2 containing STAT3-Y705F-FLAG insert. MCF-10A cells expressing dominant-negative STAT1 were generated by transduction with pQCXIP (Clontech) containing STAT1-Y701F-FLAG insert. SUM-159 cells expressing STAT3C were generated by transduction with pLNCX2 containing STAT3C-FLAG insert. Cells were selected with G418 (500μg/ml) or puromycin (2μg/ml) according to the selection marker on the vector.

High-throughput MicroRNA Screen

Doxycycline-inducible MCF-10A cells were generated by retroviral transduction with pRevTet-On and pRevTRE (Clontech) containing STAT3C-FLAG or STAT5a1*6-FLAG as the insert, then selected in hygromycin (250μg/ml) and G418 (500μg/ml). Cells were untreated or doxycycline-treated (2μg/ml) in triplicate for 48hr prior to RNA processing using the miRNeasy Mini Kit (Qiagen). The time point was chosen due to the kinetics of STAT3C induction, observation of miR-21 upregulation, and previous reports of miRNA maturation requiring 12-24hr (128). The screen was performed at the Molecular Diagnostics Laboratory of Dana-Farber Cancer Institute using a TaqMan quantitative real-time PCR (qRT-PCR)-based platform covering approximately 700 miRNAs. Results are deposited under GEO Accession: GSE44089.

Total RNA Isolation

Cell pellets were lysed in 270μl RLT Plus buffer + 1% β-mercaptoethanol and processed by QIAshredder and genomic DNA eliminator spin columns. The flow-through was mixed with

460µl 95% ethanol by pipetting up and down, and then run through an RNeasy spin column. The spin column was washed twice with 500µl RPE buffer (after ethanol addition), spun once again to remove residual ethanol, and then eluted with 50µl RNase-free H_2O. All spin steps were performed on a benchtop microcentrifuge at room temperature and 14,000 RPM for 1 minute. In side-by-side comparisons, this protocol recovered miRNAs with similar efficiency as the MicroRNeasy Mini Kit (Qiagen).

Gene Expression Analysis

For mRNA analysis, RNA was reverse transcribed using random hexamers and assayed by qRT-PCR as previously described (200). Primer sequences used are in Supplemental Table 1. For miRNA analysis, RNA was reverse transcribed with the TaqMan reverse transcription kit, followed by qRT-PCR with TaqMan miRNA assays (Life Technologies). Gene expression was analyzed in triplicate, normalized by 18S rRNA or beta actin (mRNA) or U6 snRNA (miRNA), and expressed as mean ± SEM.

Luciferase Assays

STAT3-responsive m67 and constitutive Renilla luciferase constructs were described previously (124). The miR-146b promoter luciferase was created by cloning the 3kb region upstream of miR-146b into pGL3 (Promega). PCR primers used for cloning were: forward 5'-ATGTTAACGCGTCAGGCTGGTCTCTTAGGTACTG-3'; reverse 5'TGGCTCCTCGAGCAAAGTTCTTTCAGCCTGGAC-3'. To introduce TT→AA point mutations at one or both STAT binding sites, the QuikChange Lightning Site-Directed Mutagenesis Kit (Agilent) was used. Oligonucleotides used for mutagenesis are in Table 2.2. Dual-luciferase assays were performed

as previously described (200) and expressed as mean ± SD. SssI methylase (New England BioLabs) was used as previously described (226).

Table 2.2: Oligonucleotides for QuikChange site-directed mutagenesis

Site	Forward (5'→3')	Reverse (5'→3')
1.7kb site	CTCTCCCTACCACCCTCCAAA CCCGGAACTTTCAAGTTTC	GAAACTTGAAAGTTCCGGGTTTGGA GGGTGGTAGGGAGAG
830bp site	CTCCCACACCTTCCTCCTAAC TCAGAAGAGCCAGCATG	CATGCTGGCTCTTCTGAGTTAGGAG GAAGGTGTGGGAG

EMSA

The LightShift EMSA Kit (Pierce) was used according to the manufacturer's protocol. STAT binding reactions were performed as previously described (227) using 5'-biotinylated 25bp probes. Two separate STAT3 antibodies (C-terminal and N-terminal) were used to disrupt the specific complex. For competition experiments, 40-fold excess of wild-type or mutant (TT→AA) unlabeled probe was used. Sequences of EMSA probes are in Table 2.3.

Table 2.3: Oligonucleotides for EMSA probes

Probe	Forward (5'→3')	Reverse (5'→3')
1.7kb site, wild-type	ACCCTCCATTCCCGGAACTTTCAAG	CTTGAAAGTTCCGGGAATGGAGGGT
1.7kb site, mutant	ACCCTCCAAACCCGGAACTTTCAAG	CTTGAAAGTTCCGGGTTTGGAGGGT
BCL6 Region B	GAGCTCAATTCTCGGAATTTGAGCT	AGCTCAAATTCCGAGAATTGAGCTC

Drug Treatments

5-azacytidine (Sigma) was used at 1μM for 4 days (SUM-159) or 8 days (MDA-MB-468, BT-549). JAK inhibitor 1 (Calbiochem) was used at 1μM, unless indicated otherwise. For epigenetic studies, the drugs were refreshed with new media every 2 days. U0126 and LY294002

were from Cell Signaling Technology and used at 10μM and 20μM, respectively. All drugs were dissolved in DMSO, and final DMSO volume in cell culture was 0.1-0.2%.

Western Blotting and Antibodies

Western blotting was performed as previously described (228). Antibodies to phospho-MAPK (9101), total MAPK (9102), phospho-Y705 STAT3 (9131), phospho-T308 Akt (9275), phospho-S473 Akt (9271), total Akt (9272), TRAF6 (4743), and IRAK1 (4504) were from Cell Signaling Technology. Phospho-STAT1 (33-3400) antibody was from Invitrogen. C-terminal STAT3 antibody (sc-482), N-terminal STAT3 antibody (sc-7179), and total STAT1 antibody (sc-346) were from Santa Cruz Biotechnology. Phospho-S727 STAT3 antibody was described previously (229). Anti-FLAG (F1804), tubulin (T5168), and beta actin antibody (A5316) were from Sigma. All antibodies were used at 1:10000 dilution for western blot, except for phospho-Akt antibodies, which were used at 1:2000. For use in EMSA, 2μl antibody was pre-incubated with 2μl nuclear extract on ice for 30 minutes prior to addition of binding buffer and probe. IL-6 neutralizing antibody (AB-206-NA) was from R&D Systems and used at 3μg/ml.

Transfection

Plasmid transfection was performed using Fugene HD (Promega). To introduce miRNAs (25nM) or siRNAs (10nM), cells were reverse-transfected using Lipofectamine RNAiMAX (Invitrogen); the culture media was changed 24hr later. Thermo Scientific Dharmacon was the source of miR-146b mimic (C-300754-03-0005), control mimic (CN-002000-01-05), miR-146b inhibitor (IH-300754-05-0005), and control inhibitor (IN-002005-01-05). Control siRNA (D-

001210-03) was from Thermo Scientific Dharmacon, RelA siRNA (6261) was from Cell Signaling Technology, and IL-6 siRNA (sc-39627) was from Santa Cruz Biotechnology.

ELISA

SUM-159 cells were transfected in 6-well plates with control mimic or miR-146b mimic for 48hr. Afterward, the media was replaced with 1mL fresh media for 9hr and harvested. Measurement of IL-6 concentration in the conditioned medium was performed using the Human IL-6 Quantikine ELISA Kit (R&D) according to the manufacturer's instructions.

Migration, Invasion, and Viability Assays

For motility assays, 10,000 cells per 24-well were transfected with miRNA or control mimic. After 48hr, cells were detached using trypsin, spun down with trypsin neutralizing solution (Lonza), and transferred to the apical chamber in pre-warmed DMEM/F12 without additives. Pre-warmed complete SUM-159 media was added to the basolateral chamber. Cells were allowed to migrate for 8hr through polycarbonate transwell inserts (Corning, 3422) or invade for 24hr through growth factor-reduced Matrigel-coated inserts (BD BioCoat, 354483). The inserts were then fixed and stained in 0.5% crystal violet + 6% glutaraldehyde for 30 minutes, rinsed in ddH_2O, and swabbed with pre-wet cotton tips to remove cells from the apical surface of the membrane. Migrated or invaded cells were counted in triplicate $1mm^2$ areas and expressed as mean ± SD. Cell viability was measured using Cell Titer Glo (Promega) and expressed as mean ± SD.

Computational Analyses

Level 3 miRNA expression (Illumina miRNA-Seq) and mRNA expression (Agilent 244k array), level 2 DNA methylation (Illumina 450k array), and clinical parameters (patient survival and ER, PR, HER2 status) were downloaded from The Cancer Genome Atlas (TCGA) for the breast cancer data set on September 30, 2012. Pearson correlation, rank-sum test, and log-rank test were used for statistical analyses.

Primary Breast Tumor Analysis

Phospho-STAT3 (Y705) immunohistochemistry and pathologist scoring of nuclear phospho-STAT3 staining in tumor cells were performed as previously described (124). Samples underwent miRNA expression profiling using the Nanostring nCounter system, followed by log2 transformation and quantile normalization. Statistical analysis was by rank-sum test and Pearson correlation.

CHAPTER 3:

Gene Expression-Based Discovery of Atovaquone as a STAT3 Inhibitor and Anti-Cancer Agent

INTRODUCTION

A crucial component of cancer pathogenesis and progression is the aberrant activation of oncogenic signal transduction pathways. The reliance of neoplastic but not normal cells on such pathways is the basis for targeted cancer therapy (230), which has fewer side effects and potentially higher efficacy than traditional chemotherapy. Most research on targeted therapy has focused on kinases or other enzymes because they are conceptually easier to inhibit with small molecules. However, the malignant phenotype is ultimately due to gene expression patterns exerted by the downstream action of transcription factors. Thus, using a gene expression-based readout of pathway activity may permit opportunities for novel therapeutic intervention by mechanistically diverse drugs that would be missed by a kinase-centered approach.

Signal transducers and activators of transcription (STAT) proteins are transcription factors involved in numerous aspects of tumor biology. STAT activation occurs in the cytoplasm by phosphorylation of a critical tyrosine residue, which leads to dimerization of STAT proteins mediated by reciprocal SH2/phospho-tyrosine interactions. The STAT dimer translocates to the nucleus, binds to DNA, and recruits transcriptional co-machinery to regulate the expression of target genes (186). Whereas STAT activation is transient and tightly-regulated in normal cells, it often occurs constitutively in cancer cells of many solid and hematological tumor types. Moreover, inhibiting STAT activation is deleterious to cancer cells but not normal cells (35). Thus, targeting inappropriate STAT activation in cancer is a promising therapeutic strategy and an active area of investigation.

Of the STAT proteins, STAT3 has emerged as a key cancer dependency, and genes upregulated by STAT3 promote growth, survival, angiogenesis, and metastasis (35). The Janus

kinase (JAK) family, which comprises JAK1-3 and TYK2, is frequently responsible for activating STAT3 in cancer. Currently, the only FDA-approved small molecule to target STAT activation for the treatment of cancer is ruxolitinib, a recently-introduced JAK inhibitor (30). Other small molecule inhibitors of STAT3 have been reported (231), most of which are SH2 domain antagonists, but none are clinically available. Therefore, additional FDA-approved means of inhibiting STAT3 are needed. Since STAT3-dependent cancer pathogenesis is driven by STAT3-associated gene expression patterns, we hypothesized that novel STAT3 inhibitors could be discovered by identifying chemical compounds that induce opposing gene expression changes.

To do so, we used the Connectivity Map, a database of gene expression profiles produced by treating a panel of cell lines with several thousand compounds (232). This *in silico* chemical genomic strategy has been used successfully in the past to identify drugs that achieve a specific, desired gene expression endpoint (233, 234). Moreover, this gene expression-based approach provided an unbiased means of identifying inhibitors of STAT3 that may act on any step upstream of target gene transcription. Here, we report the discovery and characterization of the FDA-approved drug atovaquone as a STAT3 inhibitor and anti-cancer agent, with evidence of anti-cancer efficacy in humans.

Attributions

Dr. Michal Bar-Natan (formerly affiliated with Dana-Farber Cancer Institute; Boston MA, USA) contributed to the cell line viability data in Figure 3.6A. Dr. Vincent Ho (Dana-Farber Cancer Institute) assisted in the generation of clinical data and procurement of patient samples in Figure 3.10.

RESULTS

Discovery of Atovaquone as a STAT3 Inhibitor

Using a 12-gene signature of STAT3 activation (124), we queried the Connectivity Map to discover compounds that elicit gene expression changes contrary to the STAT3 signature (Figure 3.1A). The compound most opposed to the STAT3 signature was atovaquone (Figure 3.1B). In addition to being the leading hit, atovaquone was attractive for several other reasons. Most importantly, it is already FDA-approved, greatly reducing the cost and latency of bench-to-bedside translation. Atovaquone, which is used clinically for infections caused by *Pneumocystis*, *Toxoplasma*, and *Plasmodium*, inhibits parasitic mitochondrial respiration and is not known to have any effects on mammalian cells (235). Furthermore, its side effects are minimal, and high plasma concentrations (15-30μg/ml; 40-80μM) are readily and routinely achieved in patients (235). For all these reasons, further investigation was focused on atovaquone as a putative STAT3 inhibitor and anti-cancer drug.

To determine if atovaquone inhibits STAT3, we tested it in a cell-based reporter system of STAT3 transcriptional activity (186). These cells lack basal STAT3 activation; upon IL-6 treatment, STAT3 becomes activated and drives transcription of a STAT3-dependent luciferase reporter gene. Pre-treatment of these cells with atovaquone caused a dose-dependent inhibition of luciferase induction by IL-6, indicating suppression of STAT3 transcriptional activity (Figure 3.1C). To determine if atovaquone inhibits STAT3 activity specifically over other transcription factors, we tested it in cell-based reporter systems for STAT1 and STAT5, two other STAT family members, and NF-κB, an unrelated transcription factor. While the activity of these other transcription factors was modestly affected at the higher doses of atovaquone, the effect on

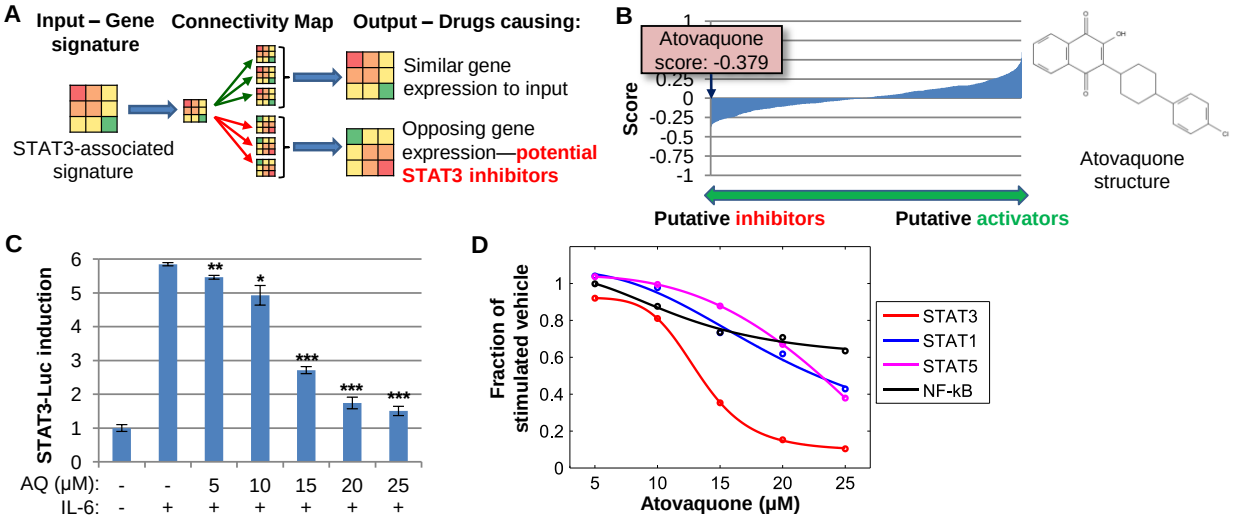

Figure 3.1: Gene expression-mediated discovery and characterization of atovaquone as a STAT3 inhibitor. (A) Overview of strategy using the Connectivity Map to identify drugs that are potential STAT3 inhibitors based on gene expression. (B) Results from the Connectivity Map analysis, with more negative scores indicating more dissimilarity with respect to the STAT3 signature. Atovaquone was the most negatively-scoring compound. (C) Atovaquone (AQ) inhibits STAT3-dependent luciferase activity. STAT3-luc reporter cells were pre-treated with drug for 1hr, then stimulated with IL-6 (10ng/ml) for 5hr. Activity of firefly luciferase was measured and normalized by cell viability (Cell Titer Glo). P-values (*, $p < 0.05$; **, $p < 0.01$; ***, $p < 0.001$) are shown relative to IL-6 stimulation in the presence of vehicle alone. (D) Atovaquone displays specificity for inhibiting STAT3. Effect of atovaquone on STAT3-luc reporter cells were compared to STAT1-luc, STAT5-luc, and NF-κB-luc cells.

STAT3 activity was much greater, indicating specificity for inhibition of STAT3 (Figure 3.1D).

These results demonstrate atovaquone to be a novel STAT3 inhibitor.

Atovaquone Inhibits STAT3 Phosphorylation, Expression of Endogenous STAT3 Target Genes, and Viability of STAT3-dependent Cancer Cells

Next, we wished to determine the mechanism by which atovaquone inhibits STAT3. Since STAT3 transcriptional activity is critically dependent on tyrosine phosphorylation, we performed western blotting to see if atovaquone affected STAT3 phosphorylation. In the STAT3 reporter cells, atovaquone pre-treatment reduced STAT3 tyrosine phosphorylation following IL-

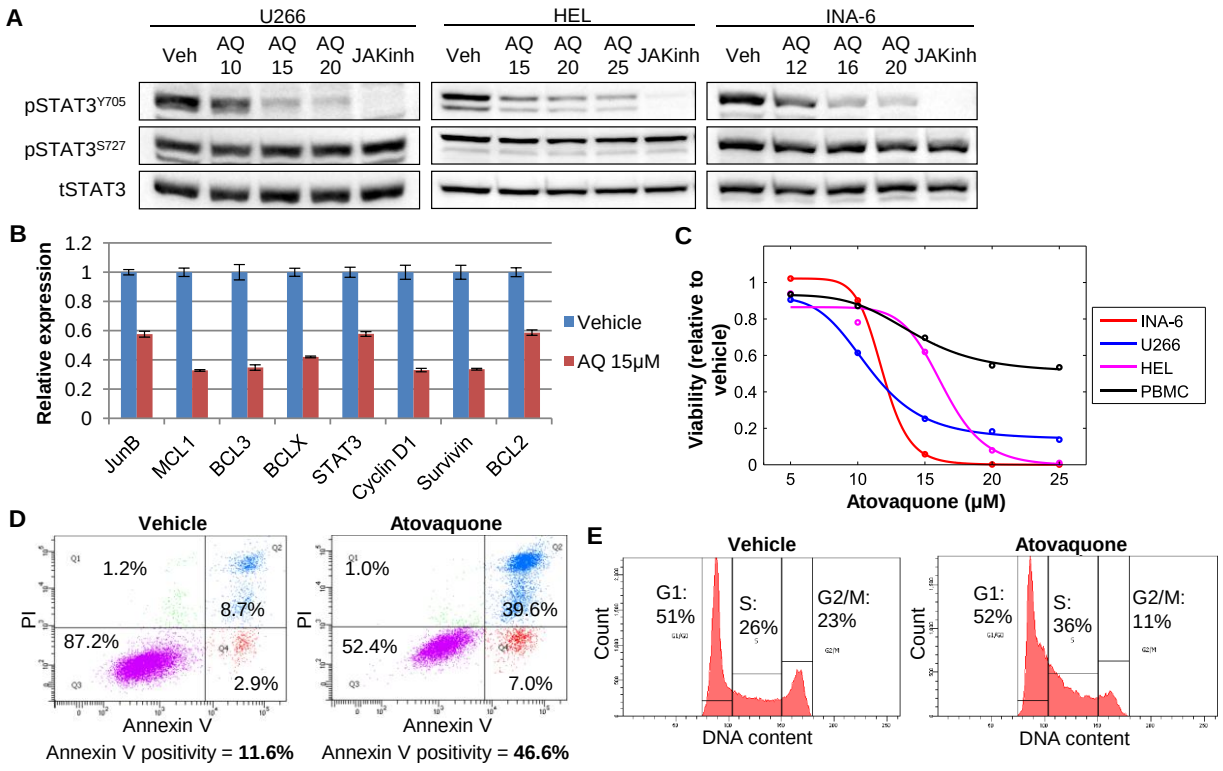

Figure 3.2: Atovaquone inhibits constitutively-activated STAT3 in cancer cells and reduces their survival and proliferation. (A) Atovaquone inhibits STAT3 tyrosine but not serine phosphorylation. Atovaquone at the indicated concentrations (μM) was used to treat U266 (2.5hr), HEL (6hr), or INA-6 cells (4hr). JAK inhibitor 1 treatment (1μM) for the same duration serves as a control and comparison. IL-6 is responsible for STAT3 activation in U266 and INA-6, while HEL harbors the JAK2-V617F mutation. (B) Endogenous STAT3 target genes were downregulated in U266 cells treated with atovaquone for 6hr. (C) Viability response curve to atovaquone (72hr) of hematologic cancer cells with activated STAT3, compared to viability of non-malignant PBMCs (average of 4 donors). (D) Atovaquone (15μM) treatment of INA-6 cells for 24hr induces apoptosis as measured by annexin V/PI staining. (E) Atovaquone (25μM) treatment of HEL cells for 24hr decreases the G2/M population by PI cell cycle analysis.

6 stimulation (Figure 3.3A). A similar effect was observed in mouse embryonic fibroblasts (MEF) (Figure 3.3B). Importantly, atovaquone additionally inhibited constitutive STAT3 tyrosine phosphorylation in multiple cancer cell lines, while STAT3 serine phosphorylation, which is not critical to transcriptional activity, was not affected (Figure 3.2A). In U266 and INA-6 cells, the source of STAT3 activation is JAK-dependent IL-6 signaling, while in HEL cells, STAT3 is activated by mutant JAK2-V617F.

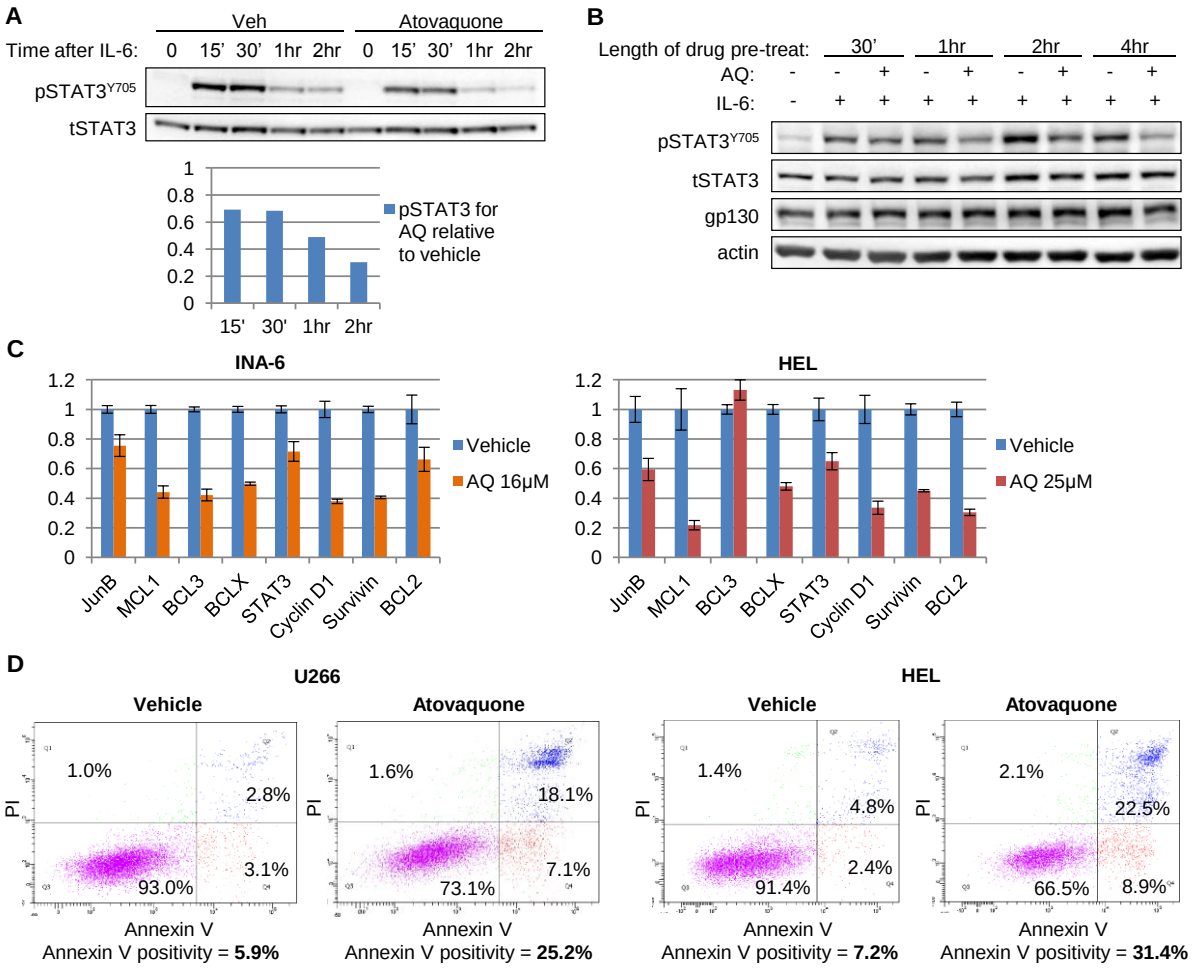

Figure 3.3: Further elucidation of effects of atovaquone on STAT3 phosphorylation, STAT3 transcriptional activity, and viability of cancer cells with constitutively-active STAT3. (A) STAT3-luc reporter cells were pre-treated with atovaquone (20μM) for 1hr, and then stimulated with IL-6 (10ng/ml) for the indicated lengths of time. Quantification of phospho-STAT3 in the presence of atovaquone, normalized by total STAT3 and relative to phospho-STAT3 in the presence of vehicle, is shown below the western blot. (B) MEFs were pre-treated with atovaquone (25μM) for the indicated time periods, then stimulated with IL-6 (5ng/ml) and soluble IL-6 receptor (20ng/ml) for 15 minutes. (C) Inhibition of endogenous STAT3 target genes in INA-6 and HEL cells treated with atovaquone for 6 hours. (D) Annexin V/PI staining of U266 and HEL cells treated with atovaquone (20μM) for 48hr demonstrates induction of apoptosis.

Given that atovaquone inhibits constitutive STAT3 activation in cancer cells, we asked whether atovaquone inhibits expression of endogenous STAT3 target genes in this context. Indeed, atovaquone substantially downregulated expression of multiple STAT3 target genes

(Figure 3.2B and 3.3C). Next, we examined the effect of atovaquone on the growth and survival of STAT3-dependent cancer cells. Survival of the multiple myeloma cell line INA-6 is exquisitely dependent on IL-6 added to culture medium and resultant STAT3 activation (236). Atovaquone suppressed the viability of INA-6 cells with an IC50 of 11.9μM, with complete loss of viability at higher doses (Figure 3.2C). The other cell lines with constitutively-active STAT3, U266 and HEL, were also killed by atovaquone. By contrast, the viability of non-malignant peripheral blood mononuclear cells (PBMC) was relatively preserved.

To ascertain how atovaquone treatment reduced the viability of STAT3-dependent cancer cells, we performed annexin V and PI staining followed by flow cytometry. This revealed atovaquone was inducing apoptotic cell death (Figure 3.2D and 3.3D). Additionally, we hypothesized atovaquone inhibits proliferation by disrupting cell cycle progression. An analysis of cell cycle distribution showed that atovaquone decreased the population of cells in G2/M and increased the proportion of cells with lower DNA content (Figure 3.2E). In summary, atovaquone inhibits constitutive STAT3 activation and target gene expression in cancer cells, and reduces their survival and proliferation.

Atovaquone Selectively Inhibits gp130 Cell-surface Expression

To understand how atovaquone inhibits STAT3 phosphorylation, we considered the possibility that atovaquone decreases the kinase activity of JAKs, which are responsible for STAT3 activation in the systems previously tested. To assess kinase activity, we first analyzed the extent of kinase auto-phosphorylation, which provides a cellular readout of kinase activity. Atovaquone treatment inhibited the auto-phosphorylation of JAK family members, showing that it diminished JAK kinase activity in cells (Figure 3.4A-B). However, *in vitro* kinase assays of

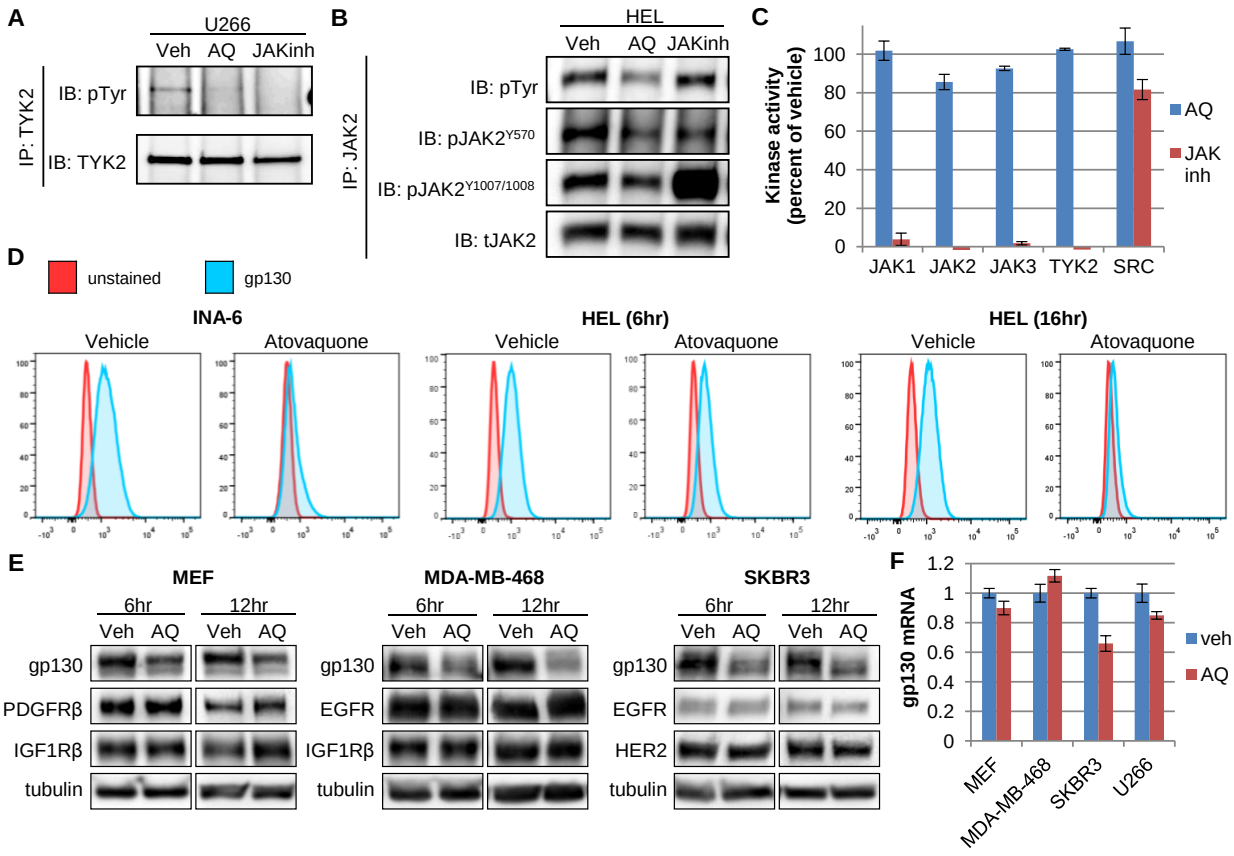

Figure 3.4: Investigation of effects of atovaquone on JAK family members and gp130. (A) Atovaquone inhibits cellular activity of the JAK family member TYK2 as measured by kinase auto-phosphorylation. U266 cells were treated with atovaquone (15μM) or JAK inhibitor 1 (1μM) for 1 hour, followed by lysis and immunoprecipitation to TYK2. The blot was probed with a pan-phospho-tyrosine antibody. Due to technical limitations, tyrosine phosphorylation of other JAK family members was not detected in U266 cells. (B) Atovaquone inhibits cellular JAK2 activity as measured by kinase auto-phosphorylation. HEL cells were treated with atovaquone (20μM) or JAK inhibitor 1 (1μM) for 6 hours, followed by lysis and immunoprecipitation to JAK2, which was selected because these cells harbor mutant JAK2-V617F. The blot was probed with a pan-phospho-tyrosine antibody, as well as antibodies specific to phospho-Tyr570 and phospho-Tyr1007/1008. Phospho-Tyr570 was previously reported to correlate better with kinase activity, whereas phospho-Tyr1007/1008 is paradoxically induced by certain JAK inhibitors, including JAK inhibitor 1, depending on binding mode (237). (C) Atovaquone (15μM) and JAK inhibitor 1 (0.5μM) were tested by *in vitro* kinase assays (Invitrogen SelectScreen) for activity against all JAK family members and Src. (D) Atovaquone downregulated cell-surface gp130 expression in INA-6 and HEL cells. Atovaquone treatment of INA-6 (20μM, 4 hours) or HEL cells (25μM, 6 or 16 hours) was followed by flow cytometry for cell-surface gp130. (E) Atovaquone decreases total cellular gp130 with prolonged treatment. MEF, MDA-MB-468, and SKBR3 cells were treated with atovaquone (25μM) for 6 or 12 hours, then analyzed by western blot for expression of gp130 and various other receptors. (F) Decreased gp130 protein is not due to decreased gp130 mRNA expression. The level of gp130 mRNA was analyzed in the cells in panel E (25μM, 12hr) and in U266 cells (20μM, 2.5 hours).

atovaquone with JAK family members showed no inhibition (Figure 3.4C), ruling out the possibility that atovaquone was a direct JAK inhibitor. Therefore, we hypothesized that atovaquone inhibits JAKs indirectly by acting on an upstream signaling component required for JAK activity.

As receptor-associated kinases, JAK signaling depends upon direct interaction with plasma membrane-localized proteins for scaffolding. This requirement also extends to mutant JAK2-V617F (238). In particular, JAKs are frequently associated with gp130, a transmembrane protein that participates in the signaling of several cytokines, including IL-6, oncostatin M (OSM), and leukemia inhibitory factor (LIF). By contrast, gp130 is not involved in the signaling of prolactin or IFN-γ, which were used to activate STAT5 and STAT1 in their respective luciferase reporter systems. For these reasons, we hypothesized that atovaquone inhibits the function or expression of gp130.

We focused on U266 cells, in which STAT3 phosphorylation was strongly suppressed by atovaquone, and performed flow cytometry to measure the cell-surface expression of gp130. Interestingly, atovaquone substantially downregulated the cell-surface expression of gp130 but not IL-6 receptor (Figure 3.5A). A pharmacological JAK inhibitor did not affect gp130 expression, indicating this effect was not secondary to inhibition of STAT3 phosphorylation. Lastly, brefeldin A, which inhibits transport of proteins from ER to Golgi, reduced the cell-surface expression of both gp130 and IL-6 receptor. Consequently, only atovaquone specifically inhibited the cell-surface expression of gp130. Atovaquone also induced downregulation of cell-surface gp130 in INA-6 and HEL cells (Figure 3.4D).

Since atovaquone reduced gp130 expression at the cell surface, we asked whether this effect was accompanied by reduced total gp130 in the cell. To address this question, we

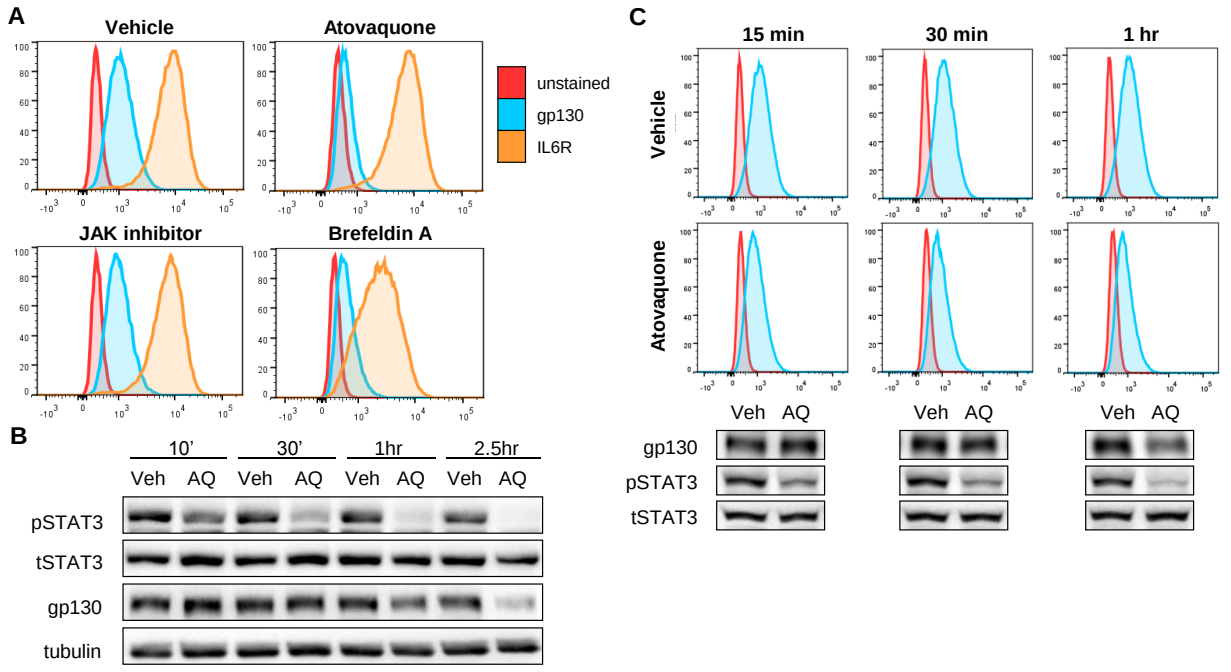

Figure 3.5: Atovaquone specifically and rapidly downregulates cell-surface gp130 expression. (A) Atovaquone downregulates levels of cell-surface gp130 but not IL-6 receptor. U266 cells were treated with atovaquone (20μM), JAK inhibitor 1 (1μM), or brefeldin A (3μg/ml) for 2.5hr, then analyzed by flow cytometry for cell-surface expression of gp130 and IL-6 receptor. (B) Atovaquone rapidly inhibits STAT3 phosphorylation and does not affect total gp130 except at much longer time points. U266 cells were treated with atovaquone at 20μM. (C) Atovaquone rapidly downregulates cell-surface gp130 expression, paralleling the kinetics of phospho-STAT3 inhibition. U266 cells were treated with atovaquone at 20μM.

performed a time course of atovaquone treatment and measured total cellular gp130 by western blotting. STAT3 phosphorylation was inhibited rapidly, after only 10 minutes, whereas total gp130 was not reduced except at much longer time points (Figure 3.5B). Thus, we surmised that atovaquone also rapidly downregulates cell-surface gp130, paralleling STAT3 inhibition and preceding the decrease in total gp130. This was confirmed by a flow cytometric time course experiment that demonstrated atovaquone rapidly inhibits the cell-surface expression of gp130, without affecting total gp130 until much later (Figure 3.5C).

Loss of cell-surface gp130 may be due to decreased entry into the plasma membrane or increased internalization. In either case, the decrease in total gp130 observed at longer time

points is likely due to degradation of relatively unstable intracellular gp130. We found that atovaquone also induced loss of total gp130 after prolonged treatment in multiple other cell lines, including MEF, SKBR3, and MDA-MB-468 cells (Figure 3.4E). In contrast, levels of other receptors—such as PDGFR-β, EGFR, HER2, and IGF1R-β—were not affected, again indicating a specific effect on gp130. Also, gp130 mRNA expression was not significantly changed by atovaquone, demonstrating that the decrease in total gp130 occurs post-transcriptionally (Figure 3.4F). In summary, atovaquone rapidly induces specific loss of cell-surface gp130, while total gp130 declines secondarily due to protein degradation.

Atovaquone Inhibits mTOR Activity by Upregulating Expression of REDD1

Having characterized the effect of atovaquone on STAT3 and STAT3-dependent cell lines, we asked if atovaquone had effects on the viability of cells that do not display constitutive STAT3 activation. Interestingly, atovaquone also reduced the viability of various malignant hematological cell lines that lack STAT3 activation (Figure 3.6A and 3.7A). Similar to cells with activated STAT3, the loss of viability occurred through apoptosis and cell cycle arrest (Figure 3.6B-C). Therefore, we hypothesized atovaquone kills cancer cells through STAT3-related and STAT3-independent mechanisms.

Accordingly, we considered the hypothesis that atovaquone inhibited another common pathway in cancer pathogenesis. In particular, we focused on the mTOR pathway, which is known to be involved in cancer cell growth and survival (239). In K562 cells lacking STAT3 activation, atovaquone inhibited phosphorylation of 4E-BP1, a direct mTOR substrate, and ribosomal protein S6 with efficacy comparable to rapamycin, but only after 5 hours of treatment (Figure 3.7B). Additionally, atovaquone inhibited phosphorylation of p70S6K, but not p42/44

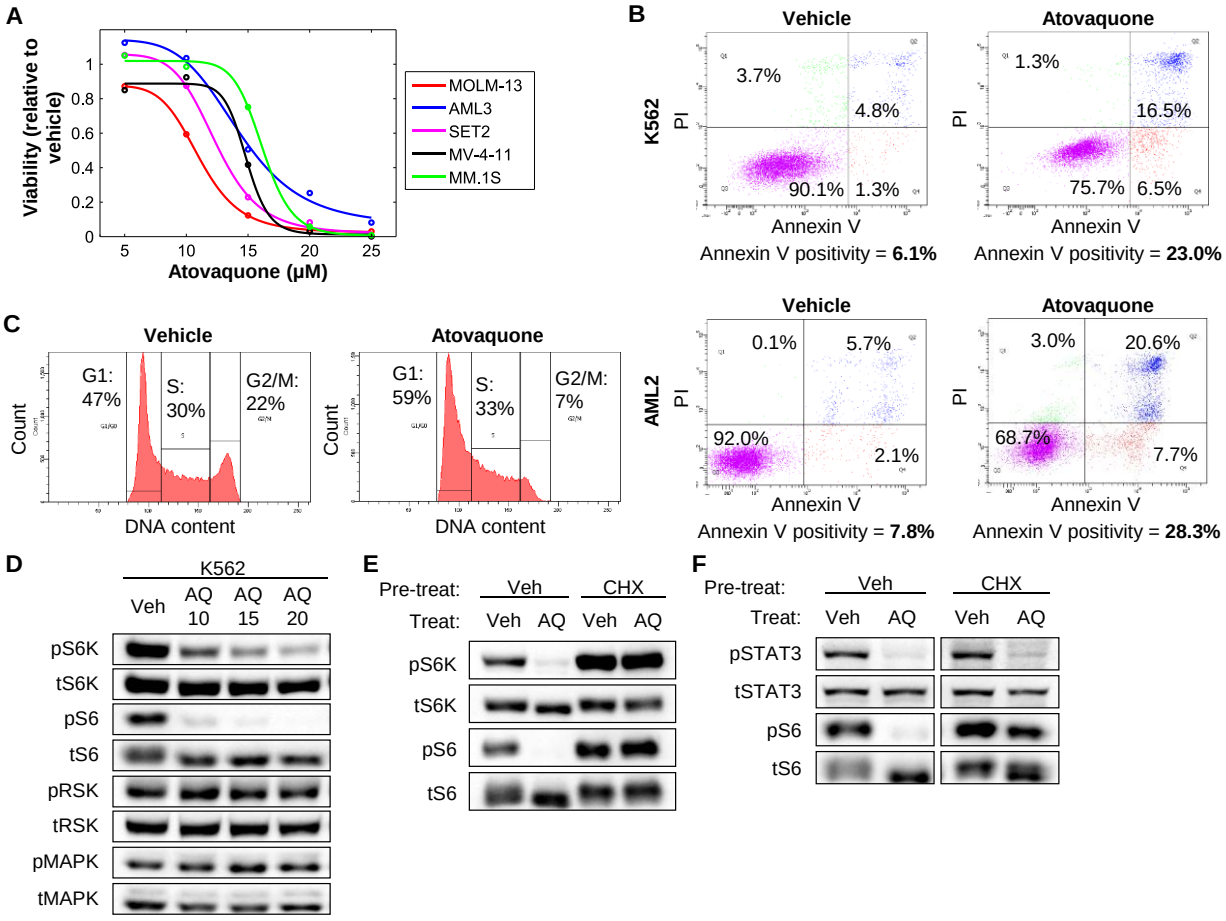

Figure 3.6: Characterization of the effects of atovaquone on cells lacking STAT3 activation and on the mTOR pathway. (A) Viability of hematologic cancer cell lines lacking STAT3 activation after 72hr treatment with atovaquone. (B) Annexin V/PI staining of K562 (20μM) and AML2 (15μM) cells treated with atovaquone for 48hr demonstrating induction of apoptosis. (C) PI cell cycle analysis of K562 cells treated with atovaquone (20μM) for 24hr demonstrating reduced G2/M population. (D) Atovaquone inhibits phospho-S6 and phospho-p70S6K, which are downstream of mTOR. K562 cells were treated with atovaquone for 6 hours. (E) Inhibition of mTOR requires *de novo* gene expression. K562 cells were pre-treated with vehicle or cycloheximide (2μg/ml) for 1 hour, then treated with vehicle or atovaquone (20μM) for 5 hours. (F) Inhibition of phospho-STAT3 does not require new gene synthesis. U266 cells were pre-treated with vehicle or cycloheximide (2μg/ml) for 1 hour, and then treated with vehicle or atovaquone (15μM) for 2.5 hours.

MAPK, p90RSK, or Akt (Figure 3.6D and data not shown). Taken together, these findings suggested that inhibition of the mTOR pathway by atovaquone was taking place at the level of mTOR itself.

The requirement for prolonged treatment to observe mTOR inhibition raised the possibility that this effect was mediated by an induced factor. To test this hypothesis, we pre-treated cells with cycloheximide, a protein synthesis inhibitor. Atovaquone inhibition of S6 phosphorylation in K562 and U266 cells was blocked in the presence of cycloheximide (Figure 3.6E-F). In contrast, cycloheximide did not affect the inhibition of STAT3 phosphorylation by atovaquone in U266 cells (Figure 3.6F), consistent with the rapid kinetics of this effect (Figure 3.5B). Similar results were obtained with actinomycin D, an inhibitor of mRNA synthesis (data not shown). These results demonstrate that atovaquone inhibition of mTOR, but not STAT3, requires *de novo* gene expression.

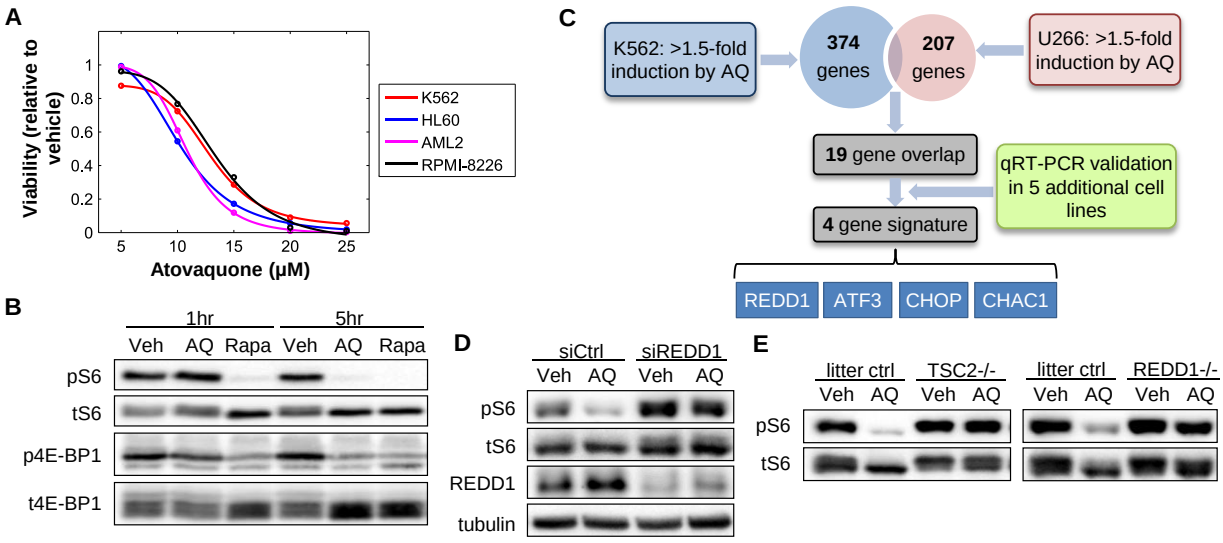

Figure 3.7: Atovaquone inhibits the mTOR pathway by inducing expression of REDD1. (A) Effect of atovaquone on viability of hematologic cancer cells lacking constitutive STAT3 activation. (B) Atovaquone inhibits the mTOR pathway. K562 cells were treated with atovaquone (20μM) or rapamycin (10nM) for 1hr or 5hr, then analyzed by western blot. (C) Strategy to identify the factor upregulated by atovaquone responsible for mTOR inhibition. (D) Knockdown of REDD1 abrogates atovaquone-mediated mTOR inhibition. SKBR3 cells were transfected with control or REDD1 siRNA for 48hr, then treated with atovaquone (25μM) for 4hr. (E) Atovaquone-mediated inhibition of mTOR requires TSC2 and REDD1. TSC2-null or REDD1-null MEFs, alongside their respective littermate control MEFs, were treated with atovaquone (25μM) for 2.5hr.

To discover the gene whose induction by atovaquone was responsible for mTOR inhibition, we performed gene expression microarrays in K562 and U266 cells. We reasoned that induction of the causative factor must be common to all cell lines in which atovaquone inhibits the mTOR pathway. Using a 1.5-fold cutoff, atovaquone upregulated several hundred genes in each cell line; however, only 19 of these genes were upregulated in both K562 and U266 cells. We then analyzed the expression of the 19 genes by qRT-PCR in additional cell lines responsive to atovaquone, resulting in the identification of a set of 4 genes that was consistently induced in all cell lines (Figure 3.7C). Of these, REDD1 is a known negative regulator of mTOR whose activity is dependent on the TSC1/2-complex (240).

To evaluate the role of REDD1, we used RNA interference to knock down its expression in adherent SKBR3 cells, given the relative ease of introducing siRNA into these cells. Knocking down REDD1 largely blocked atovaquone inhibition of S6 phosphorylation (Figure 3.7D). Moreover, atovaquone had no effect on S6 phosphorylation in MEFs with knockout of TSC2 or REDD1 itself (Figure 3.7E). Thus, atovaquone inhibits the mTOR pathway by inducing the expression of REDD1.

Atovaquone Selectively Activates the Phospho-eIF2α/ATF4 Branch of the Unfolded Protein Response (UPR)

In asking how atovaquone induces REDD1, we considered a possible role for ATF4, which regulates REDD1 expression (241). ATF4 is regulated mainly at the level of translation and is induced upon phosphorylation of eIF2α. Moreover, in the set of genes consistently induced by atovaquone, ATF3 and CHOP are also ATF4 target genes, and CHAC1 is a target gene of CHOP (242). Growth-inhibitory and pro-apoptotic functions have been reported for all

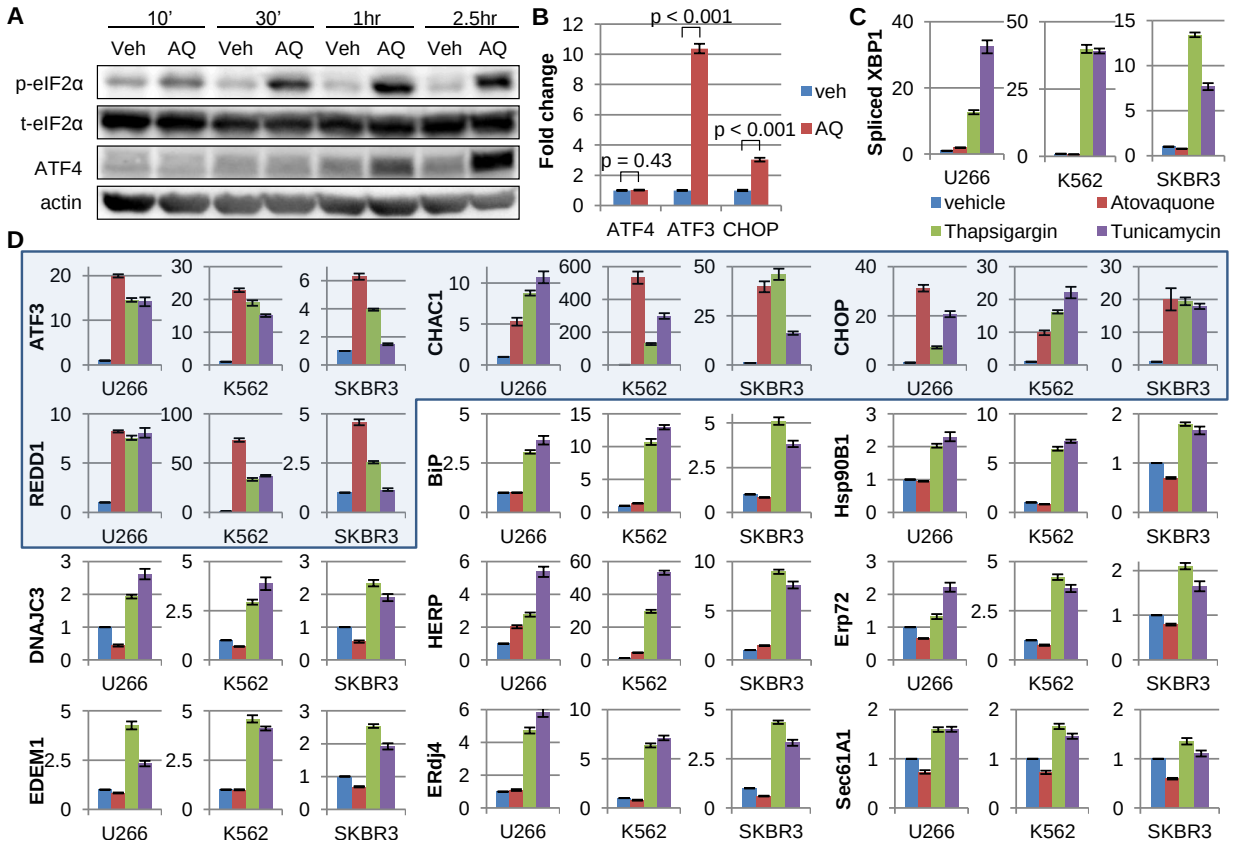

Figure 3.8: Atovaquone induces eIF2α phosphorylation and ATF4, but not other branches of the unfolded protein response. (A) Atovaquone induces phospho-eIF2α and ATF4. U266 cells were treated with atovaquone at 20μM. (B) ATF4 induction occurs at the protein but not mRNA level. U266 cells were treated with atovaquone at 15μM for 2hr. (C) Atovaquone does not induce splicing of XBP1, unlike UPR activators tunicamycin and thapsigargin. U266, K562, and SKBR3 cells were treated with atovaquone (20, 20, 25μM respectively), thapsigargin (1μM), or tunicamycin (5μg/ml) for 6hr. Afterwards, qRT-PCR was performed using primers specific to spliced XBP1. (D) Most UPR target genes are not induced by atovaquone, except for those downstream of ATF4 (highlighted in blue). Target genes were assessed in the same RNA as in panel C.

of these proteins, suggesting they may contribute to the anti-cancer activity of atovaquone. Indeed, rapamycin treatment of cancer cells lacking STAT3 activation caused only a modest decrease in viability, indicating that mTOR inhibition alone is not sufficient to fully explain the effects of atovaquone on viability of these cells (Figure 3.9A). For these reasons, we hypothesized that atovaquone induces eIF2α phosphorylation, with a resulting increase in ATF4 protein and signaling.

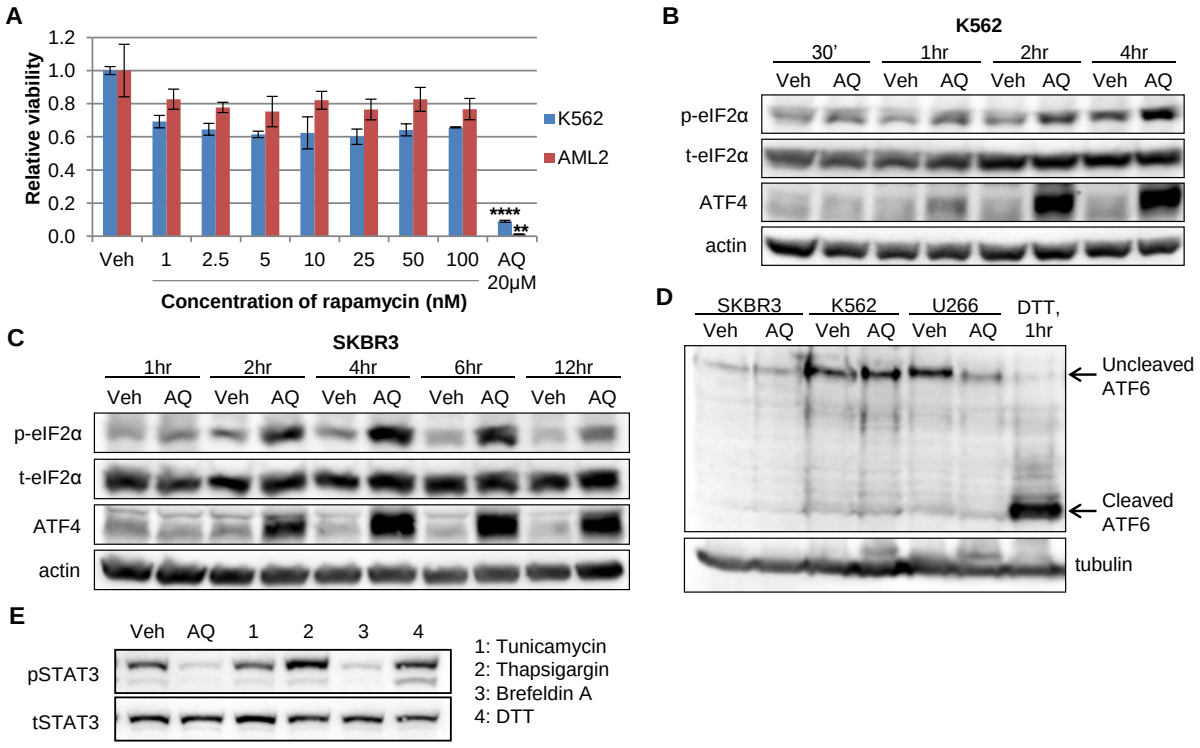

Figure 3.9: Evidence that mTOR inhibition alone does not fully account for the effect of atovaquone on viability of cancer cells lacking STAT3 activation, with further exploration of the relationships between atovaquone, the unfolded protein response (UPR), and STAT3 phosphorylation. (A) K562 and AML2 cells, which lack STAT3 activation, were treated with rapamycin for 72hr, resulting in only a modest viability decrease. P-values (**, $p < 0.01$; ****, $p < 0.0001$) are shown for the viability after 72hr atovaquone treatment (20μM) relative to 100nM rapamycin for each cell line. (B) Atovaquone induces phospho-eIF2α and ATF4. K562 cells were treated with atovaquone at 20μM. (C) Experiment similar to panel B, using SKBR3 cells and atovaquone at 25μM. (D) Atovaquone does not induce ATF6 cleavage. The last lane is a positive control, consisting of U266 cells treated with 5mM DTT for 1hr. Due to the insolubility of ATF6, all of these samples were prepared by boiling in sample buffer. (E) General UPR activation does not inhibit phospho-STAT3. U266 cells were treated with atovaquone or the UPR activators for 2.5hr.

We found that atovaquone induced eIF2α phosphorylation and increased ATF4 protein levels in multiple cell lines, including U266, K562, and SKBR3 (Figure 3.8A and 3.9B-C). While ATF4 target genes were induced, expression of ATF4 mRNA was unchanged (Figure 3.8B), demonstrating that the increase in ATF4 protein occurred at the post-transcriptional level. The phospho-eIF2α/ATF4 pathway represents one branch of the UPR, whose other branches

consist of ATF6 cleavage and IRE1-mediated XBP1 splicing. Interestingly, however, atovaquone did not induce spliced XBP1 (Figure 3.8C) or ATF6 cleavage (Figure 3.9D). Furthermore, in contrast to the UPR activators tunicamycin and thapsigargin, atovaquone did not induce any UPR target genes other than those downstream of ATF4 (Figure 3.8D). Thus, atovaquone selectively activates the phospho-eIF2α/ATF4 branch of the UPR.

Since the UPR has been reported to inhibit IL-6-dependent STAT3 activation (243), we tested various UPR activators to see if they also inhibit STAT3 phosphorylation in U266 cells. However, only brefeldin A decreased STAT3 phosphorylation (Figure 3.9E), consistent with its direct effects on cell-surface gp130 and IL-6 receptor. Consequently, atovaquone inhibition of STAT3 is not secondary to UPR activation.

Atovaquone Treatment Associates with Improved Cancer Outcomes in Patients

Atovaquone (trade name Mepron) is frequently used clinically to protect hematological cancer patients against *Pneumocystis* pneumonia during treatment and after hematopoietic stem cell transplant (HSCT). At many transplant centers, patients receive atovaquone for 20-30 days upon discharge after HSCT, and then are switched to trimethoprim-sulfamethoxazole (TMP-SMX; trade name Bactrim) for long-term prophylaxis. However, about 25% of patients are maintained on atovaquone for months or even years due to intolerance of TMP-SMX. In patients taking standard doses of atovaquone, plasma concentrations of 40-80μM are routinely achieved (235), well within the range needed to inhibit STAT3 and mTOR *in vitro*. Consequently, retrospective analysis of atovaquone exposure and clinical outcomes after HSCT provides a unique opportunity to investigate the anti-cancer effects of atovaquone in patients.

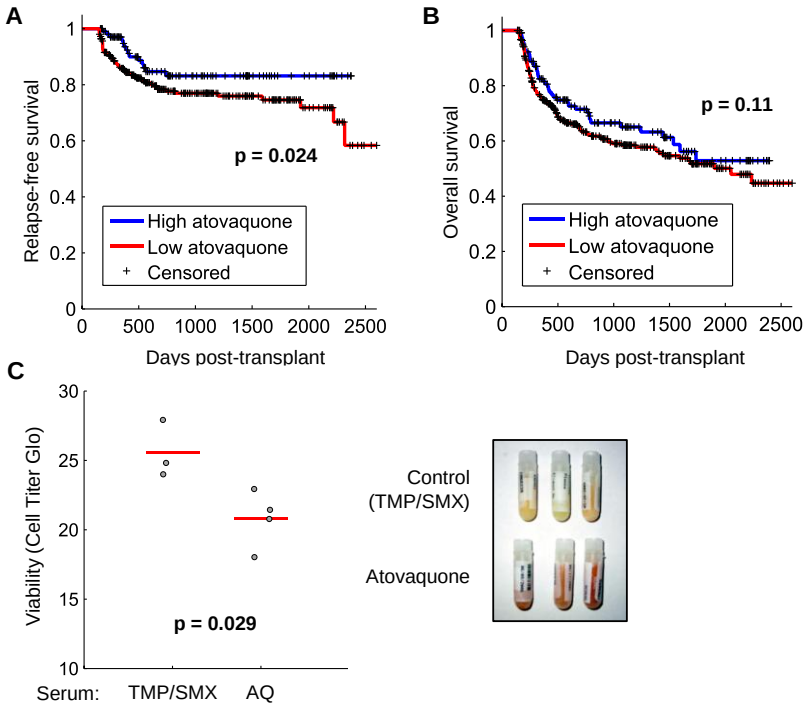

Figure 3.10: Evidence for anti-cancer activity of atovaquone in patients. (A) Greater length of atovaquone treatment (as defined in the text) after HSCT in AML is associated with improved relapse-free survival (log-rank test). (B) Analysis of overall survival in the same cohort as panel A. (C) Serum from patients treated with atovaquone inhibits viability of cancer cells in vitro. U266 cells were grown for 4 days in a 1:1 mix of RPMI-1640 and serum samples from patients taking TMP/SMX or atovaquone. Viability was then measured by Cell Titer Glo, with the absolute luminometric results shown (comparison: two-sample t-test). Right: appearance of plasma samples isolated from patients taking TMP/SMX or atovaquone.

We focused on acute myeloid leukemia (AML) due to our *in vitro* data of the effects of atovaquone in AML cell lines, frequent STAT3 activation in AML patient samples (244), association of UPR with better prognosis in AML (244), and sufficient sample size. The patient population consisted of AML patients treated with HSCT at the Dana-Farber Cancer Institute and who survived at least 150 days after transplant without relapse. Patients treated with atovaquone for at least 100 days within the 150-day period were classified as “high atovaquone” exposure, while the remaining patients were classified as “low atovaquone” exposure.

Importantly, patients in the “high atovaquone” group had significantly improved relapse-free survival, with a trend toward improved overall survival (Figure 3.10A-B).

To further investigate the anti-cancer activity of atovaquone in patients, we collected serum samples from patients approximately 100 days following HSCT who were being treated with either TMP-SMX or atovaquone. The serum from the atovaquone-treated patients reduced the viability of U266 cells compared to the serum of patients receiving TMP-SMX (Figure 3.10C). Strikingly, atovaquone is a colored compound, and its presence in patient plasma is visibly noticeable (Figure 3.10C). Taken together, these results strongly suggest that atovaquone exerts anti-cancer effects in patients.

DISCUSSION

We have identified atovaquone as a novel STAT3 inhibitor using an unbiased gene expression-based approach. Atovaquone acts by diminishing cell-surface gp130 expression and STAT3 tyrosine phosphorylation. As a consequence, critical STAT3 target genes mediating survival and proliferation are reduced, such as survivin, Bcl-2 family members, and cyclin D1. Moreover, atovaquone inhibits the viability of STAT3-dependent cancer cells by inducing apoptosis and disrupting cell cycle progression.

Since atovaquone inhibits STAT3 signaling upstream of JAK kinases, its mechanism predicts that atovaquone will also inhibit phosphorylation of other STATs if they are activated alongside STAT3 by the same upstream events. Indeed, in addition to inhibiting STAT3 phosphorylation, atovaquone inhibited IL-6-dependent phosphorylation of STAT1 in INA-6 and U266 cells and mutant JAK2-dependent phosphorylation of STAT1 and STAT5 in HEL cells (data not shown). Since STAT5 activation is crucial to cancer pathogenesis caused by JAK2-V617F (245), the additional inhibition of STAT5 in this context is a desirable effect of atovaquone. By contrast, atovaquone did not inhibit STAT5 phosphorylation in K562 cells (data not shown), in which STAT5 is activated by BCR-ABL independent of gp130.

Because the effects of atovaquone on STAT activation are restricted to gp130-dependent signaling, atovaquone inhibits STATs more selectively than direct pharmacological JAK inhibition. For example, signaling due to growth hormone, erythropoietin, and interferons is abrogated by JAK inhibitors but remains intact under atovaquone, since these hormones and cytokines do not utilize gp130. This reduces the potential side effects of atovaquone, which is already known to be extremely well-tolerated in humans. At the same time, the actions of

atovaquone extend to all cytokines that signal through gp130, including LIF and OSM, thereby exerting broader effects than therapies specifically directed against IL-6 or IL-6 receptor, such as monoclonal antibodies. This is also advantageous, since oncogenic effects of LIF and OSM have been reported (246-250).

Our work shows that IL-6-dependent STAT3 signaling, a key cancer pathway (69, 251, 252), is effectively inhibited by atovaquone. For example, IL-6 is a critical survival factor in AML and multiple myeloma (252, 253), which is pertinent to the cell lines used in this study and our findings in AML patients. Moreover, the importance of IL-6 has been established in multiple solid malignancies, including breast, lung, and melanoma (254, 255). Besides STAT3 activation due to IL-6, we also showed atovaquone inhibits STAT activation due to mutant JAK2-V617F, which is crucial to myeloproliferative neoplasms (256). Thus, we predict that atovaquone may have a role in the treatment of multiple diverse cancers, either as initial therapy or as a second-line option if JAK resistance mutations emerge following JAK inhibitor therapy. Atovaquone can also be combined with a JAK inhibitor to decrease the likelihood of developing resistance.

In addition, our work demonstrates that atovaquone activates the phospho-eIF2α/ATF4 branch of the UPR, resulting in induction of REDD1, which mediates mTOR inhibition, and induction of the pro-apoptotic factors CHOP and CHAC1. Inhibiting mTOR has intrinsic anti-cancer value due to its involvement in tumor cell survival and proliferation (239). However, recent studies also support specific benefits associated with dual blockade of the JAK/STAT and mTOR pathways, as shown in breast cancer (257) and ALL (258). Moreover, mTOR is known to phosphorylate STAT3 on serine 727 and increase its transcriptional activity (259). Although this mode of crosstalk was not observed in this study, it illustrates how the various effects of atovaquone can complement and potentially synergize with one another.

While broad UPR activation has variable effects in cancer, the ATF4/CHOP pathway has been shown to promote apoptosis in numerous cancer contexts (260-264). Additionally, the net effect of UPR activation appears to depend on the balance between induction of pro-survival BiP and pro-apoptotic CHOP (265, 266). Atovaquone strongly upregulates CHOP with no effect on levels of BiP, supporting the role of the ATF4/CHOP pathway in atovaquone-mediated apoptosis. CHAC1, an ATF4/CHOP target gene consistently upregulated by atovaquone, is also pro-apoptotic (242). Thus, atovaquone inhibits the viability of cancer cells through STAT3-related and STAT3-independent mechanisms. Multiple mechanisms of action are desirable, since the anti-cancer efficacy of single-pathway inhibitors is generally short-lived. In this case, the risk of side effects is less of a concern given the safe track record of atovaquone use in the clinic.

Our findings have laid the groundwork for further research into the biochemical and cellular effects of atovaquone. A key question for future study is the relationship between the downregulation of cell-surface gp130 and the activation of the phospho-eIF2α/ATF4 pathway. The latter is unlikely to cause the former, since other UPR activators did not affect STAT3 phosphorylation, but the reverse is a possibility. For example, atovaquone may prevent gp130 from entering the plasma membrane, causing it to accumulate in the ER and Golgi and triggering a limited form of UPR activation. Alternatively, the two effects of atovaquone may be mechanistically independent of each other. Also, the direct molecular target(s) of atovaquone are not known at this time. Their elucidation may lead to the identification of new cellular targets for cancer drug discovery efforts.

Most importantly, our analysis of patients treated with HSCT suggests atovaquone can affect clinical outcomes in AML. Due to the retrospective nature of the study, confounding cannot be ruled out. However, the choice of atovaquone over TMP-SMX is primarily due to

intolerance of TMP-SMX and not factors that might positively influence relapse. Additionally, our findings using serum samples from patients taking atovaquone supports the hypothesis that atovaquone is effective against cancer in humans. Ultimately, a randomized prospective clinical trial is needed to definitively address efficacy. AML is a disease with a 5-year survival rate of only 20-40%, and the mainstay of treatment, cytotoxic chemotherapy, has remained unchanged for decades (187). Thus, new drugs to combat AML are urgently needed, and if validated, atovaquone would be a welcome addition to the therapeutic arsenal.

In summary, we undertook a gene expression-based strategy that identified atovaquone as a novel STAT3 inhibitor. Further investigation showed that atovaquone also inhibits mTOR and activates the phospho-eIF2α/ATF4 pathway. Atovaquone kills cancer cells *in vitro* at concentrations readily achieved in patients, and significantly, we uncovered clinical evidence that supports an anti-cancer effect of atovaquone in humans. It will be worthwhile to further explore the molecular mechanisms by which atovaquone exerts these effects, and consider evaluating its anti-cancer efficacy in prospective clinical trials.

MATERIALS AND METHODS

Connectivity Map Analysis

The 12-gene STAT3 signature (124) was mapped from murine U74Av2 probes to all corresponding human U133A probes using a file downloaded from dChip (http://www.hsph.harvard.edu/cli/complab/dchip/common%20HG-U133A_MG-U74Av2.xls). Two genes downregulated by STAT3 activation were similarly mapped. The resulting probe lists (Supplemental Table 2) were used to query the Connectivity Map. Detailed results were downloaded, and the "up" score was averaged across all instances for each compound; compounds with fewer than 3 instances were excluded.

Cell Lines and Tissue Culture

Mouse embryonic fibroblasts (MEFs) were cultured in DMEM+10% FBS. TSC2-null and REDD1-null MEFs, along with their littermate controls, were kind gifts from Dr. John Blenis and Dr. Leif Ellisen, respectively. HEL was a kind gift of Dr. Daniel G. Tenen and grown in RPMI-1640+10% FBS. AML2, AML3, and MOLM-13 were kind gifts of Dr. James D. Griffin and grown in RPMI-1640+10% FBS. MM.1S was a kind gift of Dr. Kenneth C. Anderson and grown in RPMI-1640+10% FBS. SET2 was a kind gift of Dr. Ross L. Levine and grown in RPMI-1640+10% FBS. HL60 was a kind gift of Dr. James D. Griffin and grown in RPMI-1640+10% FBS. SKBR3, MDA-MB-468, U266, INA-6, RPMI-8226, K562, and MV-4-11 cells were obtained and cultured as previously reported (184, 186, 187, 224, 225). PBMCs were isolated from healthy donors by Ficoll density gradient centrifugation and maintained in

RPMI-1640+10% FBS. All cells were maintained in a humidified incubator at 37°C with 5% CO_2.

Total RNA Isolation

Cell pellets were lysed in 270µl RLT Plus buffer + 1% β-mercaptoethanol and processed by QIAshredder and genomic DNA eliminator spin columns. The flow-through was mixed with 460µl 95% ethanol by pipetting up and down, and then run through an RNeasy spin column. The spin column was washed twice with 500µl RPE buffer (after ethanol addition), spun once again to remove residual ethanol, and then eluted with 50µl RNase-free H_2O. All spin steps were performed on a benchtop microcentrifuge at room temperature and 14,000 RPM for 1 minute.

Gene Expression Analysis

Total RNA was reverse transcribed using random hexamers and assayed by qRT-PCR as previously described (200). Primer sequences used are in Supplemental Table 1. Gene expression was analyzed in triplicate, normalized by 18S rRNA, and expressed as mean ± SEM. For gene expression microarrays, RNA was isolated by Trizol, purified further on RNeasy columns, and profiled using Affymetrix Human Gene 1.0 ST arrays. Results are deposited under GEO Accession: GSE46575.

Western Blotting, Immunoprecipitation, and Antibodies

Western blotting was performed as previously described (228). Antibodies to phospho-MAPK (9101), total MAPK (9102), phospho-Y705 STAT3 (9131), phospho-S6 (2215), total S6 (2217), phospho-4E-BP1 (9451), total 4E-BP1 (9644), total RSK (9355), phospho-S6K (9234,

used at 1:5000), total S6K (2708), phospho-eIF2α (9721, used at 1:1000), total eIF2α (5324), ATF4 (11815, used at 1:1000), PDGFRβ (3169), IGF1Rβ (9750), EGFR (2232), and HER2 (2242) were from Cell Signaling Technology. Phospho-RSK antibody was from R&D (AF889). Antibodies to total STAT3 (sc-482) and gp130 (sc-656, used at 1:1000) were from Santa Cruz Biotechnology. Phospho-S727 STAT3 antibody was described previously (229). REDD1 antibody was from Proteintech (10638-1-AP, used at 1:1000). Antibody recognizing full-length and cleaved ATF6 was from Abcam (ab122897, used at 1:1000). Antibodies to tubulin (T5168) and beta actin (A5316) were from Sigma. All antibodies were used at 1:10000 dilution for western blot unless otherwise noted.

For immunoprecipitations, cells were lysed in 500ul lysis buffer (0.5% NP-40, 150mM NaCl, 50mM Tris pH 7.5, with protease and phosphatase inhibitors freshly added at 1:100 [Pierce, PI78443]) on ice for 15 minutes, then centrifuged for 10 minutes at 14,000RPM and 4°C. The supernatant was transferred to a new tube and incubated with 10µl JAK2 antibody (Santa Cruz sc-278) or a mix of two TYK2 antibodies, 10µl of each (Santa Cruz sc-5271 and Cell Signaling Technology 9312). Immunoprecipitation was performed overnight at 4°C with rotation. The next day, 75µl of protein A/G beads (Santa Cruz sc-2003) were washed twice in lysis buffer, then incubated with immunoprecipitates overnight as before. The next day, the beads were spun down (1 min. at 7,500RPM and 4°C) and washed 3 times with 650µl lysis buffer for 10 minutes at 4°C with rotation, then boiled in 50µl sample buffer + 10% β-mercaptoethanol. For western blot, 20µl were loaded per lane. For detection of phospho-tyrosine, a mixture of two pan-phospho-tyrosine antibodies (Cell Signaling Technology 9411 and 9416, 1:1000 of each) was used. Antibody to phospho-Y1007/1008 JAK2 was from Cell Signaling

Technology (3771, used at 1:1000). Antibody to phospho-Y570 JAK2 was from Millipore (09-241, used at 1:1000).

Luminometric Assays

Luciferase reporter cell lines were described previously (186). Firefly luciferase values were normalized by concurrent cell viability. Cell viability was measured as ATP-dependent luminescence by Cell Titer Glo (Promega).

Drug Treatments

For drug treatments, cells were spun down and suspended in fresh media the day prior. Atovaquone (Sigma-Aldrich A7986) was dissolved at a stock concentration of 12.5mM and used to treat cells at up to 1:500 dilution (up to 0.2% v/v DMSO final). JAK inhibitor 1 (Millipore 420097) was used at 1μM, unless indicated otherwise. DTT (Bio-Rad 1610610) was dissolved at 1M in PBS and used at 1:200 (5mM final). Tunicamycin (Sigma-Aldrich T7765) was used at 5μg/ml. Thapsigargin (T9033) was used at 1μM. Brefeldin A (Millipore 203729) was used at 3μg/ml. Rapamycin (Millipore 553210) was used at 10-100nM as indicated. DMSO was used to dissolve all drugs unless otherwise specified.

Flow Cytometry

Annexin V/PI staining was performed using Annexin V:FITC Apoptosis Detection Kit I (BD Biosciences). Staining for cell cycle analysis was performed as previously described (267). Staining for cell-surface receptors was performed in 50μl PBS + 2% FBS with 2μl antibody to IL6R (BioLegend #352803) or 5μl antibody to gp130 (BD Biosciences #555757) for 20 minutes

on ice in the dark. Cells were washed twice, then resuspended in 300μl of the same buffer. Samples were analyzed on a BD FACSCanto II machine.

Transfection and siRNA

Cells were reverse-transfected using Lipofectamine RNAiMAX (Invitrogen); the culture medium was changed 24hr later. Control siRNA (D-001210-02) and REDD1 siRNA (M-010855-01) were from Thermo Scientific Dharmacon.

Chart Review

Atovaquone start and end dates for approximately 500 AML patients who underwent HSCT at Dana-Farber Cancer Institute from 2006-2012 were obtained by chart review of the electronic medical record with DFCI IRB approval. Atovaquone was administered as a suspension, 750mg twice daily. Due to the intermittent atovaquone dosing for some patients, a discontinuation for longer than 50 days disqualified subsequent atovaquone treatment from counting toward a patient's total atovaquone exposure. Patients who received more than one HSCT were excluded (4% of total patients).

CHAPTER 4:

Conclusions and Future Directions

Discovery of Novel STAT3-Regulated MiRNAs Related to Cancer

We have conducted the first genome-wide survey of STAT3-specific miRNA alterations. This led to the discovery of four novel miRNAs that were validated to be regulated by STAT3, albeit only miR-146b was a direct STAT3 target gene. Nonetheless, some of the indirect targets may have biologically significant roles as miRNAs induced in the presence of STAT3 activation. For example, miR-137 is a well-characterized tumor suppressor miRNA that was induced 2-fold in MCF-10A cells by STAT3C. Targets of miR-137 include CDK6, Cdc42, MITF, and c-Met (268-270), and miR-137 is frequently hypermethylated in cancer. Thus, miR-137 may be another important negative regulator downstream of STAT3. On the other hand, the function of miR-95, which was induced nearly 10-fold, is poorly characterized. However, miR-95 may be oncogenic by targeting sorting nexin 1 (SNX1), thereby causing heightened EGFR signaling (271). Therefore, our inducible STAT3C system identified multiple cancer-relevant miRNAs.

Molecular Analysis of MiR-146b Regulation

We also showed STAT activation alone is sufficient to induce miR-146b, and STAT1, STAT3, and STAT5 are all involved in its regulation. Interestingly, EMSA confirmed direct STAT3 binding to the site 1.7kb upstream of miR-146b, but not to the 830bp site, despite both sites appearing equally functional in dual-luciferase reporter assays. The latter system is more physiological than EMSA, and the 830bp site, which lies in a highly GC-rich region, may bind STAT3 in its native sequence context but not as an isolated 25bp oligonucleotide. Even more physiological is chromatin immunoprecipitation (ChIP) assay of binding to endogenous DNA. Enrichment of STAT3 at these sites after IL-6 treatment was only 1.5 to 2-fold (data not shown), although this magnitude of induction can have biological significance (272, 273) and may not be

linearly correlated with the change in gene expression. It is also possible that STAT3 binding to native chromatin is transient or buried within a transcriptional complex.

Recruitment of RNA polymerase II and the transcriptional apparatus most likely occurs slightly downstream of the 830bp site, since the miR-146b primary transcript is approximately 700bp in length (199). We speculate that DNA surrounding the 1.7kb site may undergo looping to interact with the 830bp site and, in a cooperative manner, effect transcription at the miR-146b locus. This hypothesis could be tested using the chromatin conformation capture (3C) technique. Due to the report of a c-fos binding site about 600bp upstream of the 1.7kb STAT binding site (201), additional long-range interactions in the promoter region may occur. Additionally, the striking ability of MAPK to potentiate STAT-regulated miR-146b induction leads us to speculate that c-fos and related family members may act as pioneer factors for this region of chromatin. Finally, the precise roles of insulin and PI3K/Akt signaling in miR-146b regulation are more complex than for EGF and remain to be fully elucidated.

Possible Biological Significance of MiR-146b as a STAT-Responsive Gene

By identifying miR-146b as a novel STAT target, we have added a new regulatory dimension to this tumor suppressor, and we have expanded the relatively short list of known STAT miRNA targets. While STAT3 is generally considered oncogenic, studies have shown it can mediate effects that are opposed to cancer in specific situations. For example, STAT3 activation drives apoptosis during normal mammary gland involution (274). Interestingly, early involution was the mammary stage displaying the highest expression of miR-146b, which was induced over 25-fold relative to virgin tissue. In addition, STAT3 signaling inhibits the proliferation and motility of PTEN-deficient glioblastoma cells (275) and decreases *in vivo*

growth of papillary thyroid tumors (276). This is reminiscent of anti-tumor effects of oncogenic c-Myc and Ras in certain contexts (277, 278). It will be interesting to see if STAT3 regulation of miR-146b contributes to the cancer inhibitory effects of STAT3 outlined above.

Our work demonstrated that miR-146b functions as a feedback inhibitor of STAT3 via NF-κB and IL-6. However, miR-146b could modulate STAT pathway activity in other ways, which may include targeting STATs themselves. For instance, miR-146a has been reported to directly repress STAT1 (153), implying that miR-146b may do the same. In this way, STAT1 regulation of miR-146b could mediate negative feedback on STAT1. Very recently, miR-146b was shown to target two isoforms of STAT3: STAT3α and STAT3β (279). STAT3α is the normal full-length version of STAT3, whereas STAT3β has a C-terminal truncation and may inhibit STAT3α in a dominant-negative fashion (280). Thus, the interaction of miR-146b and STAT3 isoforms could affect STAT3 activity either positively or negatively, depending on the relative levels of each transcript and its affinity for miR-146b. Finally, miR-146b targeting of IRAK1 might modulate STAT3 through its role in STAT3 serine phosphorylation (281).

Additionally, some putative targets of miR-146b may influence STAT3 biology. For example, an epigenetic switch involving NF-κB and STAT3 mediates neoplastic transformation in part through upregulation of Lin28B, which contributes to persistent IL-6 (191). Interestingly, Lin28B is a predicted miR-146b target. Transfection of miR-146b mimic reduced Lin28B mRNA expression in SUM-159 cells by 50% (data not shown), with effects expected to be even larger at the protein level. Consequently, STAT3 induction of miR-146b in this context could interrupt critical oncogenic signaling networks by targeting Lin28B. However, since Lin28B is currently only a computationally predicted miR-146b target based on sequence analysis (Table 4.1), biological validation as a direct miR-146b target is required. This would be accomplished

by transferring the Lin28B 3' UTR to a luciferase reporter, followed by mutagenesis of the putative miR-146b binding sites leading to abrogated inhibition by miR-146b.

Besides targeting proteins involved in STAT3 activation, miR-146b may oppose STAT3 by targeting STAT3-dependent genes and critical mediators of STAT3-driven phenotypes, such as fibronectin, cathepsin B, and MMP-16. Except for MMP-16, these proteins have not yet been experimentally demonstrated as direct miR-146b targets, but contain predicted miR-146b binding sites in the 3' UTR that are conserved between mouse and human (Table 4.1). Fibronectin expression is elevated in STAT3C-transformed prostate epithelial cells, in which it contributes to EMT, motility, and transformation (83). Interestingly, miR-146b may also regulate EMT induced by TGF-β, as SMAD4 is a miR-146b target (282). Cathepsin B is upregulated by IL-6/STAT3 (283) and facilitates invasion of Ras-transformed MCF-10A cells (284). Lastly, MMP-16 activates the zymogen MMP-2, which is a direct STAT3 target gene and promotes invasion and metastasis (70). Therefore, miR-146b may be linked to STAT3 biology in multiple ways.

Table 4.1: Predicted miR-146b binding sites in human and mouse 3' UTRs of Lin28B, fibronectin, and cathepsin B (upper sequences, 5' → 3') aligned with miR-146b (bottom sequences, 3' → 5'). Watson-Crick base pairs are indicated as (|); wobble base pairs are shown as (:).

	Human	**Mouse**
Lin28B	5' ...GUUUUUAAGACAUCCAGUUCUCC... ::||	|| |||||||| 3' UCGGAUACCUUAAGUCAAGAGU	5' ...AGCCUGCGAACUAUUCGUUCUCU... |||||:			|: |||||| 3' UCGGAUACCUUA-AGUCAAGAGU
Fibronectin	5' ...UUGCUCUGGAGGA-AGUUCUCCA... || ||||: |||||| 3' UCGGAUACCUUAAGUCAAGAGU	5' ...UUGCUCUGGAGCCAUGUUCUCAG... || ||||: |||||| 3' UCGGAUACCUUAAGUCAAGAGU
Cathepsin B	5' ...UCAUAACCUCAAUAAAGUUCUCC... : ||| |||||| 3' UCGGAUACCUUAAGUCAAGAGU	5' ...UCAAUGGCCCAGUGCAGUUCUCU... : : |:| |||||||| 3' UCGGAUACCUUAAGUCAAGAGU

After we identified miR-146b as a STAT3 target gene, we wanted to determine if modulating miR-146b activity could affect STAT3-mediated transformation of MCF-10A cells. It has been reported that MCF-10A cells can be transformed by stable STAT3C expression (75) or transient IL-6 exposure (191). However, we were unable to reproduce these earlier findings of other groups. Possible reasons include genetic or epigenetic divergence of cell lines, as well as differences in growth conditions. Also, the low transformation efficiency of MCF-10A by STAT3C (about 1 in 2,000 cells) possibly indicates outgrowth of a rare clone. Notably, miR-146b was not among the miRNAs that were differentially expressed in MCF-10A cells transformed by Src or IL-6 (130), indicating it was not induced by STAT3 under the conditions of that study. This suggests altered regulation of miR-146b might underlie some of the inconsistent observations in MCF-10A cells.

Even if STAT3C transformed MCF-10A cells, we would not expect miR-146b to inhibit transformation through its effects on NF-κB and IL-6, since STAT3C is constitutively active independent of IL-6. It is possible miR-146b could inhibit transformation from transient IL-6 exposure if NF-κB activation converts the transient IL-6 signal into a persistent one (191). In either case, however, miR-146b may inhibit transformation of MCF-10A cells by targeting other proteins crucial to STAT3-driven transformation and cancer phenotypes, such as fibronectin and MMP-16/MMP-2 outlined above. Indeed, the incomplete rescue of motility in miR-146b-transfected SUM-159 cells by STAT3C (Figure 2.10) is probably due to continued repression of known miR-146b targets besides IL-6/STAT3, such as MMP-16, EGFR, CXCR4, ROCK1, and KLF4 (204, 208, 285). Additionally, NF-κB can promote motility separate from IL-6 and STAT3 (286), and those functions of NF-κB would remain suppressed by miR-146b even after introducing STAT3C.

Future Studies of MiR-146b

While our work strongly suggests STAT3 regulation of miR-146b is a key mechanism of tumor suppression, definitive proof requires generation of a miR-146b knockout mouse. The miR-146a knockout mouse already exists and develops lymphomas, chronic myeloproliferation, and myeloid sarcomas (287). This is consistent with the finding that deletion of miR-146a, located at 5q34, is a critical event in the pathogenesis of 5q- myelodysplastic syndrome (288). Compared to the miR-146a knockout, we speculate that mice lacking miR-146b would have an overlapping but distinct spectrum of malignancies, perhaps skewed towards IL-6-dependent cancers with dual activation of NF-κB and STAT3. Such tumors include colorectal cancer (106), breast cancer (29, 191, 219), multiple myeloma (253, 289, 290), and diffuse large B cell lymphoma (291). The mice may also exhibit disruptions in normal physiology, such as mammary gland lactation and involution, which are associated with STAT activation and miR-146b induction (279).

Our work also showed that pharmacological inhibition of STAT3 combined with miR-146b repletion can have a greater inhibitory effect than either treatment by itself in cancer cells with activation of the NF-κB/IL-6/STAT3 pathway. To further validate this approach as a viable therapy, we propose treating mouse xenografts with a JAK inhibitor and an IRAK1 inhibitor and monitoring tumor growth and metastasis. It is also reasonable to deliver a miR-146b mimetic in mice, since more targets than just IRAK1 are likely involved, and this modality may eventually become available in humans (292). Furthermore, the miR-146b locus at 10q24 is relatively close to the PTEN locus at 10q23, about 25Mbp away. Large deletions encompassing multiple tumor suppressors have been found to affect tumorigenesis (293), and it will be interesting to determine

if deletion of PTEN and miR-146b commonly occurs together in human cancers. If so, adding PI3K/mTOR inhibitors to the combination therapy regimen may be advantageous.

Discovery and Characterization of Atovaquone as a Novel STAT3 Inhibitor with Additional Anti-Cancer Effects

Using a chemical genomics database (232), we found the FDA-approved drug atovaquone to oppose the STAT3 gene expression signature (124). Therefore, we hypothesized that atovaquone could function as a STAT3 inhibitor. This was confirmed in subsequent experiments showing decreased STAT3 tyrosine phosphorylation and transcriptional activity after atovaquone treatment. Interestingly, atovaquone is not a kinase inhibitor, but downregulates the cell-surface expression of gp130 required for JAK/STAT3 activation. However, IL-6 receptor was not affected, which represents a novel drug mechanism. Additionally, atovaquone is well-tolerated in humans, achieves high plasma concentrations similar to those used in our studies (235), and kills STAT3-dependent cancer cells *in vitro.* Taken together, these observations support the potential use of atovaquone as a STAT3 inhibitor in the clinic.

On further investigation, we found the anti-cancer effects of atovaquone to be quite broad, covering diverse hematological tumor types and extending to cancer cells lacking STAT3 activation. This observation led us to hypothesize that atovaquone has additional cellular effects in addition to STAT3 inhibition. Indeed, by western blotting, we discovered atovaquone also inhibits phosphorylation of ribosomal protein S6 and p70S6K, suggesting decreased mTOR activity. However, this effect was blocked by transcription or translation inhibitors, implicating the role of an induced factor in this response. Using gene expression microarrays, upregulation of REDD1 was identified to mediate the effects of atovaquone on the mTOR pathway. Fortuitously,

these efforts also revealed UPR-related genes to be induced by atovaquone. Thus, we surmised atovaquone activates the phospho-eIF2α/ATF4 branch of the UPR, which was validated by western blot. Interestingly, however, other UPR branches are not activated.

Although atovaquone inhibits mitochondrial respiration in infectious organisms (235), and STAT3 can localize to the mitochondria (108), this is likely simply coincidental, and the effects of atovaquone on cancer cells are unlikely to involve the mitochondria. STAT3 serine phosphorylation, which is required for STAT3 mitochondrial localization, was not affected by atovaquone. Instead, atovaquone inhibition of STAT3 can be fully explained by the observed decrease of STAT3 tyrosine phosphorylation. In addition, there is no evidence that atovaquone can inhibit the activity of proteins in mammalian mitochondria, since otherwise the drug would have highly toxic side effects. Therefore, we conclude that the anti-neoplastic mechanism(s) of atovaquone ought to be distinct from its anti-microbial mechanism of action. Indeed, how atovaquone mediates its anti-cancer effects is a major question for future exploration.

In summary, atovaquone most likely kills cancer cells through a combination of its effects on STAT3, mTOR, and the UPR, depending on the cells in question. So far, the only cancer cell line not killed by atovaquone is Kasumi, in which atovaquone also fails to inhibit phospho-S6 (data not shown). Upregulation of REDD1 and inhibition of mTOR appear to be downstream of the UPR, since REDD1 is a known ATF4 target gene (241). However, the causal relationship, if any, between the downregulation of cell-surface gp130 and the activation of the phospho-eIF2α/ATF4 pathway is unclear. Since the UPR effects occur in cells lacking STAT3 activation, they are certainly not secondary to STAT3 inhibition, but could result from the altered regulation of gp130. The reverse is unlikely, as other UPR activators did not inhibit STAT3. As a

result of these various anti-cancer mechanisms, atovaquone may be able to treat a wide spectrum of tumors, and our data from patients and clinical records support its use clinically.

Role and Possible Mechanisms of Cell-Surface Gp130 Downregulation

As part of our investigation into how atovaquone inhibits STAT3, we demonstrated that reduced STAT3 phosphorylation was strongly associated with decreased cell-surface gp130 expression. By contrast, gp130 was unaffected by a pharmacological JAK inhibitor. Therefore, downregulation of cell-surface gp130 is mechanistically plausible as the explanation for STAT3 inhibition, and it would be highly coincidental if these two effects were unrelated. Nonetheless, the relationship is technically correlative at this time. To prove that gp130 downregulation causes reduced STAT3 activation, a rescue experiment is required in which blocking the effect of atovaquone on gp130 also prevents the effect on STAT3. However, designing such an experiment entails more mechanistic knowledge than is currently available. Several hypotheses concerning how atovaquone mediates its effect on gp130 have been considered, but this remains a critical question for future study.

One of the first hypotheses to be investigated was based on the report that p38 MAPK-dependent phosphorylation of gp130 at serine 782 promotes internalization from the plasma membrane and inhibits IL-6-dependent STAT3 activation (294). Encouragingly, we subsequently discovered that atovaquone rapidly induces p38 activation and gp130 phospho-S782 in U266 cells (data not shown). However, the significance of these findings was called into question when several p38 inhibitors did not rescue STAT3 phosphorylation, despite effectively blocking p38 activation and gp130 phosphorylation. Thus, in the context of atovaquone, the observed effects on p38 and phospho-S782 might serve as markers of drug treatment but seem

not to have a large role in the regulation of gp130 or STAT3. We also considered whether atovaquone might induce reactive oxygen species (ROS); however, N-acetyl cysteine (NAC), a ROS inhibitor, did not rescue STAT3 phosphorylation or cell viability, rendering this mechanism unlikely.

The relative selectivity of atovaquone for gp130 but not other transmembrane receptors raises the possibility that it might bind directly to gp130. Binding of a small molecule to a protein is difficult to detect, but could be probed using differential scanning fluorimetry (DSF) or drug affinity responsive target stability (DARTS). These techniques rely on proteins' increased resistance to thermal denaturation or proteolytic digestion, respectively, after ligand binding (295, 296). However, direct binding to gp130 is somewhat less likely due to the strikingly different kinetics of gp130 downregulation and STAT3 inhibition observed in different cell lines, ranging from rapid in U266 cells (within 10-15 minutes) to slow in HEL cells (at least 6 hours). More probably, atovaquone acts on another protein target(s), whose variability in expression and activity across different cell lines accounts for the varying kinetics of atovaquone.

Furthermore, it will be important to ascertain whether the effects on gp130 result from decreased entry to the plasma membrane or increased internalization. The latter could be shown by monitoring the intracellular appearance of antibody pre-labeled surface gp130 or by using endocytic inhibitors to block the effect. If these experiments give negative results, then gp130 may instead be hindered from entering the plasma membrane, but this would be more difficult to demonstrate experimentally. Interestingly, the natural compound ilimaquinone also impairs cell-surface protein expression (297), inhibits cell viability by upregulating CHOP (298), and shares a structural moiety with atovaquone (Figure 4.1). While the mechanistic targets of ilimaquinone are not known, it requires the activity of phospholipase D (299), and it will be interesting to see

if atovaquone has a similar requirement. However, ilimaquinone acts by causing large disruptions to the Golgi apparatus (297), and it is unclear how such a mechanism could specifically affect gp130 but not IL-6 receptor.

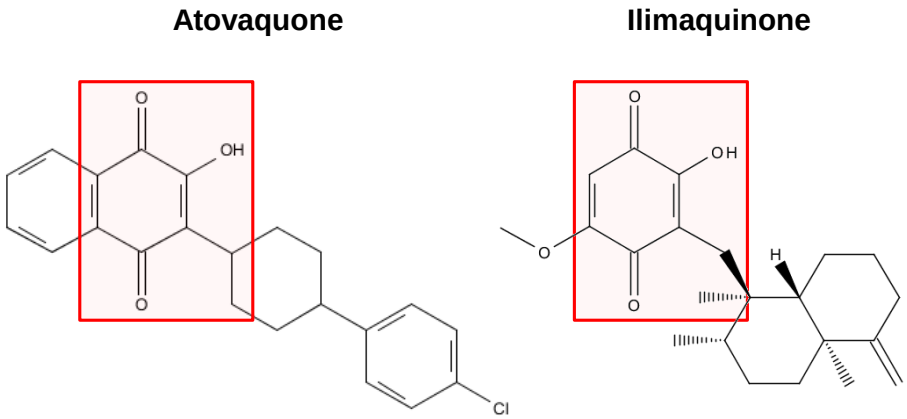

Figure 4.1: Comparison of molecular structures of atovaquone and ilimaquinone. A shared moiety is highlighted in red.

Future Studies of Atovaquone

One point of uncertainty is how atovaquone induces eIF2α phosphorylation. Four eIF2α kinases are known and respond to different stimuli: PERK (ER stress), protein kinase R (double-stranded RNA), GCN2 (amino acid starvation), and HRI (heme deficiency) (300). The role of each of these kinases can be assessed by western blot, knock down, and using knockout MEFs. Also, mass spectrometry-based phospho-proteomic profiling could uncover atovaquone-regulated pathways at a global level, leading quickly to the generation of focused hypotheses. More directly, a biotinylated version of atovaquone could help identify its molecular target(s) by pull-down of interacting proteins. Unfortunately, efforts to conjugate atovaquone to biotin have so far been hampered by its strong tendency to oxidize. In addition, this approach may fail if atovaquone binds its target(s) covalently, preventing their elution from the resin. Whether atovaquone acts reversibly or irreversibly could be tested in washout experiments.

Alternatively, an RNAi screen could be used to discover the protein target of atovaquone. However, the readout of such a screen would need to be carefully considered. One pitfall of this approach is that only one gene is knocked down at a time. If atovaquone has multiple targets, such as related members of a protein family, then they may be missed because of functional redundancy. Finally, the effects of atovaquone could be mediated through a mechanism that is not protein dependent. If that is the case, then RNAi screening and pull-down of directly interacting proteins may both prove to be unsuccessful. Fortunately, this possibility is unlikely, since it is hard to conceive of such a mechanism that is not also broadly nonspecific and highly toxic. By contrast, the side effect profile of atovaquone is extremely favorable, increasing the likelihood that it may be used as an anti-neoplastic agent.

To further demonstrate the utility of atovaquone as a cancer treatment *in vivo*, we propose conducting animal studies using xenografts of tumors that respond to atovaquone *in vitro*. Experiments with U266 cells, which form plasmacytomas when injected subcutaneously into mice, are in progress. Ultimately, we would like to conduct randomized, prospective clinical trials with cancer patients to investigate the efficacy of atovaquone on human malignancies. In the case of hematological cancers, clinical trials could be performed to administer atovaquone after stem cell transplant or as an added component to current chemotherapy regimens. Clinical trials could also be envisioned for solid tumors, pending additional laboratory study, since many display activation of STAT3 or mTOR. Also, atovaquone induction of pro-apoptotic UPR factors may be applicable to and clinically significant in various cancers.

Overall Conclusions

In summary, our work describes new physiological and pharmacological paradigms for the regulation of STAT3 in cancer. Specifically, we identified miR-146b as a novel STAT3

target gene and atovaquone as a promising STAT3 inhibitor. Both miR-146b and atovaquone modulate STAT3 activity through mechanisms not previously appreciated, and STAT3 activation by IL-6 is a major recurring theme. IL-6 has been implicated in the pathogenesis of a vast spectrum of hematological and solid cancers (301), suggesting our findings with miR-146b and atovaquone may also have broad significance. Additionally, these studies have given rise to new hypotheses for future investigation in both the laboratory and the clinic. While clinical trials can be lengthy and expensive, they are necessary to address the most important goal of this work: the advancement of therapy and patient care.

APPENDIX 1:

Supplemental Information

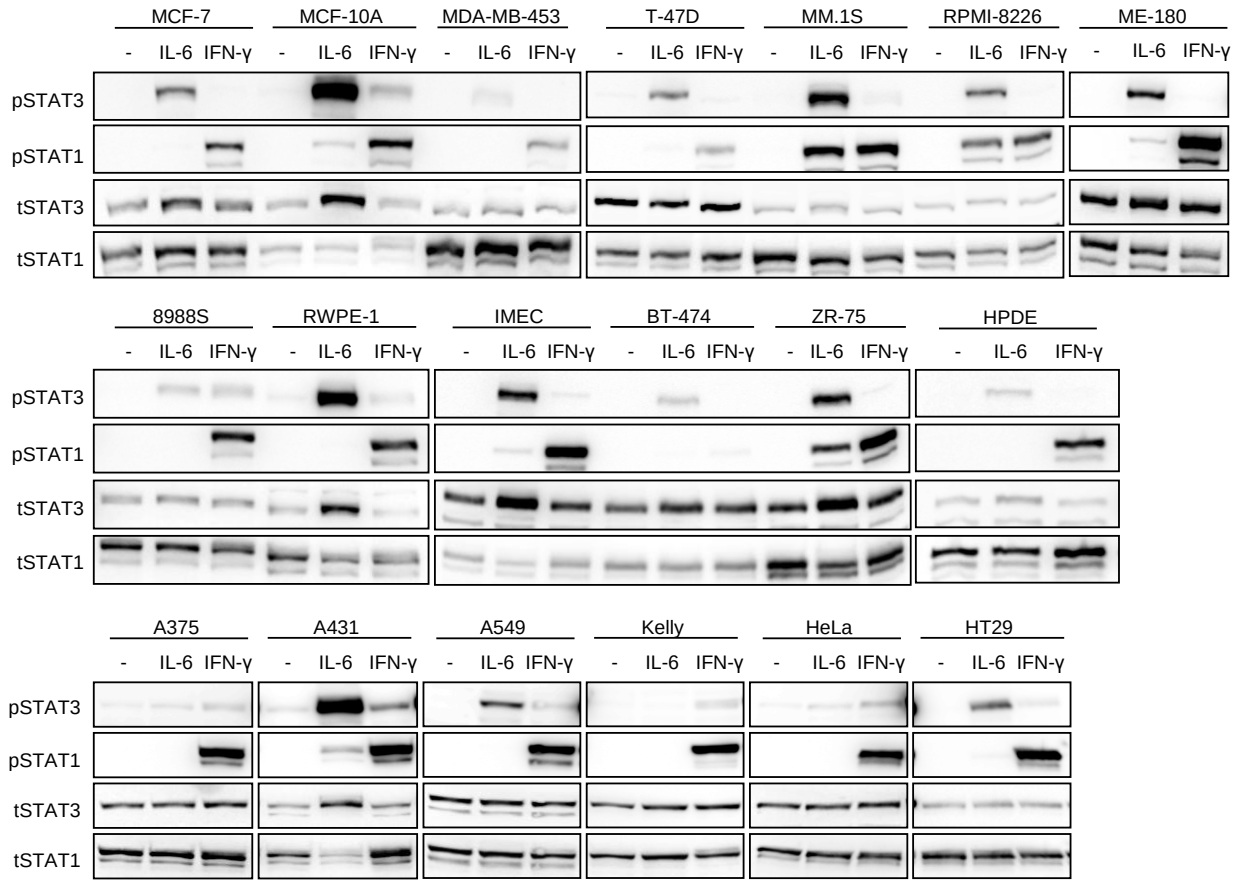

Supplemental Figure 1: STAT activation was induced in cells that lack basal STAT activation upon cytokine stimulation. Immunoblotting was performed on cells treated with IL-6 or IFN-γ (20ng/ml) for 15 minutes to detect phospho-tyrosine STAT3 or STAT1 and total STAT3 or STAT1.

Supplemental Table 1: Primer sequences used for qRT-PCR analysis

Gene	Forward (5'→3')	Reverse (5'→3')
18S rRNA	GTAACCCGTTGAACCCCATT	CCATCCAATCGGTAGTAGCG
Beta actin	TCCCTGGAGAAGAGCTACGA	AGCACTGTGTTGGCGTACAG
Pri-miR-146b	ATTCAGGGTTTTGGGGAGAT	GGGGCTTTCTGAGCTAAAGG
STAT3	ACCGGCGTCCAGTTCACTACT	CCGGGATCCTCTGAGAGCTGC
SOCS3	TCAAGACCTTCAGCTCCAAG	TGACGCTGAGCGTGAAGAAG
BIRC3	GGGAAGAGGAGAGAGAAAGAGC	TCCAGGATTGGAATTACACAAG
NFKB2	AGAGGGAGGAGGGCCTTTAG	CAGGTTCTGCTTCCCAGAAT
RELB	AGCATCCTTGGGGAGAGC	AGGCAGTCACCTCCACCTC
NFKBIE	CTCGCTCACCTACACCCTGT	CTCATGAATCACTGCCAGGT

Supplemental Table 1 (Continued)

IKB alpha	ACGAGCAGATGGTCAAGGAG	CTTCCATGGTCAGTGCCTTT
A20	CCTTGGAAGCACCATGTTTG	TTGTGTGGTTCGAGGCACAT
CCL2	TGCCCCAGTCACCTGCTGTT	CCCACTTCTGCTTGGGGTCAGC
IL6	GAAAGCAGCAAAGAGGCACT	TTTCACCAGGCAAGTCTCCT
RELA	CCACGAGCTTGTAGGAAAGG	CTGGATGCGCTGACTGATAG
JUNB	AAATGGAACAGCCCTTCT	TGTAGAGAGAGGCCACCA
MCL1	GAGACCTTACGACGGGTT	TTTGATGTCCAGTTTCCG
EGR1	AGCCCTACGAGCACCTGAC	AGCGGCCAGTATAGGTGATG
KLF4	TCCCATCTTTCTCCACGTTC	AGTCGCTTCATGTGGGAGAG
BCL6	CTGCAGATGGAGCATGTTGT	TCTTCACGAGGAGGCTTGAT
BCL3	CCTCTGGTGAACCTGCCTAC	TACCCTGCACCACAGCAATA
BCL-X	GGTATTGGTGAGTCGGATCG	TGCTGCATTGTTCCCATAGA
E-cadherin	CCTGGGACTCCACCTACAGA	TGTGAGCAATTCTGCTTGGA
Desmoplakin	GGCACCAGCAGGATGTACT	ATCAAGCAGTCGGAGCAGTT
Vimentin	TCAGAGAGAGGAAGCCGAAA	ATTCCACTTTGCGTTCAAGG
Cadherin-11	CAACGGACTATGAAACACAGGA	GAAAGGGCCATTGCTGATAA
Slug	TCGGACCCACACATTACCTT	TGACCTGTCTGCAAATGCTC
Cyclin D1	AGAGGCGGAGGAGAACAAAC	GGCGGATTGGAAATGAACTT
Survivin	GGACCACCGCATCTCTACAT	GTCTGGCTCGTTCTCAGTGG
BCL2	GCCCTGTGGATGACTGAGTA	AGGGCCAAACTGAGCAGAG
ATF4	CCAACAACAGCAAGGAGGAT	GTGTCATCCAACGTGGTCAG
BIP	CACAGTGGTGCCTACCAAGA	CAGTCAGATCAAATGTACCCAGA
Hsp90B1	AACGGGCAAGGACATCTCTA	CGTCGAAGCATGTCTCTGAT
DNAJC3	CATCTTGAATTGGGCAAGAAA	AGCCCTCCGATAATAAGCAA
HERP	GCGACTTGGAGCTGAGTGG	CCAACAACAGCTTCCCAGAAT
Erp72	AGCAGGTTTGATGTGAGTGG	TTCTCTGACCTTGGCAACAA
EDEM1	GTGAAAGCCCTTTGGAACCT	AGGCCACTCTGCTTTCCAAC
Spliced XBP1	CTGAGTCCGCAGCAGGTG	ACTGGGTCCAAGTTGTCCAG
ERdj4	TTTCACAAGTTGGCCATGAA	AAGCACTGTGTCCAAGTGTATCA
SEC61A1	AGCAGCAGATGGTGATGAGA	CCTAGGAAGTCAGCCAGGAC
gp130 (human)	GTCACCTCACACTCCTCCAAG	TTTGAACAGGTCCAATGATTTC
gp130 (mouse)	GGCACCAGCAGGATGTACT	ATCAAGCAGTCGGAGCAGTT

Supplemental Table 2: Probe lists used for Connectivity Map query

Up tags	**Down tags**
200730_s_at	202951_at
200731_s_at	216727_at
200732_s_at	212811_x_at
200733_s_at	209610_s_at
200796_s_at	209611_s_at
200797_s_at	212810_s_at
200798_x_at	
201473_at	
201693_s_at	
201694_s_at	
201995_at	
202679_at	
203140_at	
203574_at	
205962_at	
208683_at	
208743_s_at	
208875_s_at	
208876_s_at	
208877_at	
208878_s_at	
210512_s_at	
210513_s_at	
211527_x_at	
212171_x_at	
214056_at	
214057_at	
214888_at	
215990_s_at	
220266_s_at	
221841_s_at	

REFERENCES

1. Esteller M (2008) Epigenetics in cancer. *The New England journal of medicine* 358(11):1148-1159.
2. Hanahan D & Weinberg RA (2011) Hallmarks of cancer: the next generation. *Cell* 144(5):646-674.
3. Mbeunkui F & Johann DJ, Jr. (2009) Cancer and the tumor microenvironment: a review of an essential relationship. *Cancer chemotherapy and pharmacology* 63(4):571-582.
4. Kandoth C, *et al.* (2013) Integrated genomic characterization of endometrial carcinoma. *Nature* 497(7447):67-73.
5. Reis-Filho JS & Pusztai L (2011) Gene expression profiling in breast cancer: classification, prognostication, and prediction. *Lancet* 378(9805):1812-1823.
6. Nutt CL, *et al.* (2003) Gene expression-based classification of malignant gliomas correlates better with survival than histological classification. *Cancer research* 63(7):1602-1607.
7. Alizadeh AA, *et al.* (2000) Distinct types of diffuse large B-cell lymphoma identified by gene expression profiling. *Nature* 403(6769):503-511.
8. Brown S & Zeidler MP (2008) Unphosphorylated STATs go nuclear. *Current opinion in genetics & development* 18(5):455-460.
9. Braunstein J, Brutsaert S, Olson R, & Schindler C (2003) STATs dimerize in the absence of phosphorylation. *The Journal of biological chemistry* 278(36):34133-34140.
10. Lim CP & Cao X (2006) Structure, function, and regulation of STAT proteins. *Molecular bioSystems* 2(11):536-550.
11. Reich NC & Liu L (2006) Tracking STAT nuclear traffic. *Nature reviews. Immunology* 6(8):602-612.
12. Kim HS & Lee MS (2007) STAT1 as a key modulator of cell death. *Cellular signalling* 19(3):454-465.
13. Niu G, *et al.* (2005) Role of Stat3 in regulating p53 expression and function. *Molecular and cellular biology* 25(17):7432-7440.
14. Wojciak JM, Martinez-Yamout MA, Dyson HJ, & Wright PE (2009) Structural basis for recruitment of CBP/p300 coactivators by STAT1 and STAT2 transactivation domains. *The EMBO journal* 28(7):948-958.
15. Kisseleva T, Bhattacharya S, Braunstein J, & Schindler CW (2002) Signaling through the JAK/STAT pathway, recent advances and future challenges. *Gene* 285(1-2):1-24.
16. Jatiani SS, Baker SJ, Silverman LR, & Reddy EP (2010) Jak/STAT pathways in cytokine signaling and myeloproliferative disorders: approaches for targeted therapies. *Genes & cancer* 1(10):979-993.
17. Murray PJ (2007) The JAK-STAT signaling pathway: input and output integration. *J Immunol* 178(5):2623-2629.
18. Ivashkiv LB & Hu X (2004) Signaling by STATs. *Arthritis research & therapy* 6(4):159-168.
19. Silva CM (2004) Role of STATs as downstream signal transducers in Src family kinase-mediated tumorigenesis. *Oncogene* 23(48):8017-8023.
20. Schindler C & Plumlee C (2008) Inteferons pen the JAK-STAT pathway. *Seminars in cell & developmental biology* 19(4):311-318.

21. Lee JL, Wang MJ, & Chen JY (2009) Acetylation and activation of STAT3 mediated by nuclear translocation of CD44. *The Journal of cell biology* 185(6):949-957.
22. O'Sullivan LA, Liongue C, Lewis RS, Stephenson SE, & Ward AC (2007) Cytokine receptor signaling through the Jak-Stat-Socs pathway in disease. *Molecular immunology* 44(10):2497-2506.
23. Xu D & Qu CK (2008) Protein tyrosine phosphatases in the JAK/STAT pathway. *Frontiers in bioscience : a journal and virtual library* 13:4925-4932.
24. Haspel RL, Salditt-Georgieff M, & Darnell JE, Jr. (1996) The rapid inactivation of nuclear tyrosine phosphorylated Stat1 depends upon a protein tyrosine phosphatase. *The EMBO journal* 15(22):6262-6268.
25. Buettner R, Mora LB, & Jove R (2002) Activated STAT signaling in human tumors provides novel molecular targets for therapeutic intervention. *Clinical cancer research : an official journal of the American Association for Cancer Research* 8(4):945-954.
26. Koskela HL, *et al.* (2012) Somatic STAT3 mutations in large granular lymphocytic leukemia. *The New England journal of medicine* 366(20):1905-1913.
27. Scott E, Hexner E, Perl A, & Carroll M (2010) Targeted signal transduction therapies in myeloid malignancies. *Current oncology reports* 12(6):358-365.
28. Ghoshal Gupta S, Baumann H, & Wetzler M (2008) Epigenetic regulation of signal transducer and activator of transcription 3 in acute myeloid leukemia. *Leukemia research* 32(7):1005-1014.
29. Marotta LL, *et al.* (2011) The JAK2/STAT3 signaling pathway is required for growth of CD44(+)CD24(-) stem cell-like breast cancer cells in human tumors. *The Journal of clinical investigation* 121(7):2723-2735.
30. O'Shea JJ, Holland SM, & Staudt LM (2013) JAKs and STATs in immunity, immunodeficiency, and cancer. *The New England journal of medicine* 368(2):161-170.
31. Robinson DR, *et al.* (2013) Identification of recurrent NAB2-STAT6 gene fusions in solitary fibrous tumor by integrative sequencing. *Nature genetics* 45(2):180-185.
32. Merk BC, Owens JL, Lopes MB, Silva CM, & Hussaini IM (2011) STAT6 expression in glioblastoma promotes invasive growth. *BMC cancer* 11:184.
33. Das S, Roth CP, Wasson LM, & Vishwanatha JK (2007) Signal transducer and activator of transcription-6 (STAT6) is a constitutively expressed survival factor in human prostate cancer. *The Prostate* 67(14):1550-1564.
34. Klampfer L (2006) Signal transducers and activators of transcription (STATs): Novel targets of chemopreventive and chemotherapeutic drugs. *Current cancer drug targets* 6(2):107-121.
35. Frank DA (2007) STAT3 as a central mediator of neoplastic cellular transformation. *Cancer letters* 251(2):199-210.
36. Bromberg JF, Horvath CM, Besser D, Lathem WW, & Darnell JE, Jr. (1998) Stat3 activation is required for cellular transformation by v-src. *Molecular and cellular biology* 18(5):2553-2558.
37. Ning ZQ, Li J, McGuinness M, & Arceci RJ (2001) STAT3 activation is required for Asp(816) mutant c-Kit induced tumorigenicity. *Oncogene* 20(33):4528-4536.
38. Bromberg JF, *et al.* (1999) Stat3 as an oncogene. *Cell* 98(3):295-303.
39. Devarajan E & Huang S (2009) STAT3 as a central regulator of tumor metastases. *Current molecular medicine* 9(5):626-633.

40. Sinibaldi D, *et al.* (2000) Induction of p21WAF1/CIP1 and cyclin D1 expression by the Src oncoprotein in mouse fibroblasts: role of activated STAT3 signaling. *Oncogene* 19(48):5419-5427.
41. Fukada T, *et al.* (1998) STAT3 orchestrates contradictory signals in cytokine-induced G1 to S cell-cycle transition. *The EMBO journal* 17(22):6670-6677.
42. Huang H, Zhao W, & Yang D (2012) Stat3 induces oncogenic Skp2 expression in human cervical carcinoma cells. *Biochemical and biophysical research communications* 418(1):186-190.
43. Bowman T, *et al.* (2001) Stat3-mediated Myc expression is required for Src transformation and PDGF-induced mitogenesis. *Proceedings of the National Academy of Sciences of the United States of America* 98(13):7319-7324.
44. Shirogane T, *et al.* (1999) Synergistic roles for Pim-1 and c-Myc in STAT3-mediated cell cycle progression and antiapoptosis. *Immunity* 11(6):709-719.
45. Konnikova L, Simeone MC, Kruger MM, Kotecki M, & Cochran BH (2005) Signal transducer and activator of transcription 3 (STAT3) regulates human telomerase reverse transcriptase (hTERT) expression in human cancer and primary cells. *Cancer research* 65(15):6516-6520.
46. Stephanou A, Brar BK, Knight RA, & Latchman DS (2000) Opposing actions of STAT-1 and STAT-3 on the Bcl-2 and Bcl-x promoters. *Cell death and differentiation* 7(3):329-330.
47. Real PJ, *et al.* (2002) Resistance to chemotherapy via Stat3-dependent overexpression of Bcl-2 in metastatic breast cancer cells. *Oncogene* 21(50):7611-7618.
48. Grandis JR, *et al.* (2000) Constitutive activation of Stat3 signaling abrogates apoptosis in squamous cell carcinogenesis in vivo. *Proceedings of the National Academy of Sciences of the United States of America* 97(8):4227-4232.
49. Karni R, Jove R, & Levitzki A (1999) Inhibition of pp60c-Src reduces Bcl-XL expression and reverses the transformed phenotype of cells overexpressing EGF and HER-2 receptors. *Oncogene* 18(33):4654-4662.
50. Catlett-Falcone R, *et al.* (1999) Constitutive activation of Stat3 signaling confers resistance to apoptosis in human U266 myeloma cells. *Immunity* 10(1):105-115.
51. Bowman T, Garcia R, Turkson J, & Jove R (2000) STATs in oncogenesis. *Oncogene* 19(21):2474-2488.
52. Epling-Burnette PK, *et al.* (2001) Inhibition of STAT3 signaling leads to apoptosis of leukemic large granular lymphocytes and decreased Mcl-1 expression. *The Journal of clinical investigation* 107(3):351-362.
53. Puthier D, Bataille R, & Amiot M (1999) IL-6 up-regulates mcl-1 in human myeloma cells through JAK / STAT rather than ras / MAP kinase pathway. *European journal of immunology* 29(12):3945-3950.
54. Konnikova L, Kotecki M, Kruger MM, & Cochran BH (2003) Knockdown of STAT3 expression by RNAi induces apoptosis in astrocytoma cells. *BMC cancer* 3:23.
55. Gritsko T, *et al.* (2006) Persistent activation of stat3 signaling induces survivin gene expression and confers resistance to apoptosis in human breast cancer cells. *Clinical cancer research : an official journal of the American Association for Cancer Research* 12(1):11-19.
56. Kanda N, *et al.* (2004) STAT3 is constitutively activated and supports cell survival in association with survivin expression in gastric cancer cells. *Oncogene* 23(28):4921-4929.

57. Aoki Y, Feldman GM, & Tosato G (2003) Inhibition of STAT3 signaling induces apoptosis and decreases survivin expression in primary effusion lymphoma. *Blood* 101(4):1535-1542.
58. Ivanov VN, *et al.* (2001) Cooperation between STAT3 and c-jun suppresses Fas transcription. *Molecular cell* 7(3):517-528.
59. Niu G, *et al.* (2001) Overexpression of a dominant-negative signal transducer and activator of transcription 3 variant in tumor cells leads to production of soluble factors that induce apoptosis and cell cycle arrest. *Cancer research* 61(8):3276-3280.
60. Raz R, Lee CK, Cannizzaro LA, d'Eustachio P, & Levy DE (1999) Essential role of STAT3 for embryonic stem cell pluripotency. *Proceedings of the National Academy of Sciences of the United States of America* 96(6):2846-2851.
61. Zhang Q, *et al.* (2006) STAT3 induces transcription of the DNA methyltransferase 1 gene (DNMT1) in malignant T lymphocytes. *Blood* 108(3):1058-1064.
62. Gereige LM & Mikkola HK (2009) DNA methylation is a guardian of stem cell self-renewal and multipotency. *Nature genetics* 41(11):1164-1166.
63. Sherry MM, Reeves A, Wu JK, & Cochran BH (2009) STAT3 is required for proliferation and maintenance of multipotency in glioblastoma stem cells. *Stem Cells* 27(10):2383-2392.
64. Yang J, *et al.* (2013) Tumor-associated macrophages regulate murine breast cancer stem cells through a novel paracrine EGFR/Stat3/Sox-2 signaling pathway. *Stem Cells* 31(2):248-258.
65. Korkaya H, *et al.* (2012) Activation of an IL6 inflammatory loop mediates trastuzumab resistance in HER2+ breast cancer by expanding the cancer stem cell population. *Molecular cell* 47(4):570-584.
66. Scheitz CJ, Lee TS, McDermitt DJ, & Tumbar T (2012) Defining a tissue stem cell-driven Runx1/Stat3 signalling axis in epithelial cancer. *The EMBO journal* 31(21):4124-4139.
67. Tsuyada A, *et al.* (2012) CCL2 mediates cross-talk between cancer cells and stromal fibroblasts that regulates breast cancer stem cells. *Cancer research* 72(11):2768-2779.
68. Haricharan S & Li Y (2013) STAT signaling in mammary gland differentiation, cell survival and tumorigenesis. *Molecular and cellular endocrinology*.
69. Hedvat M, *et al.* (2009) The JAK2 inhibitor AZD1480 potently blocks Stat3 signaling and oncogenesis in solid tumors. *Cancer cell* 16(6):487-497.
70. Xie TX, *et al.* (2004) Stat3 activation regulates the expression of matrix metalloproteinase-2 and tumor invasion and metastasis. *Oncogene* 23(20):3550-3560.
71. Xie TX, *et al.* (2006) Activation of stat3 in human melanoma promotes brain metastasis. *Cancer research* 66(6):3188-3196.
72. Seo JM, Park S, & Kim JH (2012) Leukotriene B4 receptor-2 promotes invasiveness and metastasis of ovarian cancer cells through signal transducer and activator of transcription 3 (STAT3)-dependent up-regulation of matrix metalloproteinase 2. *The Journal of biological chemistry* 287(17):13840-13849.
73. Fukuda A, *et al.* (2011) Stat3 and MMP7 contribute to pancreatic ductal adenocarcinoma initiation and progression. *Cancer cell* 19(4):441-455.
74. Itoh M, *et al.* (2006) Requirement of STAT3 activation for maximal collagenase-1 (MMP-1) induction by epidermal growth factor and malignant characteristics in T24 bladder cancer cells. *Oncogene* 25(8):1195-1204.

75. Dechow TN, *et al.* (2004) Requirement of matrix metalloproteinase-9 for the transformation of human mammary epithelial cells by Stat3-C. *Proceedings of the National Academy of Sciences of the United States of America* 101(29):10602-10607.
76. Yamashita S, *et al.* (2004) Zinc transporter LIVI controls epithelial-mesenchymal transition in zebrafish gastrula organizer. *Nature* 429(6989):298-302.
77. Yadav A, Kumar B, Datta J, Teknos TN, & Kumar P (2011) IL-6 promotes head and neck tumor metastasis by inducing epithelial-mesenchymal transition via the JAK-STAT3-SNAIL signaling pathway. *Molecular cancer research : MCR* 9(12):1658-1667.
78. Cheng GZ, *et al.* (2008) Twist is transcriptionally induced by activation of STAT3 and mediates STAT3 oncogenic function. *The Journal of biological chemistry* 283(21):14665-14673.
79. Pakala SB, *et al.* (2013) MTA1 promotes STAT3 transcription and pulmonary metastasis in breast cancer. *Cancer research*.
80. Cho KH, *et al.* (2013) STAT3 mediates TGF-beta1-induced TWIST1 expression and prostate cancer invasion. *Cancer letters*.
81. Lo HW, *et al.* (2007) Epidermal growth factor receptor cooperates with signal transducer and activator of transcription 3 to induce epithelial-mesenchymal transition in cancer cells via up-regulation of TWIST gene expression. *Cancer research* 67(19):9066-9076.
82. Xiong H, *et al.* (2012) Roles of STAT3 and ZEB1 proteins in E-cadherin down-regulation and human colorectal cancer epithelial-mesenchymal transition. *The Journal of biological chemistry* 287(8):5819-5832.
83. Azare J, *et al.* (2007) Constitutively activated Stat3 induces tumorigenesis and enhances cell motility of prostate epithelial cells through integrin beta 6. *Molecular and cellular biology* 27(12):4444-4453.
84. Guo W, *et al.* (2006) Beta 4 integrin amplifies ErbB2 signaling to promote mammary tumorigenesis. *Cell* 126(3):489-502.
85. Snyder M, Huang XY, & Zhang JJ (2011) Signal transducers and activators of transcription 3 (STAT3) directly regulates cytokine-induced fascin expression and is required for breast cancer cell migration. *The Journal of biological chemistry* 286(45):38886-38893.
86. Ng DC, *et al.* (2006) Stat3 regulates microtubules by antagonizing the depolymerization activity of stathmin. *The Journal of cell biology* 172(2):245-257.
87. Silver DL, Naora H, Liu J, Cheng W, & Montell DJ (2004) Activated signal transducer and activator of transcription (STAT) 3: localization in focal adhesions and function in ovarian cancer cell motility. *Cancer research* 64(10):3550-3558.
88. Rundhaug JE (2005) Matrix metalloproteinases and angiogenesis. *Journal of cellular and molecular medicine* 9(2):267-285.
89. Niu G, *et al.* (2002) Constitutive Stat3 activity up-regulates VEGF expression and tumor angiogenesis. *Oncogene* 21(13):2000-2008.
90. Wei D, *et al.* (2003) Stat3 activation regulates the expression of vascular endothelial growth factor and human pancreatic cancer angiogenesis and metastasis. *Oncogene* 22(3):319-329.
91. Wei LH, *et al.* (2003) Interleukin-6 promotes cervical tumor growth by VEGF-dependent angiogenesis via a STAT3 pathway. *Oncogene* 22(10):1517-1527.

92. Yahata Y, *et al.* (2003) Nuclear translocation of phosphorylated STAT3 is essential for vascular endothelial growth factor-induced human dermal microvascular endothelial cell migration and tube formation. *The Journal of biological chemistry* 278(41):40026-40031.
93. Kujawski M, *et al.* (2008) Stat3 mediates myeloid cell-dependent tumor angiogenesis in mice. *The Journal of clinical investigation* 118(10):3367-3377.
94. Xu Q, *et al.* (2005) Targeting Stat3 blocks both HIF-1 and VEGF expression induced by multiple oncogenic growth signaling pathways. *Oncogene* 24(36):5552-5560.
95. Niu G, *et al.* (2008) Signal transducer and activator of transcription 3 is required for hypoxia-inducible factor-1alpha RNA expression in both tumor cells and tumor-associated myeloid cells. *Molecular cancer research : MCR* 6(7):1099-1105.
96. Burdelya L, *et al.* (2005) Stat3 activity in melanoma cells affects migration of immune effector cells and nitric oxide-mediated antitumor effects. *J Immunol* 174(7):3925-3931.
97. Groner B, Lucks P, & Borghouts C (2008) The function of Stat3 in tumor cells and their microenvironment. *Seminars in cell & developmental biology* 19(4):341-350.
98. Bollrath J & Greten FR (2009) IKK/NF-kappaB and STAT3 pathways: central signalling hubs in inflammation-mediated tumour promotion and metastasis. *EMBO reports* 10(12):1314-1319.
99. Nefedova Y, *et al.* (2004) Hyperactivation of STAT3 is involved in abnormal differentiation of dendritic cells in cancer. *J Immunol* 172(1):464-474.
100. Wang T, *et al.* (2004) Regulation of the innate and adaptive immune responses by Stat-3 signaling in tumor cells. *Nature medicine* 10(1):48-54.
101. Cheng F, *et al.* (2003) A critical role for Stat3 signaling in immune tolerance. *Immunity* 19(3):425-436.
102. Kortylewski M, *et al.* (2005) Inhibiting Stat3 signaling in the hematopoietic system elicits multicomponent antitumor immunity. *Nature medicine* 11(12):1314-1321.
103. Lee H, *et al.* (2010) STAT3-induced S1PR1 expression is crucial for persistent STAT3 activation in tumors. *Nature medicine* 16(12):1421-1428.
104. Deng J, *et al.* (2012) S1PR1-STAT3 signaling is crucial for myeloid cell colonization at future metastatic sites. *Cancer cell* 21(5):642-654.
105. Lesina M, *et al.* (2011) Stat3/Socs3 activation by IL-6 transsignaling promotes progression of pancreatic intraepithelial neoplasia and development of pancreatic cancer. *Cancer cell* 19(4):456-469.
106. Grivennikov S, *et al.* (2009) IL-6 and Stat3 are required for survival of intestinal epithelial cells and development of colitis-associated cancer. *Cancer cell* 15(2):103-113.
107. Bollrath J, *et al.* (2009) gp130-mediated Stat3 activation in enterocytes regulates cell survival and cell-cycle progression during colitis-associated tumorigenesis. *Cancer cell* 15(2):91-102.
108. Gough DJ, *et al.* (2009) Mitochondrial STAT3 supports Ras-dependent oncogenic transformation. *Science* 324(5935):1713-1716.
109. Demaria M, *et al.* (2010) A STAT3-mediated metabolic switch is involved in tumour transformation and STAT3 addiction. *Aging* 2(11):823-842.
110. Reddy MM, *et al.* (2012) The JAK2V617F oncogene requires expression of inducible phosphofructokinase/fructose-bisphosphatase 3 for cell growth and increased metabolic activity. *Leukemia* 26(3):481-489.
111. Gao X, Wang H, Yang JJ, Liu X, & Liu ZR (2012) Pyruvate kinase M2 regulates gene transcription by acting as a protein kinase. *Molecular cell* 45(5):598-609.

112. Garzon R, Calin GA, & Croce CM (2009) MicroRNAs in Cancer. *Annu Rev Med* 60:167-179.
113. Winter J, Jung S, Keller S, Gregory RI, & Diederichs S (2009) Many roads to maturity: microRNA biogenesis pathways and their regulation. *Nat Cell Biol* 11(3):228-234.
114. Okamura K, Liu N, & Lai EC (2009) Distinct mechanisms for microRNA strand selection by Drosophila Argonautes. *Molecular cell* 36(3):431-444.
115. Hu HY, *et al.* (2009) Sequence features associated with microRNA strand selection in humans and flies. *BMC genomics* 10:413.
116. Carthew RW & Sontheimer EJ (2009) Origins and Mechanisms of miRNAs and siRNAs. *Cell* 136(4):642-655.
117. Bartel DP (2009) MicroRNAs: target recognition and regulatory functions. *Cell* 136(2):215-233.
118. Liu J (2008) Control of protein synthesis and mRNA degradation by microRNAs. *Curr Opin Cell Biol* 20(2):214-221.
119. Lewis BP, Burge CB, & Bartel DP (2005) Conserved seed pairing, often flanked by adenosines, indicates that thousands of human genes are microRNA targets. *Cell* 120(1):15-20.
120. Miranda KC, *et al.* (2006) A pattern-based method for the identification of MicroRNA binding sites and their corresponding heteroduplexes. *Cell* 126(6):1203-1217.
121. Schmittgen TD (2008) Regulation of microRNA processing in development, differentiation and cancer. *J Cell Mol Med* 12(5B):1811-1819.
122. Calin GA, *et al.* (2004) Human microRNA genes are frequently located at fragile sites and genomic regions involved in cancers. *Proc Natl Acad Sci U S A* 101(9):2999-3004.
123. Shi XB, Tepper CG, & deVere White RW (2008) Cancerous miRNAs and their regulation. *Cell Cycle* 7(11):1529-1538.
124. Alvarez JV, *et al.* (2005) Identification of a genetic signature of activated signal transducer and activator of transcription 3 in human tumors. *Cancer research* 65(12):5054-5062.
125. Hu G, *et al.* (2010) miR-221 suppresses ICAM-1 translation and regulates interferon-gamma-induced ICAM-1 expression in human cholangiocytes. *Am J Physiol Gastrointest Liver Physiol* 298(4):G542-550.
126. Schmitt MJ, *et al.* (2012) Interferon-gamma-induced activation of Signal Transducer and Activator of Transcription 1 (STAT1) up-regulates the tumor suppressing microRNA-29 family in melanoma cells. *Cell communication and signaling : CCS* 10(1):41.
127. Li G, *et al.* (2010) STAT5 requires the N-domain for suppression of miR15/16, induction of bcl-2, and survival signaling in myeloproliferative disease. *Blood* 115(7):1416-1424.
128. Loffler D, *et al.* (2007) Interleukin-6 dependent survival of multiple myeloma cells involves the Stat3-mediated induction of microRNA-21 through a highly conserved enhancer. *Blood* 110(4):1330-1333.
129. Yang CH, Yue J, Fan M, & Pfeffer LM (2010) IFN induces miR-21 through a signal transducer and activator of transcription 3-dependent pathway as a suppressive negative feedback on IFN-induced apoptosis. *Cancer research* 70(20):8108-8116.
130. Iliopoulos D, Jaeger SA, Hirsch HA, Bulyk ML, & Struhl K (2010) STAT3 activation of miR-21 and miR-181b-1 via PTEN and CYLD are part of the epigenetic switch linking inflammation to cancer. *Molecular cell* 39(4):493-506.

131. Ohno M, *et al.* (2009) The modulation of microRNAs by type I IFN through the activation of signal transducers and activators of transcription 3 in human glioma. *Molecular cancer research : MCR* 7(12):2022-2030.
132. Brock M, *et al.* (2009) Interleukin-6 modulates the expression of the bone morphogenic protein receptor type II through a novel STAT3-microRNA cluster 17/92 pathway. *Circulation research* 104(10):1184-1191.
133. He L, *et al.* (2005) A microRNA polycistron as a potential human oncogene. *Nature* 435(7043):828-833.
134. Hong L, *et al.* (2010) The miR-17-92 cluster of microRNAs confers tumorigenicity by inhibiting oncogene-induced senescence. *Cancer research* 70(21):8547-8557.
135. Chen L, *et al.* (2011) miR-17-92 cluster microRNAs confers tumorigenicity in multiple myeloma. *Cancer letters* 309(1):62-70.
136. Olive V, Jiang I, & He L (2010) mir-17-92, a cluster of miRNAs in the midst of the cancer network. *The international journal of biochemistry & cell biology* 42(8):1348-1354.
137. Dai B, *et al.* (2011) STAT3 mediates resistance to MEK inhibitor through microRNA miR-17. *Cancer research* 71(10):3658-3668.
138. Ghosh AK, *et al.* (2009) Aberrant regulation of pVHL levels by microRNA promotes the HIF/VEGF axis in CLL B cells. *Blood* 113(22):5568-5574.
139. Wu W, *et al.* (2013) MicroRNA-18a modulates STAT3 activity through negative regulation of PIAS3 during gastric adenocarcinogenesis. *British journal of cancer* 108(3):653-661.
140. Brock M, *et al.* (2011) MicroRNA-18a enhances the interleukin-6-mediated production of the acute-phase proteins fibrinogen and haptoglobin in human hepatocytes. *The Journal of biological chemistry* 286(46):40142-40150.
141. Pichiorri F, *et al.* (2008) MicroRNAs regulate critical genes associated with multiple myeloma pathogenesis. *Proceedings of the National Academy of Sciences of the United States of America* 105(35):12885-12890.
142. Foshay KM & Gallicano GI (2009) miR-17 family miRNAs are expressed during early mammalian development and regulate stem cell differentiation. *Developmental biology* 326(2):431-443.
143. Carraro G, *et al.* (2009) miR-17 family of microRNAs controls FGF10-mediated embryonic lung epithelial branching morphogenesis through MAPK14 and STAT3 regulation of E-Cadherin distribution. *Developmental biology* 333(2):238-250.
144. Zhang M, *et al.* (2011) Both miR-17-5p and miR-20a alleviate suppressive potential of myeloid-derived suppressor cells by modulating STAT3 expression. *J Immunol* 186(8):4716-4724.
145. Cascio S, *et al.* (2010) miR-20b modulates VEGF expression by targeting HIF-1 alpha and STAT3 in MCF-7 breast cancer cells. *Journal of cellular physiology* 224(1):242-249.
146. Hatziapostolou M, *et al.* (2011) An HNF4alpha-miRNA inflammatory feedback circuit regulates hepatocellular oncogenesis. *Cell* 147(6):1233-1247.
147. Yang X, *et al.* (2013) MicroRNA-26a suppresses tumor growth and metastasis of human hepatocellular carcinoma by targeting IL-6-Stat3 pathway. *Hepatology*.
148. Zhu H, *et al.* (2013) NPM-ALK up-regulates iNOS expression through a STAT3/microRNA-26a-dependent mechanism. *The Journal of pathology* 230(1):82-94.

149. Liu LH, *et al.* (2011) miR-125b suppresses the proliferation and migration of osteosarcoma cells through down-regulation of STAT3. *Biochemical and biophysical research communications* 416(1-2):31-38.
150. Surdziel E, *et al.* (2011) Enforced expression of miR-125b affects myelopoiesis by targeting multiple signaling pathways. *Blood* 117(16):4338-4348.
151. Dentelli P, *et al.* (2010) microRNA-222 controls neovascularization by regulating signal transducer and activator of transcription 5A expression. *Arteriosclerosis, thrombosis, and vascular biology* 30(8):1562-1568.
152. Gregersen LH, *et al.* (2010) MicroRNA-145 targets YES and STAT1 in colon cancer cells. *PloS one* 5(1):e8836.
153. Tang Y, *et al.* (2009) MicroRNA-146A contributes to abnormal activation of the type I interferon pathway in human lupus by targeting the key signaling proteins. *Arthritis and rheumatism* 60(4):1065-1075.
154. Wang Y, *et al.* (2010) Lethal-7 is down-regulated by the hepatitis B virus x protein and targets signal transducer and activator of transcription 3. *Journal of hepatology* 53(1):57-66.
155. Chen Q, *et al.* (2012) Inducible microRNA-223 down-regulation promotes TLR-triggered IL-6 and IL-1beta production in macrophages by targeting STAT3. *PloS one* 7(8):e42971.
156. Wei J, *et al.* (2013) miR-124 inhibits STAT3 signaling to enhance T cell-mediated immune clearance of glioma. *Cancer research*.
157. Du L, *et al.* (2012) miR-337-3p and its targets STAT3 and RAP1A modulate taxane sensitivity in non-small cell lung cancers. *PloS one* 7(6):e39167.
158. Majid S, *et al.* (2011) MicroRNA-205 inhibits Src-mediated oncogenic pathways in renal cancer. *Cancer research* 71(7):2611-2621.
159. Wu H, *et al.* (2012) MiR-135a targets JAK2 and inhibits gastric cancer cell proliferation. *Cancer biology & therapy* 13(5):281-288.
160. Matsuyama H, *et al.* (2011) miR-135b mediates NPM-ALK-driven oncogenicity and renders IL-17-producing immunophenotype to anaplastic large cell lymphoma. *Blood* 118(26):6881-6892.
161. Moffatt CE & Lamont RJ (2011) Porphyromonas gingivalis induction of microRNA-203 expression controls suppressor of cytokine signaling 3 in gingival epithelial cells. *Infection and immunity* 79(7):2632-2637.
162. Su C, Hou Z, Zhang C, Tian Z, & Zhang J (2011) Ectopic expression of microRNA-155 enhances innate antiviral immunity against HBV infection in human hepatoma cells. *Virology journal* 8:354.
163. Jiang S, *et al.* (2010) MicroRNA-155 Functions as an OncomiR in Breast Cancer by Targeting the Suppressor of Cytokine Signaling 1 Gene. *Cancer Res*.
164. Kutty RK, *et al.* (2010) Inflammatory cytokines regulate microRNA-155 expression in human retinal pigment epithelial cells by activating JAK/STAT pathway. *Biochemical and biophysical research communications* 402(2):390-395.
165. Zhuang G, *et al.* (2012) Tumour-secreted miR-9 promotes endothelial cell migration and angiogenesis by activating the JAK-STAT pathway. *The EMBO journal* 31(17):3513-3523.
166. Krichevsky AM, Sonntag KC, Isacson O, & Kosik KS (2006) Specific microRNAs modulate embryonic stem cell-derived neurogenesis. *Stem Cells* 24(4):857-864.

167. Johnston PA & Grandis JR (2011) STAT3 signaling: anticancer strategies and challenges. *Molecular interventions* 11(1):18-26.
168. Minegishi Y, *et al.* (2007) Dominant-negative mutations in the DNA-binding domain of STAT3 cause hyper-IgE syndrome. *Nature* 448(7157):1058-1062.
169. Debnath B, Xu S, & Neamati N (2012) Small molecule inhibitors of signal transducer and activator of transcription 3 (Stat3) protein. *Journal of medicinal chemistry* 55(15):6645-6668.
170. Sansone P & Bromberg J (2012) Targeting the interleukin-6/Jak/stat pathway in human malignancies. *Journal of clinical oncology : official journal of the American Society of Clinical Oncology* 30(9):1005-1014.
171. Alvarez JV, Greulich H, Sellers WR, Meyerson M, & Frank DA (2006) Signal transducer and activator of transcription 3 is required for the oncogenic effects of non-small-cell lung cancer-associated mutations of the epidermal growth factor receptor. *Cancer research* 66(6):3162-3168.
172. Sen B, Saigal B, Parikh N, Gallick G, & Johnson FM (2009) Sustained Src inhibition results in signal transducer and activator of transcription 3 (STAT3) activation and cancer cell survival via altered Janus-activated kinase-STAT3 binding. *Cancer research* 69(5):1958-1965.
173. Flowers LO, Subramaniam PS, & Johnson HM (2005) A SOCS-1 peptide mimetic inhibits both constitutive and IL-6 induced activation of STAT3 in prostate cancer cells. *Oncogene* 24(12):2114-2120.
174. Turkson J, *et al.* (2004) Novel peptidomimetic inhibitors of signal transducer and activator of transcription 3 dimerization and biological activity. *Molecular cancer therapeutics* 3(3):261-269.
175. Becker S, Groner B, & Muller CW (1998) Three-dimensional structure of the Stat3beta homodimer bound to DNA. *Nature* 394(6689):145-151.
176. Song H, Wang R, Wang S, & Lin J (2005) A low-molecular-weight compound discovered through virtual database screening inhibits Stat3 function in breast cancer cells. *Proceedings of the National Academy of Sciences of the United States of America* 102(13):4700-4705.
177. Siddiquee K, *et al.* (2007) Selective chemical probe inhibitor of Stat3, identified through structure-based virtual screening, induces antitumor activity. *Proceedings of the National Academy of Sciences of the United States of America* 104(18):7391-7396.
178. Schust J, Sperl B, Hollis A, Mayer TU, & Berg T (2006) Stattic: a small-molecule inhibitor of STAT3 activation and dimerization. *Chemistry & biology* 13(11):1235-1242.
179. Xi S, Gooding WE, & Grandis JR (2005) In vivo antitumor efficacy of STAT3 blockade using a transcription factor decoy approach: implications for cancer therapy. *Oncogene* 24(6):970-979.
180. Zhang X, Zhang J, Wang L, Wei H, & Tian Z (2007) Therapeutic effects of STAT3 decoy oligodeoxynucleotide on human lung cancer in xenograft mice. *BMC cancer* 7:149.
181. Sen M, *et al.* (2012) First-in-human trial of a STAT3 decoy oligonucleotide in head and neck tumors: implications for cancer therapy. *Cancer discovery* 2(8):694-705.
182. Turkson J, *et al.* (2005) A novel platinum compound inhibits constitutive Stat3 signaling and induces cell cycle arrest and apoptosis of malignant cells. *The Journal of biological chemistry* 280(38):32979-32988.

183. Lee YK, Isham CR, Kaufman SH, & Bible KC (2006) Flavopiridol disrupts STAT3/DNA interactions, attenuates STAT3-directed transcription, and combines with the Jak kinase inhibitor AG490 to achieve cytotoxic synergy. *Molecular cancer therapeutics* 5(1):138-148.
184. Nelson EA, *et al.* (2011) The STAT5 inhibitor pimozide decreases survival of chronic myelogenous leukemia cells resistant to kinase inhibitors. *Blood* 117(12):3421-3429.
185. Takakura A, *et al.* (2011) Pyrimethamine inhibits adult polycystic kidney disease by modulating STAT signaling pathways. *Human molecular genetics* 20(21):4143-4154.
186. Nelson EA, *et al.* (2008) Nifuroxazide inhibits survival of multiple myeloma cells by directly inhibiting STAT3. *Blood* 112(13):5095-5102.
187. Nelson EA, *et al.* (2012) The STAT5 Inhibitor Pimozide Displays Efficacy in Models of Acute Myelogenous Leukemia Driven by FLT3 Mutations. *Genes & cancer* 3(7-8):503-511.
188. Hodge DR, Hurt EM, & Farrar WL (2005) The role of IL-6 and STAT3 in inflammation and cancer. *Eur J Cancer* 41(16):2502-2512.
189. Grivennikov S & Karin M (2008) Autocrine IL-6 signaling: a key event in tumorigenesis? *Cancer cell* 13(1):7-9.
190. Libermann TA & Baltimore D (1990) Activation of interleukin-6 gene expression through the NF-kappa B transcription factor. *Molecular and cellular biology* 10(5):2327-2334.
191. Iliopoulos D, Hirsch HA, & Struhl K (2009) An epigenetic switch involving NF-kappaB, Lin28, Let-7 MicroRNA, and IL6 links inflammation to cell transformation. *Cell* 139(4):693-706.
192. Ndlovu MN, *et al.* (2009) Hyperactivated NF-{kappa}B and AP-1 transcription factors promote highly accessible chromatin and constitutive transcription across the interleukin-6 gene promoter in metastatic breast cancer cells. *Molecular and cellular biology* 29(20):5488-5504.
193. Matsumoto G, *et al.* (2005) Targeting of nuclear factor kappaB Pathways by dehydroxymethylepoxyquinomicin, a novel inhibitor of breast carcinomas: antitumor and antiangiogenic potential in vivo. *Clinical cancer research : an official journal of the American Association for Cancer Research* 11(3):1287-1293.
194. Xiao W, *et al.* (2004) Co-operative functions between nuclear factors NFkappaB and CCAT/enhancer-binding protein-beta (C/EBP-beta) regulate the IL-6 promoter in autocrine human prostate cancer cells. *The Prostate* 61(4):354-370.
195. Domingo-Domenech J, *et al.* (2006) Interleukin 6, a nuclear factor-kappaB target, predicts resistance to docetaxel in hormone-independent prostate cancer and nuclear factor-kappaB inhibition by PS-1145 enhances docetaxel antitumor activity. *Clinical cancer research : an official journal of the American Association for Cancer Research* 12(18):5578-5586.
196. Yang J, *et al.* (2012) Ikk4a/Arf inactivation with activation of the NF-kappaB/IL-6 pathway is sufficient to drive the development and growth of angiosarcoma. *Cancer research* 72(18):4682-4695.
197. Liang J, *et al.* (2012) Sphingosine-1-Phosphate Links Persistent STAT3 Activation, Chronic Intestinal Inflammation, and Development of Colitis-Associated Cancer. *Cancer cell*.

198. Neilson LM, *et al.* (2007) Coactivation of janus tyrosine kinase (Jak)1 positively modulates prolactin-Jak2 signaling in breast cancer: recruitment of ERK and signal transducer and activator of transcription (Stat)3 and enhancement of Akt and Stat5a/b pathways. *Mol Endocrinol* 21(9):2218-2232.
199. Taganov KD, Boldin MP, Chang KJ, & Baltimore D (2006) NF-kappaB-dependent induction of microRNA miR-146, an inhibitor targeted to signaling proteins of innate immune responses. *Proceedings of the National Academy of Sciences of the United States of America* 103(33):12481-12486.
200. Walker SR, Nelson EA, & Frank DA (2007) STAT5 represses BCL6 expression by binding to a regulatory region frequently mutated in lymphomas. *Oncogene* 26(2):224-233.
201. Shao M, *et al.* (2011) PDGF induced microRNA alterations in cancer cells. *Nucleic acids research* 39(10):4035-4047.
202. Bhaumik D, *et al.* (2008) Expression of microRNA-146 suppresses NF-kappaB activity with reduction of metastatic potential in breast cancer cells. *Oncogene* 27(42):5643-5647.
203. Hurst DR, *et al.* (2009) Breast cancer metastasis suppressor 1 up-regulates miR-146, which suppresses breast cancer metastasis. *Cancer research* 69(4):1279-1283.
204. Xia H, *et al.* (2009) microRNA-146b inhibits glioma cell migration and invasion by targeting MMPs. *Brain research* 1269:158-165.
205. Kontzias A, Kotlyar A, Laurence A, Changelian P, & O'Shea JJ (2012) Jakinibs: a new class of kinase inhibitors in cancer and autoimmune disease. *Current opinion in pharmacology* 12(4):464-470.
206. Sansone P, *et al.* (2007) IL-6 triggers malignant features in mammospheres from human ductal breast carcinoma and normal mammary gland. *The Journal of clinical investigation* 117(12):3988-4002.
207. Rokavec M, Wu W, & Luo JL (2012) IL6-mediated suppression of miR-200c directs constitutive activation of inflammatory signaling circuit driving transformation and tumorigenesis. *Molecular cell* 45(6):777-789.
208. Katakowski M, *et al.* (2010) MiR-146b-5p suppresses EGFR expression and reduces in vitro migration and invasion of glioma. *Cancer investigation* 28(10):1024-1030.
209. Li Y, *et al.* (2010) miR-146a suppresses invasion of pancreatic cancer cells. *Cancer research* 70(4):1486-1495.
210. Hou Z, Xie L, Yu L, Qian X, & Liu B (2012) MicroRNA-146a is down-regulated in gastric cancer and regulates cell proliferation and apoptosis. *Med Oncol* 29(2):886-892.
211. Xu B, *et al.* (2012) MiR-146a suppresses tumor growth and progression by targeting EGFR pathway and in a p-ERK-dependent manner in castration-resistant prostate cancer. *The Prostate* 72(11):1171-1178.
212. Lin SL, Chiang A, Chang D, & Ying SY (2008) Loss of mir-146a function in hormone-refractory prostate cancer. *RNA* 14(3):417-424.
213. Grivennikov SI & Karin M (2010) Dangerous liaisons: STAT3 and NF-kappaB collaboration and crosstalk in cancer. *Cytokine & growth factor reviews* 21(1):11-19.
214. Fan Y, Mao R, & Yang J (2013) NF-kappaB and STAT3 signaling pathways collaboratively link inflammation to cancer. *Protein & cell* 4(3):176-185.
215. Lee H, *et al.* (2009) Persistently activated Stat3 maintains constitutive NF-kappaB activity in tumors. *Cancer cell* 15(4):283-293.

216. Tye H, *et al.* (2012) STAT3-Driven Upregulation of TLR2 Promotes Gastric Tumorigenesis Independent of Tumor Inflammation. *Cancer cell* 22(4):466-478.
217. Ebert MS & Sharp PA (2012) Roles for microRNAs in conferring robustness to biological processes. *Cell* 149(3):515-524.
218. Kanaan Z, *et al.* (2012) Differential microRNA expression tracks neoplastic progression in inflammatory bowel disease-associated colorectal cancer. *Human mutation* 33(3):551-560.
219. Liu M, *et al.* (2010) The canonical NF-kappaB pathway governs mammary tumorigenesis in transgenic mice and tumor stem cell expansion. *Cancer research* 70(24):10464-10473.
220. Grivennikov SI, Greten FR, & Karin M (2010) Immunity, inflammation, and cancer. *Cell* 140(6):883-899.
221. Debnath J, Muthuswamy SK, & Brugge JS (2003) Morphogenesis and oncogenesis of MCF-10A mammary epithelial acini grown in three-dimensional basement membrane cultures. *Methods* 30(3):256-268.
222. DiRenzo J, *et al.* (2002) Growth factor requirements and basal phenotype of an immortalized mammary epithelial cell line. *Cancer research* 62(1):89-98.
223. Ouyang H, *et al.* (2000) Immortal human pancreatic duct epithelial cell lines with near normal genotype and phenotype. *The American journal of pathology* 157(5):1623-1631.
224. Walker SR, Chaudhury M, Nelson EA, & Frank DA (2010) Microtubule-targeted chemotherapeutic agents inhibit signal transducer and activator of transcription 3 (STAT3) signaling. *Molecular pharmacology* 78(5):903-908.
225. Walker SR, *et al.* (2009) Reciprocal effects of STAT5 and STAT3 in breast cancer. *Molecular cancer research : MCR* 7(6):966-976.
226. Singal R, van Wert J, & Bashambu M (2001) Cytosine methylation represses glutathione S-transferase P1 (GSTP1) gene expression in human prostate cancer cells. *Cancer research* 61(12):4820-4826.
227. Battle TE & Frank DA (2003) STAT1 mediates differentiation of chronic lymphocytic leukemia cells in response to Bryostatin 1. *Blood* 102(8):3016-3024.
228. Battle TE, Arbiser J, & Frank DA (2005) The natural product honokiol induces caspase-dependent apoptosis in B-cell chronic lymphocytic leukemia (B-CLL) cells. *Blood* 106(2):690-697.
229. Frank DA, Mahajan S, & Ritz J (1997) B lymphocytes from patients with chronic lymphocytic leukemia contain signal transducer and activator of transcription (STAT) 1 and STAT3 constitutively phosphorylated on serine residues. *The Journal of clinical investigation* 100(12):3140-3148.
230. Sawyers C (2004) Targeted cancer therapy. *Nature* 432(7015):294-297.
231. Haftchenary S, Avadisian M, & Gunning PT (2011) Inhibiting aberrant Stat3 function with molecular therapeutics: a progress report. *Anti-cancer drugs* 22(2):115-127.
232. Lamb J, *et al.* (2006) The Connectivity Map: using gene-expression signatures to connect small molecules, genes, and disease. *Science* 313(5795):1929-1935.
233. Hieronymus H, *et al.* (2006) Gene expression signature-based chemical genomic prediction identifies a novel class of HSP90 pathway modulators. *Cancer cell* 10(4):321-330.
234. Wei G, *et al.* (2006) Gene expression-based chemical genomics identifies rapamycin as a modulator of MCL1 and glucocorticoid resistance. *Cancer cell* 10(4):331-342.

235. Baggish AL & Hill DR (2002) Antiparasitic agent atovaquone. *Antimicrobial agents and chemotherapy* 46(5):1163-1173.
236. Burger R, *et al.* (2009) Janus kinase inhibitor INCB20 has antiproliferative and apoptotic effects on human myeloma cells in vitro and in vivo. *Molecular cancer therapeutics* 8(1):26-35.
237. Andraos R, *et al.* (2012) Modulation of activation-loop phosphorylation by JAK inhibitors is binding mode dependent. *Cancer discovery* 2(6):512-523.
238. Lu X, *et al.* (2005) Expression of a homodimeric type I cytokine receptor is required for JAK2V617F-mediated transformation. *Proceedings of the National Academy of Sciences of the United States of America* 102(52):18962-18967.
239. Guertin DA & Sabatini DM (2005) An expanding role for mTOR in cancer. *Trends in molecular medicine* 11(8):353-361.
240. DeYoung MP, Horak P, Sofer A, Sgroi D, & Ellisen LW (2008) Hypoxia regulates TSC1/2-mTOR signaling and tumor suppression through REDD1-mediated 14-3-3 shuttling. *Genes & development* 22(2):239-251.
241. Whitney ML, Jefferson LS, & Kimball SR (2009) ATF4 is necessary and sufficient for ER stress-induced upregulation of REDD1 expression. *Biochemical and biophysical research communications* 379(2):451-455.
242. Mungrue IN, Pagnon J, Kohannim O, Gargalovic PS, & Lusis AJ (2009) CHAC1/MGC4504 is a novel proapoptotic component of the unfolded protein response, downstream of the ATF4-ATF3-CHOP cascade. *J Immunol* 182(1):466-476.
243. Lee HK, *et al.* (2009) Capsaicin inhibits the IL-6/STAT3 pathway by depleting intracellular gp130 pools through endoplasmic reticulum stress. *Biochemical and biophysical research communications* 382(2):445-450.
244. Schardt JA, Weber D, Eyholzer M, Mueller BU, & Pabst T (2009) Activation of the unfolded protein response is associated with favorable prognosis in acute myeloid leukemia. *Clinical cancer research : an official journal of the American Association for Cancer Research* 15(11):3834-3841.
245. Yan D, Hutchison RE, & Mohi G (2012) Critical requirement for Stat5 in a mouse model of polycythemia vera. *Blood* 119(15):3539-3549.
246. Chen Y, *et al.* (2010) Gprc5a deletion enhances the transformed phenotype in normal and malignant lung epithelial cells by eliciting persistent Stat3 signaling induced by autocrine leukemia inhibitory factor. *Cancer research* 70(21):8917-8926.
247. Fossey SL, Bear MD, Kisseberth WC, Pennell M, & London CA (2011) Oncostatin M promotes STAT3 activation, VEGF production, and invasion in osteosarcoma cell lines. *BMC cancer* 11:125.
248. Kellokumpu-Lehtinen P, *et al.* (1996) Leukemia-inhibitory factor stimulates breast, kidney and prostate cancer cell proliferation by paracrine and autocrine pathways. *International journal of cancer. Journal international du cancer* 66(4):515-519.
249. Li Q, *et al.* (2011) Oncostatin M promotes proliferation of ovarian cancer cells through signal transducer and activator of transcription 3. *International journal of molecular medicine* 28(1):101-108.
250. West NR, Murray JI, & Watson PH (2013) Oncostatin-M promotes phenotypic changes associated with mesenchymal and stem cell-like differentiation in breast cancer. *Oncogene*.

251. Reynaud D, *et al.* (2011) IL-6 controls leukemic multipotent progenitor cell fate and contributes to chronic myelogenous leukemia development. *Cancer cell* 20(5):661-673.
252. Schuringa JJ, Wierenga AT, Kruijer W, & Vellenga E (2000) Constitutive Stat3, Tyr705, and Ser727 phosphorylation in acute myeloid leukemia cells caused by the autocrine secretion of interleukin-6. *Blood* 95(12):3765-3770.
253. Klein B, Zhang XG, Lu ZY, & Bataille R (1995) Interleukin-6 in human multiple myeloma. *Blood* 85(4):863-872.
254. Hoejberg L, Bastholt L, & Schmidt H (2012) Interleukin-6 and melanoma. *Melanoma research* 22(5):327-333.
255. Schafer ZT & Brugge JS (2007) IL-6 involvement in epithelial cancers. *The Journal of clinical investigation* 117(12):3660-3663.
256. Kiladjian JJ (2012) The spectrum of JAK2-positive myeloproliferative neoplasms. *Hematology / the Education Program of the American Society of Hematology. American Society of Hematology. Education Program* 2012:561-566.
257. Britschgi A, *et al.* (2012) JAK2/STAT5 inhibition circumvents resistance to PI3K/mTOR blockade: a rationale for cotargeting these pathways in metastatic breast cancer. *Cancer cell* 22(6):796-811.
258. Tasian SK, *et al.* (2012) Aberrant STAT5 and PI3K/mTOR pathway signaling occurs in human CRLF2-rearranged B-precursor acute lymphoblastic leukemia. *Blood* 120(4):833-842.
259. Yokogami K, Wakisaka S, Avruch J, & Reeves SA (2000) Serine phosphorylation and maximal activation of STAT3 during CNTF signaling is mediated by the rapamycin target mTOR. *Current biology : CB* 10(1):47-50.
260. Little JL, Wheeler FB, Fels DR, Koumenis C, & Kridel SJ (2007) Inhibition of fatty acid synthase induces endoplasmic reticulum stress in tumor cells. *Cancer research* 67(3):1262-1269.
261. Liu G, *et al.* (2012) Salermide up-regulates death receptor 5 expression through the ATF4-ATF3-CHOP axis and leads to apoptosis in human cancer cells. *Journal of cellular and molecular medicine* 16(7):1618-1628.
262. Oyadomari S & Mori M (2004) Roles of CHOP/GADD153 in endoplasmic reticulum stress. *Cell death and differentiation* 11(4):381-389.
263. Rao R, *et al.* (2010) Treatment with panobinostat induces glucose-regulated protein 78 acetylation and endoplasmic reticulum stress in breast cancer cells. *Molecular cancer therapeutics* 9(4):942-952.
264. Sanchez AM, *et al.* (2008) Induction of the endoplasmic reticulum stress protein GADD153/CHOP by capsaicin in prostate PC-3 cells: a microarray study. *Biochemical and biophysical research communications* 372(4):785-791.
265. Wang HQ, Du ZX, Zhang HY, & Gao DX (2007) Different induction of GRP78 and CHOP as a predictor of sensitivity to proteasome inhibitors in thyroid cancer cells. *Endocrinology* 148(7):3258-3270.
266. Kim R, Emi M, Tanabe K, & Murakami S (2006) Role of the unfolded protein response in cell death. *Apoptosis : an international journal on programmed cell death* 11(1):5-13.
267. Krishan A (1975) Rapid flow cytofluorometric analysis of mammalian cell cycle by propidium iodide staining. *The Journal of cell biology* 66(1):188-193.
268. Zhu X, *et al.* (2013) miR-137 inhibits the proliferation of lung cancer cells by targeting Cdc42 and Cdk6. *FEBS letters* 587(1):73-81.

269. Bemis LT, *et al.* (2008) MicroRNA-137 targets microphthalmia-associated transcription factor in melanoma cell lines. *Cancer research* 68(5):1362-1368.
270. Luo C, *et al.* (2013) miR-137 inhibits the invasion of melanoma cells through downregulation of multiple oncogenic target genes. *The Journal of investigative dermatology* 133(3):768-775.
271. Huang Z, *et al.* (2011) MicroRNA-95 promotes cell proliferation and targets sorting Nexin 1 in human colorectal carcinoma. *Cancer research* 71(7):2582-2589.
272. Walter J, Hartung HP, & Dihne M (2012) Interferon gamma and sonic hedgehog signaling are required to dysregulate murine neural stem/precursor cells. *PloS one* 7(8):e43338.
273. Leroy G, *et al.* (2012) Proteogenomic characterization and mapping of nucleosomes decoded by Brd and HP1 proteins. *Genome biology* 13(8):R68.
274. Desrivieres S, *et al.* (2006) The biological functions of the versatile transcription factors STAT3 and STAT5 and new strategies for their targeted inhibition. *Journal of mammary gland biology and neoplasia* 11(1):75-87.
275. de la Iglesia N, *et al.* (2008) Deregulation of a STAT3-interleukin 8 signaling pathway promotes human glioblastoma cell proliferation and invasiveness. *The Journal of neuroscience : the official journal of the Society for Neuroscience* 28(23):5870-5878.
276. Couto JP, *et al.* (2012) STAT3 negatively regulates thyroid tumorigenesis. *Proceedings of the National Academy of Sciences of the United States of America* 109(35):E2361-2370.
277. Meyer N & Penn LZ (2008) Reflecting on 25 years with MYC. *Nature reviews. Cancer* 8(12):976-990.
278. Pylayeva-Gupta Y, Grabocka E, & Bar-Sagi D (2011) RAS oncogenes: weaving a tumorigenic web. *Nature reviews. Cancer* 11(11):761-774.
279. Elsarraj HS, *et al.* (2013) Novel role of microRNA146b in promoting mammary alveolar progenitor cell maintenance. *Journal of cell science*.
280. Dewilde S, Vercelli A, Chiarle R, & Poli V (2008) Of alphas and betas: distinct and overlapping functions of STAT3 isoforms. *Frontiers in bioscience : a journal and virtual library* 13:6501-6514.
281. Huang Y, Li T, Sane DC, & Li L (2004) IRAK1 serves as a novel regulator essential for lipopolysaccharide-induced interleukin-10 gene expression. *The Journal of biological chemistry* 279(49):51697-51703.
282. Geraldo MV, Yamashita AS, & Kimura ET (2012) MicroRNA miR-146b-5p regulates signal transduction of TGF-beta by repressing SMAD4 in thyroid cancer. *Oncogene* 31(15):1910-1922.
283. Kitamura H, *et al.* (2005) IL-6-STAT3 controls intracellular MHC class II alphabeta dimer level through cathepsin S activity in dendritic cells. *Immunity* 23(5):491-502.
284. Premzl A, Zavasnik-Bergant V, Turk V, & Kos J (2003) Intracellular and extracellular cathepsin B facilitate invasion of MCF-10A neoT cells through reconstituted extracellular matrix in vitro. *Exp Cell Res* 283(2):206-214.
285. Labbaye C & Testa U (2012) The emerging role of MIR-146A in the control of hematopoiesis, immune function and cancer. *Journal of hematology & oncology* 5:13.
286. Helbig G, *et al.* (2003) NF-kappaB promotes breast cancer cell migration and metastasis by inducing the expression of the chemokine receptor CXCR4. *The Journal of biological chemistry* 278(24):21631-21638.

287. Zhao JL, *et al.* (2011) NF-kappaB dysregulation in microRNA-146a-deficient mice drives the development of myeloid malignancies. *Proceedings of the National Academy of Sciences of the United States of America* 108(22):9184-9189.
288. Starczynowski DT, *et al.* (2010) Identification of miR-145 and miR-146a as mediators of the 5q- syndrome phenotype. *Nature medicine* 16(1):49-58.
289. Brocke-Heidrich K, *et al.* (2004) Interleukin-6-dependent gene expression profiles in multiple myeloma INA-6 cells reveal a Bcl-2 family-independent survival pathway closely associated with Stat3 activation. *Blood* 103(1):242-251.
290. Demchenko YN, *et al.* (2010) Classical and/or alternative NF-kappaB pathway activation in multiple myeloma. *Blood* 115(17):3541-3552.
291. Lam LT, *et al.* (2008) Cooperative signaling through the signal transducer and activator of transcription 3 and nuclear factor-{kappa}B pathways in subtypes of diffuse large B-cell lymphoma. *Blood* 111(7):3701-3713.
292. Khatri N, Rathi M, Baradia D, Trehan S, & Misra A (2012) In vivo delivery aspects of miRNA, shRNA and siRNA. *Critical reviews in therapeutic drug carrier systems* 29(6):487-527.
293. Xue W, *et al.* (2012) A cluster of cooperating tumor-suppressor gene candidates in chromosomal deletions. *Proceedings of the National Academy of Sciences of the United States of America* 109(21):8212-8217.
294. Radtke S, *et al.* (2010) Cross-regulation of cytokine signalling: pro-inflammatory cytokines restrict IL-6 signalling through receptor internalisation and degradation. *Journal of cell science* 123(Pt 6):947-959.
295. Niesen FH, Berglund H, & Vedadi M (2007) The use of differential scanning fluorimetry to detect ligand interactions that promote protein stability. *Nature protocols* 2(9):2212-2221.
296. Lomenick B, *et al.* (2009) Target identification using drug affinity responsive target stability (DARTS). *Proceedings of the National Academy of Sciences of the United States of America* 106(51):21984-21989.
297. Takizawa PA, *et al.* (1993) Complete vesiculation of Golgi membranes and inhibition of protein transport by a novel sea sponge metabolite, ilimaquinone. *Cell* 73(6):1079-1090.
298. Lu PH, *et al.* (2007) Ilimaquinone, a marine sponge metabolite, displays anticancer activity via GADD153-mediated pathway. *European journal of pharmacology* 556(1-3):45-54.
299. Sonoda H, Okada T, Jahangeer S, & Nakamura S (2007) Requirement of phospholipase D for ilimaquinone-induced Golgi membrane fragmentation. *The Journal of biological chemistry* 282(47):34085-34092.
300. Kim SM, *et al.* (2010) Activation of eukaryotic initiation factor-2 alpha-kinases in okadaic acid-treated neurons. *Neuroscience* 169(4):1831-1839.
301. Guo Y, Xu F, Lu T, Duan Z, & Zhang Z (2012) Interleukin-6 signaling pathway in targeted therapy for cancer. *Cancer treatment reviews* 38(7):904-910.